EFFECT OF ADDITIVES AND COMONOMERS ON CRYSTALLIZATION AND SOLID STATE POLYMERIZATION OF POLYESTERS

Thesis submitted to the

UNIVERSITY OF PUNE

for the degree of

DOCTOR OF PHILOSOPHY

in

CHEMISTRY

by

E. BHOJE GOWD

Division of Polymer Science and Engineering

National Chemical Laboratory

PUNE: 411 008

INDIA

January 2005

EFFECT OF ADDITIVES AND COMONOMERS ON CRYSTALLIZATION AND SOLID STATE POLYMERIZATION OF POLYESTERS

By

E. Bhoje Gowd

January 2005

Dedicated to My Parents
and
Lord Venkateswara Swami

DECLARATION

Certified that the work incorporated in this thesis entitled **"Effect of additives and comonomers on crystallization and solid state polymerization of polyesters"** submitted by **E. Bhoje Gowd** was carried out under my supervision. Such material as obtained from other sources has been duly acknowledged in this thesis.

January 2005 **Dr. C. Ramesh**

Pune (Research Guide)

DECLARATION

I hereby declare that the thesis entitled **"Effect of additives and comonomers on crystallization and solid state polymerization of polyesters"** submitted for Ph. D. degree to the University of Pune has been carried out at National Chemical Laboratory, Pune, India under the supervision of **Dr. C. Ramesh,** Division of Polymer Science and Engineering, National Chemical Laboratory, Pune-411008. The work is original and has not been submitted in part or full by me for any degree or diploma to this or any other University.

January 2005 (**E. Bhoje Gowd)**

Pune

Acknowledgements

I take this opportunity to express my gratitude to Dr. C. Ramesh, my research supervisor, mentor, for his invaluable guidance, teaching, support and advice throughout the course of this investigation. It is only because of him that my career has been escalated to a height where I stand today. I have learnt from him to interpret, concise and correct my approach to science from formulation to the presentation of results. Although this eulogy is insufficient, my sincere regards and reverence are for him, forever.

It is my honour to acknowledges Dr. S. Sivaram, Director NCL, who was my inspiration to choose this career and who gave me an opportunity to work in NCL. I am very lucky to associate with him many times and I shall be grateful to him for the encouragement and support I got from him during my course.

I am extremely grateful to Dr. S. Ponrathnam for the stimulating scientific discussions and suggestions. Whenever I approached him with some problems he readily helped. I am thankful to my collaborators Prof. Tashiro (Japan) and Dr. N. Sanjeeva Murthy (USA) for their valuable discussions and suggestions.

I owe deeply to ever-trustful friends Smitha S. Nair, S. R. Mallikarjuna and K. Raghunath Reddy for always being with me. I sincerely thank them for all their affection and help. I must thank Smitha especially for all the support she has given me.

I am thankful to Drs. C. V. Avadhani, D. Baskaran, T. P. Mohandas, M.G. Kulkarni, R. P. Singh, S. P. Vernekar, B. B. Idage, P. P. Wadgaonkar and C. Bhaskar on this occasion for their suggestions, advice and valuable discussions we have had in this period. I am also thankful to Mrs. D. A. Dhoble, Dr. (Mrs). S. B. Idage, Mr. S. K. Menon and Dr. Jadhav for their help during the course of this work.

I express my heartfelt thanks to Dr. V. Raghunadh, Dr. M. J. Yanjarappa, Dr. G. Jayasimha Reddy, Dr. A. V. Sainath, Dr. Nabi Saheb and Mr. Sreekanth Reddy for their willing help at initial stages of my thesis work and friendly support. I specially thank Dr. (Mrs) Nirmala James, Mr. Tony Mathew, Mr. S. Rajesh, Mr. P. Govindaiah and Mr. Rajkumar Patel for their timely help during the course of my work.

The friendly attitude of my colleagues in polymer chemistry division helped to have cheerful atmosphere in the laboratory. I extend my deep sense of gratitude towards them. Also I wholeheartedly thank the ***Telugu group****, who made my stay at NCL memorable and pleasant. My endless thanks to my M. Sc. (Tech) classmates and SKUPAA members for everything they have done.*

On this special occasion, I also remember and express my gratitude to some of my earlier teachers (Late) Sri Narasingha Rao and family, Sri P. Subbarayudu, (Late) Prof. A. Kameswara Rao, Prof. Varada Rajulu, Prof. S. Venkata Naidu, Dr. K. Chowdoji Rao and Dr. K. Mohana Raju who literally steered my vision of career. I must remember my childhood friends Nagendra, Seena, Kumara Swami, Ravindra and Rangaswamy for everything they have done.

I thank authorities of NMR facility and PPC of NCL for their timely help. I also thank CSIR for the senior research fellowship.

Finally, I am deeply and thoroughly indebted to my family members for all the freedom and moral support they have given to my choice of career and life style.

(E. Bhoje Gowd)

ABSTRACT

This thesis presents the results of the study of the structure and morphology development in PET based copolymers during chain extension reaction (solid state polymerization). To that end comonomers having distinct properties are chosen: 1) comonomer which is semi-rigid 2) highly flexible comonomer which can plasticize the PET and 3) rigid monomer which can form liquid crystal with PET.

Another important aspect of polymer crystallization is the role of orientation on crystallization. Hence, very specially spun PET fibers with varying degree of amorphous orientation are studied for the crystallization behavior and correlated with the amorphous orientation factor.

Poly(ethylene terephthalate) (PET) (IV:0.15 dL/g) oligomer was obtained by depolymerisation of high molecular weight PET. Polycarbonate (PC) oligomer (IV: 0.15 dL/g) was synthesized by standard melt polymerization procedure using bisphenol A and diphenyl carbonate in the presence of a basic catalyst. Blends of varying compositions were prepared by melt blending the chemically distinct PET and PC oligomers. The copolymer, poly(ethylene terephthalate-*co*-bisphenol A carbonate) was synthesized by simultaneous solid state polymerization and ester-carbonate interchange reaction between the oligomers of PET and PC. The reaction was carried out under reduced pressure at temperatures below the melting temperature of the blend samples. DSC and WAXS techniques characterized the structure and morphology of the blends, while ^{1}NMR spectroscopy was used to monitor the progress of interchange reactions between the oligomers. The studies have indicated the amorphisation of the PET and PC crystalline phases in solid state with the progress of solid-state polymerization and interchange reaction.

Poly (ethylene glycol) and end capped poly (ethylene glycol) [Poly(ethylene glycol) dimethyl ether (PEGDME)] of number average molecular weight 1000 was melt blended with PET oligomer. NMR, DSC and WAXS techniques characterized the structure and morphology of the blends. Both these samples showed reduction in T_g and similar crystallization behavior. Solid-state polymerization was performed on these blend samples using Sb_2O_3 as catalyst under reduced pressure at temperatures below the melting temperature of the samples. Inherent viscosity data indicated that for the blend sample

with PEG, there was enhancement of SSP rate while for the sample with PEGDME the SSP rate was suppressed. NMR data showed that PEG was incorporated in to the PET chain, while PEGDME did not react with PET.

Solid state polymerization was performed on PET and POB oligomer blends to obtain PET/POB copolymer. Oligomer blends were crystallized thermally to obtain suitable precursors for SSP. DSC results showed that T_m of oligomers decreased in the blend sample. Melt crystallization temperature of PET increased with the progress of reaction indicating the enhancement of crystallization rate with the progress of reaction. It could be due to the nucleation of PET by unmelted long POB chains. On the other hand, melt quenched samples showed that the crystallization rate reduced with the progress of the SSP and interchange reaction. Thus the POB had profound influence on the crystallization of PET. A copolymer of same composition was also prepared by melt polymerization and compared with the copolymer formed by SSP.

Amorphous poly (ethylene terephthalate) fibers in which the skin was removed were studied to expressly study the effect of amorphous molecular orientation on crystallization behavior. Thermal analysis was carried out on fibers with a wide range of molecular orientation using differential scanning calorimetry (DSC) under constrained and unconstrained conditions. The thermal behavior was correlated with structural characteristics such as amorphous orientation determined using wide-angle x-ray diffraction. We show for the first time a quantitative inverse linear relationship between the degree of amorphous orientation and the cold crystallization temperatures and heat of crystallization. Crystallization begins at a critical amorphous orientation of 0.18, and extrapolation shows that even at modest amorphous orientation of 0.27, the cold crystallization can start spontaneously at T_g and with no change in free energy.

CONTENTS

GLOSSARY

ASSP	After solid state polymerization
ABA	*p*-Acetoxybenzoic acid
B_{B1}	Degree of randomness
BSSP	Before solid state polymerization
DEG	Diethylene glycol
DMT	Dimethyl terephthalate
DSC	Differential scanning calorimetry
DT	Degree of transesterification
EG	Ethylene glycol
F	Degree of orientation
f_{am}	Degree of amorphous orientation or Hermann orientation factor
F_{am}	Oriented amorphous phase
f_c	Degree of crystallite orientation
FWHM ($\Delta\phi$)	Full width at half maxima
ΔH	Enthalpy of melting
ΔH_c	Heat of crystallization
$I(\phi)$	Azimuthal intensity
IR	Infra red
IV	Inherent viscosity
M_n	Number average molecular weight
NMR	Nuclear magnetic resonance
PBT	Poly(butylene terephthalate)
PBG	Poly(butylene glycol)
PC	Polycarbonate
PEN	Poly(ethylene 2,6-dimethyl naphthalate)

PEG	Poly(ethylene glycol)
PEGDME	Poly(ethylene glycol) dimethyl ether
PET	Poly(ethylene terephthalate)
P(ET/CT)	Poly(ethylene terephthalate-co-1,4-cyclohexylenedimethylene terephthalate)
PHB	Poly(hydroxybutyrate)
PHV	Poly(hydroxyvalerate)
PS	Polystyrene
PTT	Poly(trimethylene terephthalate)
ΔS	Change of entropy
Sb_2O_3	Antimony trioxide
SAXS	Small angle X-ray scattering
SSP	Solid state polymerization
T_{cc}	Crystallization temperature upon heating (cold crystallization)
T_c	Crystallization temperature upon cooling
TCE	1,1',2,2'-tetrachloroethane
TEM	Transmission electron microscopy
TMS	Trimethyl silane
T_g	Glass transition temperature
$Ti(O^iPr)_4$	Titanium tetraisopropoxide
T_m	Melting temperature
TFA	Trifluoro acetic acid
WAXS	Wide angle X-ray scattering
XRD	X-ray diffraction
$[\eta]$	Intrinsic viscosity
η_{inh}	Inherent viscosity
δ	Solubility parameter

List of Figures

List of Schemes

List of Tables

CHAPTER 1

GENERAL INTRODUCTION

1.1 Introduction

The importance of polymer crystallization has increased in modern polymer industry, despite the recent decline in research activities. More than 80% of the commodity polymers made today are crystalline, and the subject of crystallization is still the number one issue concerning the performance of semicrystalline polymers. Although many believe the field of polymer crystallization has "matured", new problems and new knowledge continue to emerge, making research and education of this topic ever more challenging.

Polymer crystallization is a process whereby an ordered (crystalline) phase is produced from a disordered amorphous phase (melt or solution). Crystallization and crystallinity are important properties of polyesters, and have been studied by various methods for poly(ethylene terephthalate) (PET) and poly(butylene terephthalate) (PBT)[1-11]. The properties of crystallizable polyesters are strongly dependent on the morphological features (size, shape, perfection, volume fraction and orientation of crystallites), which are formed by the crystallization from the molten state. Thus, crystallization behavior is a tool to control the morphological structure and the resultant properties[12]. This chapter discusses the information available on the effect of additives and comonomers on crystallization of PET and structure and morphology changes during the SSP of polyester oligomers and its blends.

1.1.1 Poly(ethylene terephthalate)

Since its discovery in 1941,[13] poly(ethylene terephthalate) (PET) has been the subject of countless studies. Its popularity as a research material grew at the same time as it is becoming a commodity product, and along with polyethylene and polypropylene, it became a sort of textbook example for the study of polymer crystallization[14]. It is particularly often considered as a model for the study of the class of semi rigid semicrystalline polymers, comprising among others aromatic polyesters, polyamides, and poly(aryl ether ketone)'s; all polymers are characterized by a relatively rigid backbone compared to that of polyethylene.

With the high level of production and its low price, PET can be positioned between the technical polymers and commodities. The most important applications of PET are its use in textile filaments, packaging materials, and bottle production. PET can be processed by melt spinning, injection molding, blow molding or film extrusion. Its application as an engineering plastic accounts for only 7% of the total use. Table 1.1 shows some of the main producers of PET. However, apart from good physical properties and chemical

stability, PET is not outstandingly successful as an injection molding resin due to its low rate of crystallization in a cold mould. The mould has to be heated to 130-140°C, well above the glass transition temperature (T_g), to obtain adequate crystallization rates. Depending upon cooling and shear conditions of injection molding operations, complex morphologies may develop[15,16]. These structural features dictate mechanical properties of the molded parts. On the other hand, such a structural development process also controls some aspects of injection molding, e.g. cycle time. Thus, it is essential to understand and to be able to predict crystallization under molding conditions, i.e. high shear rates and high cooling rates.

Table 1.1: Overview of some of the main producers of PET

Manufacturer	Trade name PET
Eastmann	Eastapak
ICI	Melinar
Hoechst	Impet*
DuPont	Dacron
Shell	Caripak
Bayer	Makroblend**
DSM	Arnite

* glass fiber reinforced

** PET/Polycarbonate blend

However, most studies address crystallization kinetics under quiescent and isothermal conditions, except in a few cases where shear rate and cooling rate are considered[17]. During the mid-1960s and later in years, fast-crystallizing grades of PET are developed which gave uniform and controlled morphology because of the presence of specific additives such as nucleating agents.

1.1.2 Nucleating agents for PET

Using nucleating agents to increase crystallization kinetics of PET has been well documented[18-24]. The nucleating agents can reduce the surface energy required for nucleation and therefore promote nucleation process, and this can be refereed as a physical nucleation mechanism. On the other hand, it has been demonstrated that certain strong nucleating agents are based on a chemical nucleation mechanism, i.e. these nucleating agents react with polymer chains and result in ionic chain-ends serving as nucleating

centres. Furthermore, homogeneous nucleation can be promoted by incorporation of rigid segments in polymer backbone via copolymerization. Table 1.2 is a partial list of nucleating agents utilized in PET.

Table 1.2: A list of nucleating agents for PET*

Inorganic compounds
• chalk, gypsum, clay, kaolin, mica, talc, silicate
• cadmium red, cobalt yellow, chromium oxide, phthalocyanine
• titanium oxide, magnesium oxide, antimony trioxide (added or remnants)
• phosphates, carbonates, sulfates, sodium fluoride, boron and sodium nitrides
• metal hydrides of Al, Cu, Ni, In, Ba, Co, La
Organic compounds
• salts of monocarboxylic or polycarboxylic acids
• montan wax and montanic esters
• alkali metal salts of ethylene terephthalate oligmers and benzonic acids
• amine carboxylate (also plasticizer)
• diphenylamine, tetrachloroethane
• nitromethane, sodium benzene acetone,, toluene (also plasticizer)
• chlorobenzonate (e.g. Na)
• benzophenone, tetralin
• disolium terephthalate
• aromatic alcohols, amines
• alkali aralkylsulfonates
• epoxides
Residual catalysts
• catalysis remnants in transesterification (derivatives of Ca, Mn, Mg, Zn, Ti, Sn, etc.)
• catalysis remnants in polycondensation (derivatives of Sb, Ti, Ge, etc.)
• Catalysis deactivators (phosphorous derivatives)
Polymers
• polyolefins (PE, PP, PMP, PB-1), fluoropolymers (PTFE)
• coploymers of ethylene and unsaturated carboxylic esters
• copolymers of styrene derivatives and conjugated dienes

• ionomers (Surlyn) • blending with faster crystallizing polymers (PBT, PBN, PPS and PA) and LCP's • incorporation of rigid chain segments by copolymerization
Others • any additives, including fibers(glass), carbon black, etc, in resin formulation

* Based on Gachter/Muller, *Plastics Additives*, Chapt. 17, Hanser Publisher, 1992

1.1.3 Enhancement of PET crystallization rate by copolymerization.

A small amount (0.01%) of certain faster crystallizing units, normally rigid and polar ones, is incorporated into the backbone of the neat polymer. Examples of homogeneous nucleation include block copolymers of PET and PBT[25] and random co-polymers of PET and 4, 4.- biphenylene terephthalate or paraphenylene terephthalate[26] and random co-polymers of PBT and N,N.-bis-(p-carbomethoxybenzoyl)-1,4- butanediamine (T4T)[27] as well.

The crystallization rate of PET can be increased by incorporation of low amount (2 mol%) of diamide segments, such as T6T, T4T, T2T and TϕT (Figure 1.1) either during polymerization[28], or during a subsequent extrusion process[29]. These diamide segments are incorporated into PET by copolymerization at a concentration of 2 mol%, using $Ti(i\text{-}OC_3H_7)_4$ as a catalyst. Diamide segments are able to form hydrogen bonds and therefore are expected to self- assemble in the melt, thus inducing the adjacent ordering of the ester segments and thereby increasing the crystallization rate of PET. All of the diamide segments are able to nucleate PET, as the undercooling is decreased, however, T2T is found to be the most effective nucleator, the undercooling being decreased from 74 to 58°C, a decrease of 16°C, indicating a considerable improvement in the crystallization rate. The T2T segment is of approximately the same length as the repeating unit of PET, whereas the diamide segments T4T and TϕT are longer than the repeating unit of PET. Although the T2T and ester segments of PET are expected to be non-isomorphous, T2T probably has a good fit in the crystal lattice of PET.

Agarwal et al[30] describe a solid-state process for ethylene diamine incorporation as amide segments into commercial PET pellets, without melting, and without using water or diluents. On diffusion into the polymer pellets, the functional monomer can undergo reaction with the –COOH and –OH functionalities at chain ends, or with the –O–(CO)– functionality along the chains. Besides, exchange reaction can aid the distribution of the comonomer so incorporated. As expected, molecular weight of the polymer decreases, but

can be built up to the original level by a subsequent solid state polymerization (SSP). They observed that the amide functionality so incorporated is effective in enhancing the crystallization rate of PET, sufficiently to substitute talc as a nucleating agent.

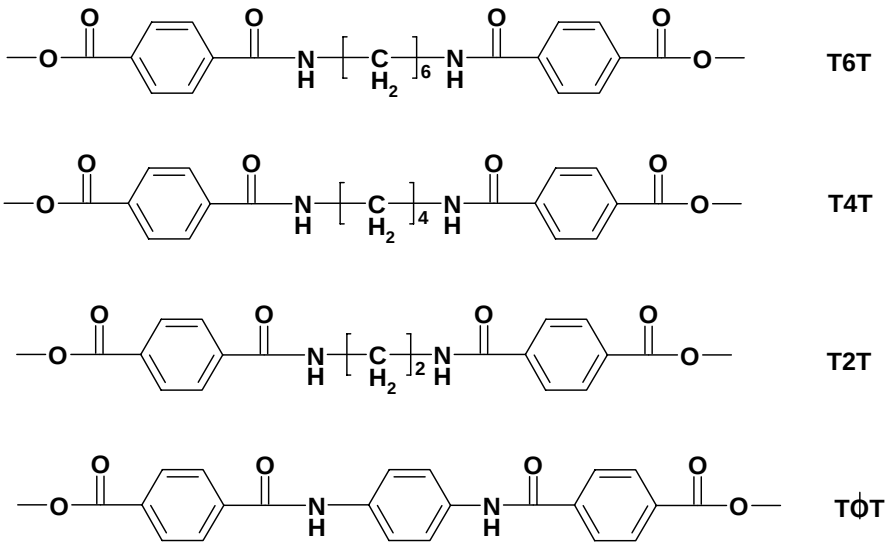

Figure 1.1: Structure of diamide segments

1.1.4 Crystallization of PET with short and long codiols

The nucleation rate of PET can be enhanced by the incorporation of short[31] and long diols[32]. Codiols have a lower surface free energy, and therefore are able to enhance the nucleation rate of PET. The PET chain is not very flexible, however, by the incorporation of long, flexible segments, the chain mobility of the amorphous phase can be increased. The presence of long diols in the PET chain will influence the crystallization.

1.1.4.1 PET with short codiols

Short codiols usually disturb the order of PET; however, when they are present in small quantities, they are able to act as nucleators. Codiols fold easily and have a lower surface tension than ethanediol[31,33]. The codiols are not incorporated in the crystalline phase because they do not fit into the crystalline lattice of PET and are present in the amorphous phase. The codiols are also present in the chain fold and thereby lower the free energy of the fold surface, resulting in an increase in the nucleation rate. Branched diols such as 2,5-hexanediol and 3-methyl-2,4-pentanediol are particularly effective, and the optimum concentration is in the range of 5 mol %[31]. Branched diols have methyl side groups; it is probable that these pending groups decrease the surface free energy to a greater extent

than linear diols. At higher concentrations, the disturbance of the chain order dominates the crystallization rates are then reduced.

During the synthesis of PET, the dimer of EG, diethylene glycol (DEG), is always formed, such that PET usually contains between 2 and 4 mol % DEG. The glass-transition temperature (T_g), as well as the melting temperature (T_m), of PET are known to decrease with increasing DEG content. Frank and Zachmann[34] investigated samples with DEG contents up to 15 mol %. Their study shows that when crystallizing from the melt, increasing the DEG content increases the half time of crystallization, indicating a decrease in the rate of crystallization. However, on crystallizing from the glassy state, rate of crystallization increases with increasing DEG content. They explained these differences as being associated with the decrease of T_m and T_g with increasing DEG contents. Farikov et al[35] confirmed the decrease in T_m and T_g with increase in the DEG concentration. They concluded that when crystallizing from the glassy state, at crystallization temperatures higher than 200°C, the crystallization rate decreases with increasing DEG content; but at lower temperatures, it is insensitive to the DEG content. Golike and Cobbs[36] studied the crystallization of PET, when cooling from the melt, for samples containing 5 and 10 mol % DEG at temperatures ranging from 110 to 240°C. They concluded that at temperatures just above T_g where molecular motion is rate determining, higher DEG content increases the rate of crystallization. This is attributed to the flexible aliphatic chains introduced by the presence of DEG. At higher temperatures, where the rate is determined by the degree of supercooling, addition of the copolymer decreases the crystallization rate.

1.1.4.1 PET containing long codiols

PET can be modified using a small amount of polyether segments to form segmented copolymers having a lower T_g (PET is internally plasticized)[37]. Lowering the T_g allows the use of lower mold temperatures; this is an advantage because the usual mold temperatures required for PET are high (120-140°C) and are therefore impractical[38]. PET can be modified with the polyethers like poly(ethylene glycol) (PEG) and poly(butylene glycol) (PBG); unfortunately these polyethers are thermally unstable. The modification of PET with an olefinic diol (C_{36}-diol) is a relatively new approach. The C_{36}-diol (Figure 1.2) is a branched alkane with a functionality of approximately 2. The C_{36}-diol is more thermally stable than PEG and PBG segments and is therefore possibly better suited for use in high melting PET, if it forms single amorphous phase with PET. When the C_{36}-diol is copolymerized with PBT, the segmented copolymer has one T_g[39].

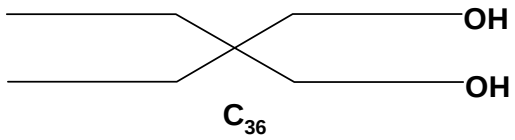

Figure 1.2: Schematic representation of C_{36} dimerized fatty diol

Bouma et al[40] compared the effect of linear, branched, and aromatic codiols such as 1,5-pentanediol, 1,8-octanediol, 2,5-hexanediol, and 1,3-dihydroxymethyl benzene on crystallization of PET.

1.1.4.3 Crystallization behavior of PET in PET/PEG gel

Degrees of crystallinity in an annealed PET typically vary between 20 and 50%, as measured by wide-angle X-ray diffraction[41]. Roland has investigated the annealing of PET at higher temperature[42]. The crystallinity of PET is found to increase from about 45 % to 60 % for samples annealed at 260°C for 700 h. Xue et al[43,44] showed an effective method for preparing highly crystalline PET. PET is first dissolved in an oligomer which has shorter chains, like a low molecular weight poly(ethylene glycol) (PEG) or an epoxy resin. At elevated temperature, a homogeneous solution consisting of PET and the oligomer is obtained, which formed rapidly a thermo reversible gel on cooling. After the solvent is removed, a highly crystalline PET is recovered.

1.1.5 Solvent induced crystallization

The process involves diffusion of solvent in the polymer and interruption of the intersegmental forces due to solvent polymer interaction. The extent of crystallization is proportional to the penetration distance of solvent. The crystallization process is thus diffusion controlled and it can be described by Fick's classical equation.

Many authors studied the solvent induced crystallization of PET[45-50]. It is reported that polarity, type, molar volume and the solubility parameter of the solvent plays a major role in solvent induced crystallization.

1.1.6 Crystallization under pressure

Crystallization under pressure results in a different morphology, higher densities, and higher melting temperatures compared to those obtained from crystallization at atmospheric pressure. Wei and Cuculo[51] observed a two-stage crystallization process at high pressures. Philips[52] observed that the nucleation density increased 10-fold and the crystallinity also increased upto 80% under 2 k-bar pressure. Siegmann and Harget[53]

observed extended chain crystals under pressure in their study of crystallization and melting of PET. There have been few studies on the effect of pressure on the crystallization of PET, it is observed that crystallization under pressure leads to extended chain crystals and associated high melting temperatures.

1.1.7 Effect of molecular orientation on crystallization

1.1.7.1 Orientation

Chain orientation the principle factor, which dominates the mechanical properties of fibers[54]. Orientation in synthetic fibers is usually achieved by deformation in the solid state. The traditional method to achieve polymer chain orientation in the fiber direction is based on the drawing or stretching of fiber around glass transition temperature[55-57]. Chain mobility in solid polymer is very limited due to strong chain interaction and/or crystallization. In a solid-state deformation process, the interaction between chains restricts the achievable orientation and creates a high level of stretching tension. The degree of orientation can be calculated using the Hermen's orientation equation.

$$F = \frac{1}{2}\left(3\,\mathrm{Cos}^2\theta - 1\right)$$

Where $\mathrm{Cos}^2\theta$ is the mean-square cosine, averaged over all of the molecules, of the angle between a given crystal axis and a reference direction. The crystal axis is usually the chain axis, while the reference direction is the fiber axis. F values of 1, 0, -1/2 describe systems with perfect, random and perpendicular alignment of the polymer chains relative to the reference direction respectively.

1.1.7.2 Structural changes on drawing

The structural and morphological changes that occur when low speed spun yarns are drawn uniaxially at 90-100°C are rather complex. Initially, an enhancement in molecular orientation takes place and later crystallization occurs at many places, and the same molecules get trapped in several growing crystals. As each crystal grows, the entanglements and chain ends are expelled and form part of the amorphous regions between the crystals, which also contain the tie molecules. These strained regions prevent the large-scale growth of crystals. Ultimately, a fibrillar structure develops, with alternating crystalline and amorphous regions stacked vertically along the fiber axis. Since the filament has been cold drawn, it has high orientation, low crystallinity, no clear-cut

boundaries between the crystalline and amorphous phases, and little chain folding. PET filaments spun at high speeds develop a fibrillar morphology, with relatively large crystals with considerable folding, fewer defects and lower amorphous orientation. A detailed study made by Huisman and Heuvel[58] in which low speed and high speed spun PET yarns are stretched so that both drawn yarns had a final extensibility of 10%, led to morphological models, supporting the scheme of structure formation described above. Brody[59] showed that filaments spun at high winding speeds are structurally not the same as partially drawn filaments, originally spun at low winding speeds.

1.1.7.3 Structural changes on heat-setting

The as-drawn PET filaments that have not been heat-set have adequate mechanical properties, but cannot be used for most textile and technical purposes because they exhibit thermal shrinkage. Heat setting imparts dimensional stability to these structures by bringing the macromolecules closer to their equilibrium state, so that they attain resistance to thermal shrinkage, dimensional changes, curling or snarling of twisted yarns, creasing of fabrics, etc[60]. Improvement of mechanical properties often results from heat-setting.

Detailed studies on heat-setting of as-drawn multifilament yarns[61-63], in which the yarn is either held at constant length or left to shrink during heat setting at temperatures between 100 and 250°C, provided insight into how structural and morphological changes occur in the filaments. The oriented non-crystalline phase is predominant in the as-drawn PET filament and influences to a great extent its properties. The effects of heat-setting on the morphology of this filament are distinctly different in the different temperature regime. When the heat set temperature range is 100-180°C the parts of the oriented amorphous phase crystallize as a result of heat setting, forming small crystallites with sizes of same magnitude as the existing crystallites in the as-drawn fiber. These newly formed crystallites introduce more constraints that limit the mobility of the remaining amorphous phase, thus resulting in a rise of the glass transition temperature. When the heat-set temperature range is 180-250°C, crystallization occurs through transverse growth of existing crystallites and significant reorganization of the structure, which in addition to bringing about lateral order, also results in enhancement of longitudinal order. In this temperature range heat setting results in substantial improvement in crystal perfection with significant degree of chain folding; leading to small number of large crystals. Consequently, the constraints on the amorphous regions are reduced and the T_g of the heat-set filaments reduces as the heat-setting temperature increases from 180 to 250°C.

1.1.7.4 Effect of molecular orientation on crystallization of PET

The effect of chain orientation on the crystallization of PET has also attracted wide attention because of its relevance in polymer processing. In the presence of chain orientation, it has been shown that the rate of crystallization is strongly dependent on the degree of orientation and the key parameters being the initial orientation of the chains and the temperature of crystallization[64-69]. Orientation induced crystallization in PET is thought to be occurring through an intermediate phase called mesophase or transient phase[69,70]. Yeh and Gail observed paracrystalline order in quenched PET under electron microscopy[71,72]. Murthy et al suggested that short-range order, as evidenced by the occurrence of two different interchain distances, act as incipient crystals for further crystallization[73]. *In situ* monitoring of the development of structure using synchrotron radiation source further reinforced the existence of mesophase order just before the crystallization[55-57].

1.2 Structure and morphology of PET

The mechanical properties of polymers depend on their morphological structures. The structures of the polymer are so complicated that they have been the subject of much interest. It is quite obvious that polymeric materials may differ fundamentally in many important aspects according to the manner, in which the polymer is prepared, and it is well known that by varying the crystallization and processing conditions it is possible to obtain technologically significant variations in structure and mechanical properties. Many studies have therefore been carried out to establish relationships between the properties and morphological characteristics of polymers[74-78].

Extensive literature is published on morphology of PET at different conditions using various experimental techniques: transmission electron microscopy (TEM), differential scanning calorimetry (DSC), density measurements and x-ray diffraction at small (SAXS) and wide (WAXS) angles.

1.2.1 Crystal structure of PET

Upon crystallization, PET forms a triclinic unit cell[79] with a = 4.56 Å, *b* = 5.94 Å, c = 10.75 Å, α = 98.5°, β = 118°, and γ = 112°. Kitano et al[80] showed that extremely highly crystalline PET has shown different morphology compared to ordinary PET. They observed unit cell is smaller than that of ordinary PET. Highly crystalline material is proposed to consist of molecules which are either fully extended or which contain only a

few folds. This new crystalline specimen shows good double orientation without any treatment: the crystallites not only have their a axes parallel, but they also have their (001) planes approximately parallel to the main plane of the specimen. In highly crystalline PET specimen, there are only two directions of unit cell orientation and crystal growth in a particular direction is predominant, although usually for a triclinic unit cell there are four different orientations in a doubly oriented specimen. The structure determined from the intensity data is basically consistent with that obtained by Daubeny et al[79] although there are small differences between the atomic dimensional parameters. Different authors have intensively studied the crystal structure of PET[56,70,79,81,82] and unit cell parameters are reported elsewhere[83]. The variation in unit cell parameters is clearly not due to the experimental errors, but must be attributed, primarily to the variation in sample history. It has been reported that the unit cell parameters of PET crystals vary with crystallization temperature, draw ratio, and subsequent annealing temperature and time[63].

1.2.2 Effect of deformation and annealing on the morphology of the glassy amorphous PET

Zimmermann et al reported that stretching of semicrystalline PET caused changes in *d*-spacings of the (100) and (010) planes[84]. Porter et al observed that the lattice parameters of stress induced crystallites in PET are different from those in the closest packing[85]. However, PET can also form an amorphous glass. Bonart is the first scientist who reported the formation of a "paracrystalline" structure in PET induced by drawing[86]. He observed that the structure of PET changed during stretching of a totally amorphous sample, first forming a nematic phase and then a smectic phase. Here and below, we follow the terminology of the original authors to call these lattice distortions "paracrystalline" although it has been shown a long time ago that the paracrystalline model of disorder breaks down in more than one dimension[87]. Yeh and Geil pointed out that the quenched amorphous PET consisted of granule like structures in which molecules exhibited a paracrystalline order, based on their electron microscopic observation[71,72]. They argued that strain-induced crystallization could be explained by rotation, alignment, and perfection of the internal order of the paracrystalline granule like structure.

Balta Calleja et al investigated the structural changes during annealing of cold-drawn amorphous PET films by X-ray diffraction and microindentation techniques[88]. Their results revealed the appearance of a smectic order at 60°C having a spacing of 10.7 Å. The SAXS maxima observed at 70°C indicate that a density fluctuation of 110 Å appears as a

precursor before triclinic crystallization. From the SAXS pattern it is inferred that the layer structure is initially inclined about 62° from the draw direction. Triclinic crystal formation starts above 80°C, where the (010) planes are inclined by 10° from the draw direction. The crystallization mechanism from the smectic structure, via the precursor state, into the final triclinic crystal is explained by a tilting mechanism.

Recently, Blundell et al studied the in situ structural development of PET films during fast-drawing using synchrotron X-ray techniques[56,82]. Their results indicated a strong dependence of the crystallization rate on both temperature and molecular orientation. They also observed a highly oriented weak transient diffraction peak on the meridian prior to crystallization and identified it with the mesophase structure. They suggested that this transient structure is a precursor for strain-induced crystallization. Recently strain-induced crystallization of PET was investigated after an amorphous PET film was stretched to an extension of 100% below T_g using *in situ* synchrotron WAXD techniques by Ran et al[89]. Their results indicated that the mesophase developed immediately upon the neck formation. They concluded that strain-induced crystallization occurred mainly in the mesophase region, which supports the hypothesis that the mesophase acts as the precursor for strain-induced crystallization.

1.2.3 Effect of annealing on the melting behavior

The melting behaviour of PET has been investigated extensively[90-95]. Groennckx et al[90,91] studied isothermally crystallized PET and annealed PET. They explained double melting behavior of PET as follows. During isothermal crystallization only one melting temperature is observed at $T_c > 215$°C and $T_c < 150$°C. At intermediate crystallization temperature ($150 < T_c > 215$°C) two endotherms appears. Because the most stable crystalline structures are formed at the highest crystallization temperatures, it is concluded that the crystallites obtained at $T_c > 215$°C do not transform during scanning at 8°C/min. Part of the crystallites formed at lower T_c ($150 < T_c > 215$°C) can reorganize during heating in the DSC and thus melt at higher temperatures (endotherm II) than the unreorganized fraction (endotherm I); consequently two endotherms appear. The crystallites formed at $T_c < 150$°C completely transform at a DSC scanning rate 8°C/min and again one endotherm is observed. From the annealing data they concluded that the appearance of double melting endotherms does not necessarily imply a crystal thickening mechanism. An equilibrium melting point ($T°_m$) 290°C is obtained using Hoffmann's relationship between T_c and T_m[96]. They showed that the degree of crystallinity, the

morphological structure, and the melting temperature depend strongly on the crystallization temperature. The increase of melting temperature with crystallization temperature can be accounted for by an increase in lamellar thickness, fold-surface smoothening, and higher crystallite perfection. The influence of annealing conditions on the morphology and melting behavior of poly(ethy1ene terephthalate) (PET) is studied by Raheil[97,98]. They attributed the multiple melting behaviors to different types of crystals or to partial melting of crystals formed during heating and recrystalIization.

1.3 Solid state polymerization

Solid state polymerization (SSP) is one of the areas that holds high scientific and industrial interest because polymers with properties that are not obtainable by usual processes or which cannot be prepared by any other method can be synthesized. Studies on solid state polymerization suggest that the subject can be better discussed under two headings according to whether the starting materials are crystalline monomers or semi-crystalline pre-polymers[99]. In the first case the monomer is polymerized at a temperature lower than the melting point of both monomer and polymer. This method so far remains confined to laboratories where it is chiefly used to obtain highly oriented polymers. In the latter case, the polymerization is carried out on low or medium molecular weight semi-crystalline pre-polymers at a temperature below the melting point of the pre-polymer. This method has received considerable industrial attention because of the high quality polymers obtained by this process.

1.3.1 Solid state polymerization of PET

The poly(ethylene terephthalate) (PET) resin obtained by the standard synthetic routes (melt process) generally has an average molecular weight of 15000-20000 kg/kmol and an intrinsic viscosity (η) of 0.55-0.65 dL/g, which is unsuitable for molding application (η = 0.72-0.85 dL/g) or high-strength fibers (η = 0.95-1.05 dL/g). The solid state polymerization (SSP) process is the only feasible way to obtain such high molecular weight of PET and also of other step-growth polymers such as poly(trimethylene terephthalate) (PTT), poly(butylene terephthalate) (PBT), poly(ethylene naphthalate) (PEN), and nylon 6,6. In fact, the melt viscosity during the melt-phase polymerization increases rapidly with the molecular weight, reaching prohibitively high values in the final stages. Higher temperatures could effectively reduce the melt viscosities, but undesired degradation side reactions would also take place. In the SSP process the polycondensation

reactions continue within solid pellets, 2-3-mm-long extruded particles, initially heated in a dedicated unit (preheater) to 200-230°C well above the PET glass transition temperature ($T_{g,\ PET}$ = 78-80°C) but appreciably below the PET melting ($T_{m,\ PET}$ = 257-263°C) and sticking (*T*s, $_{PET}$ = 245°C) temperatures. This temperature is high enough to activate the terminal ester linkages, so that interchange reactions between the hydroxyl groups of one PET molecule and the adjacent terminal linkage of another molecule can still take place. In this reaction ethylene glycol will go off and the number average molecular weight is increased[100]. Only by SSP, it is possible to obtain PET free of DEG[101]. It is known that DEG content strongly affects PET structure and properties[102-104].

The mechanism of the SSP can be summarized as consisting of the following three stages: (1) diffusion of the polymer chains and reaction of the corresponding end groups (reaction step)[100,105-111], (2) diffusion of the byproducts (water and ethylene glycol) through the polymer matrix (internal diffusion step) to the surface[111-116], and then finally the (3) diffusion of these byproducts from the surface to the gas bulk (interphase diffusion step)[100,105,117]. Polycondensation reactions are reversible, and therefore, the removal of the byproducts plays a key role in shifting the equilibrium to the right direction. The forward reactions are facilitated by the byproduct removal either by flow of inert gas or by maintaining reduced pressure, or a combination of the two[118,119]. Recently, there has been a growing interest in applying microwave heating to synthetic polymer technology. Microwave irradiation produces heat, which is generated in the material itself, instead of using external heating. Mallon et al and Yoo et al reported that SSP rates could be enhanced by using microwave irradiation[120,121]. Theoretical analysis and experimental evidence show that the increase in SSP rate is not due to an increase in bulk temperature. Instead, the effect is consistent with directed heating of the condensates leading to enhanced diffusion rates.

Transesterification/Polycondensation

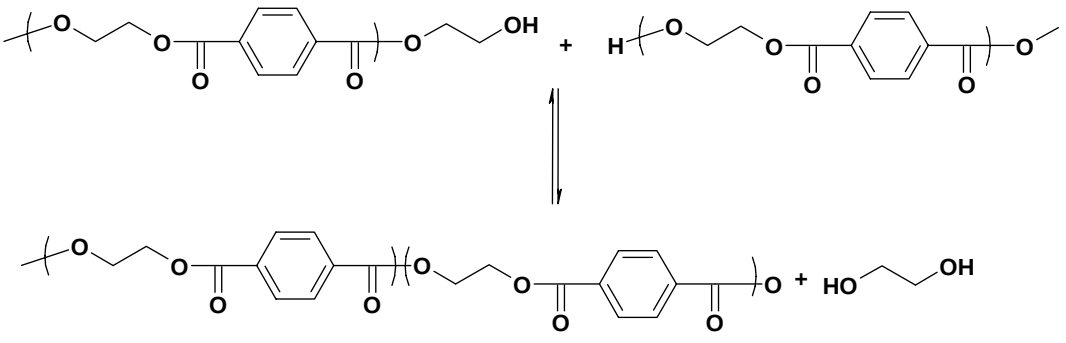

Esterification

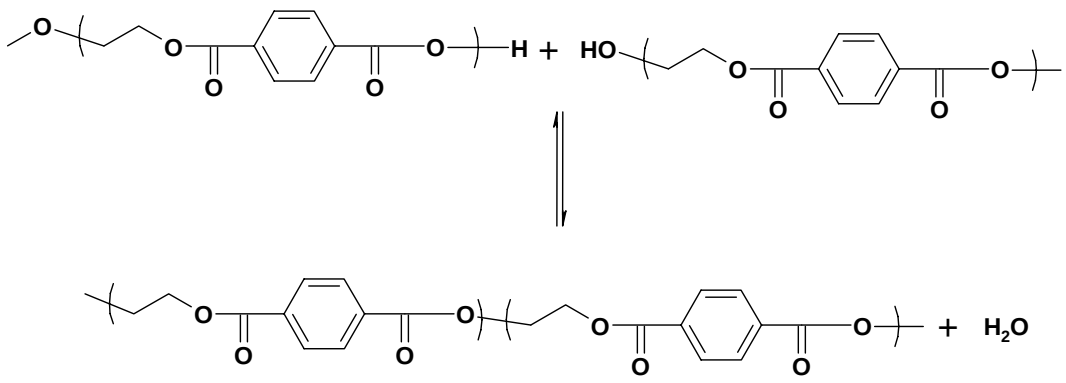

Scheme 1: Transesterification and esterification reactions in PET

1.3.2 Ultrahigh molecular weight PET by SSP

PET having IV ~ 0.15 – 1.0 dL/g is very commonly available. Very high molecular weight PET (IV as high as 3 dL/g) can also achieved by SSP. The table 1.3 summarizes the reports describing SSP of PET to IV higher than 1.5 dL/g or M_n higher than 70,000. Ultrahigh molecular weight PET is also obtained by swollen state polymerization in specific diluents under bubbling nitrogen gas at atmosphere pressure[122-124]. Suitable diluents are those, which can swell PET but not dissolve it. Diluents having a solubility parameter similar to PET are desirable for attaining higher ultimate molecular weight at the same polymerization temperature. The material obtained by swollen state polymerization showed honeycomb like structure.

Major factors influencing the SSP rate include the catalyst (type and concentration)[125, 126], temperature[100,112,127,138,139], particle size[100,112,138-141], crystallinity level [105,138,139,142,143], nature and rate of carrier gas[100,105,114,115,139,144], molecular weight of starting material[145] and concentration of carboxyl end groups or carboxyl content[146,147]. Kinetics and mechanisms[101,109,120,148-150] of PET SSP is discussed in detail in the literature.

1.3.3 Structure and morphology changes during solid state polymerization for homopolymers

Understanding the structure and morphology of the SSP precursors (prepolymer) and the morphology changes during the SSP is important for both scientific and practical reasons. Even though the general characteristics of SSP of PET are well known, there have not been many reports on morphological analysis of the main variables involved in the process of polymerization.

Table 1.3: SSP of PET to ultrahigh molecular weight

Sl No.	Authors	Characteristics of initial PET	SSP conditions	Final M_n or IV (dL/g)
1	Hsu[100]	0.18 – 0.25 mm particle M_n = 16,500	250°C, 40 h, N_2 ~ 2cm/s	M_n = 120,000 IV = 2.27
2	Kurita[128]	Standard chips IV = 0.6	237°C, 12 h, N_2	IV = 3.42
3	Cohn[129,130]	Porous fibrous pellet, IV = 1.9	220-240°C, 10 h, N_2	IV = 5.3
4	Rinehart[131]	Porous pills made by compacting 0.84 mm particles, IV = 0.5	250°C, 5 h, N_2	IV = 2.39
5	Ito et al[132]	Solution grown crystals, 2 – 10 μm, IV = 0.67	253°C, 24 h, vacuum	IV = 2.41
6	Ito et al [133,134]	Porous and fibrous aggregates IV = 0.61	240°C, 12 h, vacuum (10 mtorr)	IV = 3.2, up to 4.9 in multiple steps
7	Sasaki et al. [135]	Film, 0.01 mm, IV = 0.15	320°C (melt), 1.5 min, vacuum (0.5 torr)	IV = 2.31
8	Boiko and Marikhin[136]	100 μm film, M_n = 15,000	250°C, 20 h, vacuum (0.05 mtorr)	M_n = 151,680
9	Ma et al[137]	180 μm thick PET chips, IV = 0.5	250°C, 6 h, vacuum (10 mtorr)	IV = 2.75

It is generally accepted that the solid state condensation reactions take place in the amorphous regions[143, 151, 152]. So far this assumption is valid; the crystallinity of the starting polymer or oligomer should have a strong effect on the reaction rate.

For the starting semi-crystalline poly-condensate, there are two possible effects on the reaction rate. Firstly, the crystalline phase, as such, restricts chain mobility and diffusivity and so reduces the reaction rate. On the other hand, as the end groups are concentrated in the amorphous regions, a higher reaction rate may be expected. A further advantage of the use of semi-crystalline polymer as the starting material is that polymer particles do not agglomerate in the reactor[151]. In conventional SSP the prepolymer has a typical inherent

viscosity of 0.6 dL/g[153-159]. PET prepolymer in the form of chips or pellets have to undergo a crystallization process prior to solid state polymerization[160] and the pellets are crystallized at 180^{o}C for more than 1 h. The SSP is performed at 210^{o}C for about 15 h. However, crystallization and the morphology of the high molecular weight PET precursors is different from the oligomers having [η] ~0.1-0.2 dL/g. Recently the process of preparing high molecular weight PET[160,161] from crystallized oligomers having [η] ~0.2 dL/g is developed. In these processes oligomers are initially crystallized at temperatures where its crystallization rate is maximum and the SSP is performed at temperatures close to melting point. The salient feature of the process is that the sample is brought to crystallization temperature very rapidly (called shock crystallization). This has been achieved either by bringing the amorphous pellet in a preheated oven at about 500^{o}C or dropping melt extruded sample on a preheated turn table kept at about 175^{o}C. Also these samples have high carboxyl group content (~200 ppm). The crystallized samples show large crystal size of about 12 nm.

James et al[152] used crystallized oligomers of PET and PEN having [η] ~ 0.2 dL/g as prepolymers for SSP to understand the effect of crystallization and morphology on the SSP rate. Crystallization of the oligomers is found to be very rapid and is completed within a minute. The crystallized oligomers show very well defined diffraction patterns with large crystal sizes. The DSC thermograms show no premelting endotherms in these samples and the presence of it would indicate small or imperfect crystallites, which might cause sticking during SSP[160]. The crystallinity and crystal size achieved in these samples during the crystallization process are higher when compared with the crystallinity and the crystal size obtained in a typical high molecular weight PET (40%, 5 nm)[92].

The crystallization results indicate that the catalyst plays an important role in the crystallization of oligomeric PET. The oligomer containing $Ti(O^{i}Pr)_4$ has the lowest crystallization rate. The lower crystallization rate in the case of $Ti(O^{i}Pr)_4$ has been attributed to the extensive interactions of PET terminal groups with the catalyst[162] which increases the apparent molecular weight. Because of the low crystallization rate, the sample could be quenched into fully amorphous material, while the samples containing Sb_2O_3 could not be quenched into fully amorphous state. Though the crystallization rate is lower for the sample with $Ti(O^{i}Pr)_4$, the crystallinity and the crystal size achieved are comparable to the other samples. Carboxyl end group concentration does not affect the crystallization rate of these oligomers. This is evident from the observation that oligomers

having very high carboxyl end group also have T_{cc} similar to the oligomers with lower carboxyl end group. Pilati et al[162] also suggest that carboxyl content plays a significant role in controlling T_{cc} of high molecular weight PET but not in oligomers. From these results it is apparent that with increase in viscosity, T_{cc} will decrease indicating a reduction in crystallization rates.

The structure and morphology of the PET can be inferred from the WAXS, SAXS and DSC studies on pre SSP and post SSP samples of oligomer prepared with $Ti(O^iPr)_4$. The WAXS patterns do not show any obvious difference, indicating that there is no significant change in crystallinity or crystal size during SSP. However the long period showed a small increase during SSP. The lamellar thickness also exhibits marginal increase. These results indicate that the crystalline regions do not undergo major structural reorganization during SSP. However, DSC data shows an increase in melting point after SSP and this could be attributed to the smoothening of the lamellar surface[91]. It is worthwhile to note that the lamellar thickness is about 7.1 nm, while the length of the fully extended oligomer chain is about 12 nm (degree of polymerization is 12 and extended length of the monomer[163] is 1.07 nm). Hence the possibility of chain folding is less and the chain ends are outside the crystals. The large crystal width also indicates that the chain ends are excluded from the lattice and reside in the amorphous phase. Miyagi and Wunderlich[164] produced similar oligomer crystals by etching folded chain PET crystals. During SSP, the chains grow *via* the reaction between the molecules that further remove chains in the same or different lamella or with the chains from the adjacent lamella and this leads to more tie molecules. The presence of tie molecules is indicated by the super heating of the crystals at higher heating rate in DSC experiments[165]. A super heating of 5^oC is observed for a heating rate of 50^oC/minute for sample with $Ti(O^iPr)_4$ and is in agreement with the data reported by Miyagi and Wunderlich. Based on the data, a structural model is proposed and is shown in figure 1.3 for pre and post SSP samples. The rapid increase in η_{inh}, during the initial stages of SSP could be due to the availability of large number of end groups in the amorphous phase. With progress in time, the chains grow and entanglements increase. This increase in entanglement as well as decrease in the end group concentration could retard the rate of SSP during the later stages of SSP.

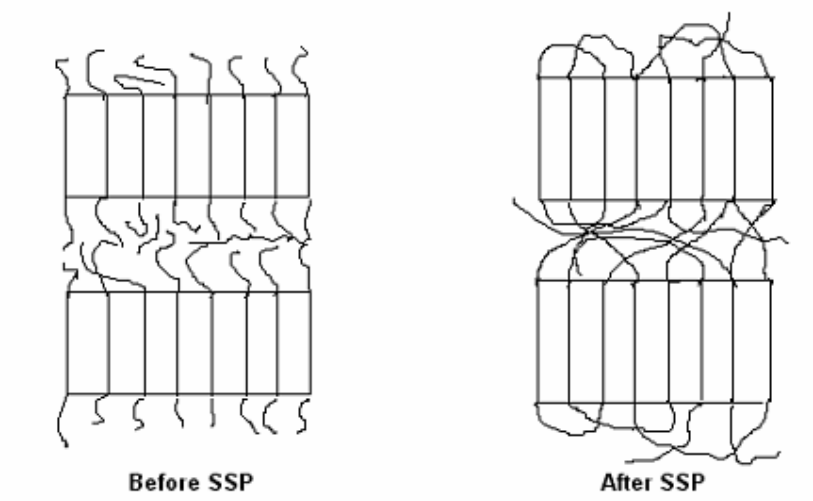

Figure 1.3: Proposed structural model for PET before and after SSP

Desimone et al[151,165] studied crystallization and SSP of polycarbonate using supercritical CO_2. They showed that supercritical CO_2 induces the crystallinity in polycarbonate and also enhances the SSP rates. The amorphous polycarbonate beads with an Mw of 2500 are exposed to supercritical CO_2 and are rendered 19% crystalline with a T_m of 197°C. There is no chain extension during crystallization. As the polymerization proceeded, the samples became progressively more crystalline and additionally, the T_m increased significantly with time. An increase in crystallinity with chain extension during solid-state polymerization has been observed by Sivaram et al[166,167]. This phenomena is explained by the fact that the polymer is greatly reorganized in the solid phase, leading to the development of more perfect crystallites[168]. The observed change in rate is a composite of a number of effects including the increase in reaction temperature and polymer crystallinity along with a decrease in end group concentration. The role of polymer crystallinity is 2-fold. An increase in polymer crystallinity should concentrate the end groups in the amorphous regions of the polymer, leading to an increased reaction rate. However, the increase in crystallinity with time should decrease the rate of diffusion of phenol, which may limit the molecular weight that can be achieved in a given time.

Chang et al[139] showed that in SSP, preheat process not only promotes the molecular weight of prepolymer, but, more importantly, it increases the crystallinity of prepolymer. Higher crystallinity materials have sharper melting points and higher sticking points. Then reaction can occur at higher temperatures to enhance the reaction rate. However, the reaction rate is not always increased; because the high crystallinity inhibits the diffusion of byproducts.

Rodriguez et al[143] studied the effect of precursor crystallinity on the SSP of PET. The SSP process demands the molecular ends to collide for the reaction to occur. Therefore, and considering the lack of molecular mobility associated with the polymerization process itself, the only way to promote this interaction is through morphological variables of the precursors such as crystallinity. The previous results are, therefore, correlated with a morphological variable (crystallinity) to explain the observed results. They reported that for the purpose of obtaining a large increase in molecular weight, high crystallinity in precursors are required. This is contrary to suggestions given by Chang et al[139] and Karayannidis et al[169] who concluded that because of the high crystallinity present, there would not be a high increase in molecular weight after SSP. Understanding these effects is complicated because of the thermal treatments involved. However it has been explained as follows. It is considered that the macromolecular chain ends have to meet first before getting bound together. As a consequence, any source of molecular orientation will help the process. This can be found in a lamellar-stacked system. Low average molecular weights develop either thicker or more perfect crystals (i.e., those with a higher melting point). Thick crystals originate as a consequence of a higher probability of segmental orientation in the thin amorphous portion of the lamellar-stacked system. On the contrary, high molecular weights give rise to thinner or more imperfect crystals or to a stacked system with thicker amorphous portions that overall decrease the average orientation of chain ends. In this last case, a lower increase in molecular weight could be expected in agreement with the results mentioned before.

1.4 Synthesis of copolymers

1.4.1 Melt blending

It is common for polymer chemists to attempt to use blends of known polymers as new materials, rather than design and synthesize a totally novel polymer. This has the advantage of being much cheaper, quicker and the physical properties of a blend of known polymers can be easier to predict than the properties of a completely new polymer.

In the 1970's and 80's a series of papers are produced documenting the results of miscibility tests carried out on various pairs of polymers[170-176]. Some of the common polymer blends are polyesters (PET, PBT, PEN) with other polyesters and polyesters with polycarbonates (PC). There are initial differences in opinion as to whether these blends are compatible. PET and PC are also fully miscible when the blend is more than 70% PC[172,173], and this conclusion is supported by Linder and coworkers[174] Chen and co-

workers concluded that the PET/PC system is immiscible over the entire composition range[175] and this is then backed up by Hanrahan et al[176]. These discrepancies are explained by the realization that the longer one mixed the two in the molten state, the more compatible they became, indicating that there is a reaction going on between the two polymers. Glass transition temperatures (T_g) would merge together and melting points (T_m) would shift and/or disappear altogether[177]. This is shown to be the result of the copolymerization reaction between the polyester and polyester/polycarbonate, a reaction known as transesterification. Since this discovery many papers and patents have been produced on the subject, explaining the mechanism and kinetics of several blends[178-181]. This indicates the high levels of industrial and academic interest in transesterification. This interest stems from the fact that transesterification can provide novel materials with varying degrees of randomness, composition and physical properties from well known and well documented materials. The product obtained will be a copolymer of the two monomers present, and the properties of this product will be a mixture of the properties of the two initial homopolymers. Transesterification is also a good way to compatibilize two immiscible polymers.

However, when the transesterification between the two polymers reaches very high levels, the crystallinity and resultant physical properties of the blends can be reduced[182]. Thus it is important to control the transesterification in order to obtain products with desirable properties. The optimum degree of transesterification is ~ 25-35%. Transesterification reactions occur rapidly in the melt, as reported by Stewart et al[183]. For example, a PET/PEN blend containing 50 wt % PET mixed at 305°C in an extruder resulted in transesterification levels of 7.8%, 20.2% and 26.6% for reaction times of approximately 1.5 min., 3 min. and 4.5 min. respectively. The film of the blend is hazy with 7.8% transesterification but clear at the higher levels of transesterification. However, controlling the transesterification level between about 10 and about 20% is difficult and blends with levels of transesterification greater than about 30% start to behave like random copolymers. Degree of transesterification is a function of temperature, mixing/copolmerization time, catalyst/residual catalyst, composition of the blend[178,184-186]. Transesterification reactions can be controlled by solid state polymerization of polymer blends.

1.4.2 Solid state polymerization

Very limited literature has been published on the synthesis of copolyesters by solid state polymerization. In 1992 Cox et al[187] produced a copolymer of PET and PEN by solid state polymerization. They found that transesterification can also occur during solid state operation where melt blended, crystallized blend is held at temperature below the melting point and subjected to an inert gas flow to increase the inherent viscosity (IV). In this patent degree of transesterification is controlled by the addition of a phosphorous stabilizer.

Hoffmann et al[188] found that blends of PET and PEN with low levels of transesterification from the melt (immiscible blends) can be polymerized in the solid state to produce blends with higher levels of transesterification, higher inherent viscosities (IV's), lower acetaldehyde (AA) levels and improved color than the blends which are transesterified in a melt extruder. When the solid state polymerized blends are remelted and processed into articles, the resultant articles are clear, have lower AA levels and improved color than clear blends prepared via conventional melt blending. The process eliminates the need for multiple extruders passes, additional handling steps and can be readily implemented in a continuous manufacturing system.

However, in the earlier studies blends of high molecular weight samples are used as precursors (IV~ 0.6 dL/g) for solid state polymerization. Sivaram et al[189,190] synthesized poly(ethylene terephthalate-*co*-bisphenol A carbonate) by ester-carbonate interchange reaction in the solid state using PET/PC oligomer blend (IV~ 0.15 dL/g) as SSP precursors. Oligomers are solution blended and crystallized by refluxing for 4h in acetone induce sufficient crystallinity to enable their polymerization in the solid state. The solid state polymerization of PC-PET oligomer mixtures is performed at atmospheric pressure under a flow of nitrogen in the temperature range 180–230°C for 15 h. It is evident that the polymerization reaction proceeds in the solid state with a steady increase in molecular weight.

It is well known that several exchange reactions can take place (*via* intra or intermolecular reactions) during melt mixing of PC and PET[170,191,192]. Hait et al[189,190] show that many of the exchange reactions previously reported during the melt blending of PET and PC also occur in the solid state at temperatures below 240°C. The most important reactions, which occur, are shown in Scheme 1. Reactions 5–7 occur at a relatively higher rate in the melt compared to the others. In solid state, as the hydroxyl groups are the active species;

reactions 1 and 2 are the most probable reactions along with reactions 5–7. Reactions 3 and 4 cannot take place, as it is reported[192] that, with the increase in carboxyl group concentration, the rate of solid state reaction decreases. From the ^{1}H NMR the formation of ether confirms that reaction 8 also occurs during the reaction.

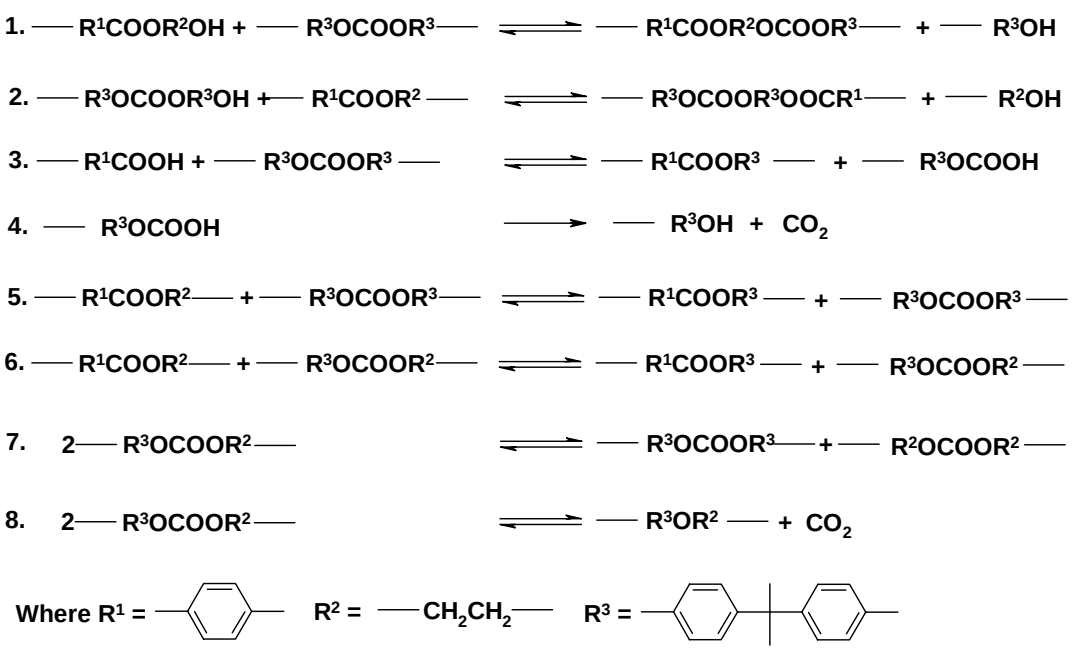

Scheme1.2: Most important reactions, which occur during, melt mixing of PET and PC

Nirmala et al[194] studied the simultaneous solid state and exchange reactions in PET/PEN oligomers. The semicrystalline blends of PET and PEN oligomers are prepared by melt mixing PET and PEN oligomers and then allowed to fall onto a hot plate, which is maintained at a constant temperature of 175°C. Hemispherical particles are formed upon the hot plate that underwent crystallization at 175°C. The residence time in the extruder is less than 2 min. to minimize the transesterification in the extruder.

Crystallized oligomer blends are subjected to SSP at 220°C for 20 h in a nitrogen flow of 3 L/min. It is apparent from the results that the majority of changes in the structure occur during the first two hours of reaction, subsequent to which there are only marginal changes. During initial stages of SSP, the percentage transesterification and degree of randomness increases while the average sequence length decreases. This indicates that the transesterification reactions are active during the initial stages of SSP. If the progress of SSP and transesterification is compared, the results indicate that transesterification reactions are less active after 2 h of SSP. On the other hand, η_{inh} keeps on increasing

monotonically during SSP, albeit, at a reduced rate after 2 to 3 h. So, along with transesterification the chain ends react leading to an increase in molecular weight. A comparison of increase in transesterification and viscosity during reaction indicates that SSP favors reactions predominantly among chain ends.

Neil et al[195] reported a method of making block copolycarbonates by solid state polymerization. A mixture of a partially crystallized polycarbonate having activated terminal aryloxy groups, for example terminal Me salicyl groups, when heated together with an oligomeric polyester having reactive terminal hydroxy groups under solid state polymerization conditions gives block copolymers.

The synthesis of catenane-containing polycarbonates, the first mechanically linked analogues of a commercial polymer, has been achieved by solid-state copolymerization by Fustin et al[196,197]. This method, involving solution blending of the comonomers, crystallization of the blend, and prolonged heating under vacuum, has been shown to quantitatively incorporate the catenane into bisphenol A polycarbonate. The unexpectedly small influence of the catenane on T_g is suggestive of considerable internal mobility/flexibility of the catenane, certainly when compared to the strong influence of very rigid comonomers such as fluorene bisphenol. These studies are the first examples of the effects on structure and properties of incorporating mechanical linkages into a polymer backbone.

1.4.3 Structure and morphology of copolymers by melt blending

The blends of condensation polymers are of particular interest because of their unique ability to undergo interchange reactions[198]. It is generally accepted that, as a result of direct ester-ester interchange reactions, the blend of homopolymers transforms into block copolymers which subsequently turns into a random copolymer as block lengths gradually decrease[199]. Hanna et al discuss the order in random copolymers and its influence upon their crystallization ability[200].

1. In polymer blends comprising at least one crystallizable component, the transreactions lead to a formation of copolymer chains in which two or more different types of chemical units are joined in a random sequence. Such chains are unable to fully contribute to the three-dimensional periodicity of a crystal lattice. As a consequence, one has to predict amorphisation of blends in which transreactions are possible leading to a high degree of randomization, which is practically observed by Kimura et al for PET/polyarylate copolymers[201].

2. Alternately[200] copolymers containing units of crystallizable polymers, can show a certain crystallization ability even at very high degree of randomness. The authors prove this idea by means of computer models of systems of random copolymer chains. It is thereby demonstrated that there is a probability for certain proportions of similar units, exceeding a given length, to segregate and form rather perfect albeit small and isolated crystals. Also it is found possible for identical but random sequences to segregate creating lateral order in unit with no periodicity in the direction of the chain axis.

1.4.4 Co-crystallization in copolymers

Cocrystallization behavior in copolymers whose component homopolymers are both crystalline is a rare phenomenon. Only a few systems including poly(3-hydroxybutyrate-*co*-3-hydroxyvalerate) (P(3HB-*co*-3HV)) copolymers[205-210] have been reported to show cocrystallization which is manifested by the presence of a clear melting temperature over the entire range of composition. Cocrystallization is divided into two groups, i.e., isomorphism and isodimorphism. When two components have the similar chemical structure and thus occupy approximately the same volume, the excess free energy of cocrystallizaion would be very small, and therefore the chain conformation of both corresponding homopolymers becomes compatible with either crystal lattice, so called isomorphism[211]. As a result, only one crystalline phase containing both comonomer units is detected at all compositions. On the other hand, copolymers may show isodimorphism where two crystalline phases, each of which contains comonomer units as a minor component, are observed. In this case, an increase in the content of the minor component in each crystalline phase is accompanied by a lowering of the melting and crystallization temperatures. In this case, a melting point minimum is observed in the plot of melting point versus copolymer composition.

The co-crystallization behavior can be divided into three types depending on the chemical structure of the A and B comonomeric units.

A). Crystallization of A or B units takes place either in an A-polymer or a B-polymer crystal with complete rejection of the comonomer units from the crystals, exhibiting the crystal lattice transition from the A-crystal to the B-crystal at some intermediate copolymer composition.

B). A units can crystallize with complete rejection of the B units from the crystals, whereas B units can co-crystallize with incorporation of A units to some extent, depending on the copolymer composition. In both (i) and (ii) the T_m is dependent on the copolymer composition and exhibits a minimum (eutectic point) at some intermediate composition at which the crystal lattice transition is usually observed.

C). A and B units can co-crystallize into a single crystal structure (copolymer isomorphism) over the full range of copolymer composition, exhibiting a continuous change in the lattice parameters from the A-crystal to the B-crystal and in the melting temperatures without reaching a minimum point.

The crystallization behavior in random copolymers is controlled by local crystallization due to fractionation of the crystallizable sequences. The short parts of the crystallizable sequences cannot be involved in crystallization but the longer parts are capable of undergoing crystallization. The crystallizability of each comonomer unit may be a function of the crystallizable sequence distribution, the cohesive energy of molecules, the molecular mobility and the surface free energy of the crystal such as the end and lateral crystal surface energies. All of these parameters should be dependent on the copolymer composition. The crystallization behavior of a random copolymer system is strongly influenced by copolymer sequence distribution. A small variation in the chemical structure brings about considerable changes in the crystallization behaviour.

Okui et al[205] have studied the crystallization behavior of poly(ethylene terephthalate-co-1,4-cyclohexylenedimethylene terephthalate) P(ET/CT) random copolyesters. The copolyesters rich in ET units form crystals with complete rejection of the CT units, whereas CT units can co-crystallize with ET units to some extent in the composition region rich in CT units. The T_m of these copolymers are depressed with an increase in CT in the compositions and show a minimum at the intermediate composition of about 30-40 mol% CT at which the crystal lattice transition occurred.

Baozhong Li et al[212,213] have studied the crystallization behavior of poly(ethylene terephthalate-co-isophthalate) PET/PEI random copolyesters with different molar ratios. With increasing PEI, the copolyesters become less crystallizable and even amorphous when the composition of PEI is above 20%. The WAXD profiles of the crystallizable copolyesters shows that the crystals come from PET homopolymers. The crystallinities of

the crystallizable copolyester become lower and crystals grow imperfectly when the composition of PEI increases.

1.4.5 Structure and morphology of copolymers by solid state polymerization

It is generally accepted that interchain reactions will take place only in amorphous polymers or in the amorphous part of semicrystalline polymers. Even if exchange reactions occur in crystallites[214-216] they take place only in crystal defects. Nirmala et al synthesized PET/PEN copolymers by solid state polymerization. NMR results indicate that the degree of randomness is always below unity, indicating the presence of blocks of homopolymer chains. The invariance in WAXD pattern and DSC data indicate that the SSP and transesterification take place in the amorphous phase while crystalline phase remains unaltered.

Reorganization of the copolymer structures in the solid state has also been reported in the literature[217-222]. Lenz and Go demonstrated the conversion of a random copolymer into block copolymers for materials annealed at temperatures lower than the melting points of the corresponding homopolymers. The driving force for sequence reorganization and block copolymer formation is the crystallization of at least one of the two kinds of blocks. The reactions of this kind have been classified as crystallization induced reactions.

1.5 References

1. Tashiro K, Nakai Y. Macromolecules 1980; 13: 137.
2. Siesler HW. J. Polym. Sci., Polym. Chem. 1979; 17: 453.
3. Stambaugh B, Koenig JL, Lando JB. J. Polym. Sci., Polym. Phys. 1979; 17: 1053.
4. Ward IM, Wilding MA. Polymer 1977; 18: 327.
5. Jakeways R. J. Polym. Sci. Poly. Lett. Ed. 1976; 14: 41.
6. Coleman MM, Painter PC. J. Macromol. Sci. Rev. Macromol. Chem. Part C 1977; C16: 197.
7. Escala A, Balizer E, Stein RS. Polym. Prepr. Am. Chem. Soc. Div. Polym. Chem. 1978; 19: 152.
8. Edelman K, Wyden H. Kautsch. Gummi Kunstst., 1972; 25: 353.
9. Muzzy JD, Bright DG, Hoyos GH. Polym. Eng. Sci., 1979; 18: 107.
10. Chang EP, Kirsten RO, Slagowski EL. Polym. Eng. Sci. 1978; 18: 932.
11. a) Jabarin SA, Polym. Eng. Sci. 1982; 22:815. b) Lin CC. Polym. Eng. Sci. 1983; 23: 113.

12. Lee SW, Ree M, Park CE, Jung YK, Park CS, Jin YS, Bae DC. Polymer 1999; 40: 7137.
13. Whinfield JR, Dickson JT. US Patent 1949; 2,465,319.
14. Wunderlich, B. Prog. Polym. Sci. 2003; 28: 383.
15. Katti SS, Schultz JM. Polym. Eng. Sci. 198; 222: 1001.
16. Hsiung C, TRIP 1996; 4: 342.
17. Janeshitz H, Fleischmann E, Geymayer W. Polypropylene, Structure, Blends and Composites, De. J. Karger-Kocsis, Chapman & Hall, 1995
18. Cormia RL, Price FP, Turnbull D. J. Chem. Phys., 1962; 37: 1333.
19. Gornick F, Ross GS, Frlen LJ. J. Polym. Sci., Part C 1967; 18: 79.
20. Ross GS, Frolen LJ. J. Res. Natl. Bur. Stand. 1975; 79A: 701.
21. Barham PJ, Jarvis DA, Keller A. J. Polym. Sci., Polym. Phys. Ed. 1982; 20: 1733.
22. Barham PJ. J. Mater. Sci. 1984; 19: 3826.
23. Binsbergen FL. J. Polym. Sci., Polym. Phys. Ed. 1930; 11: 253.
24. Chatterijee AM, Price FP. J. Polym. Sci., Polym. Phys. Ed. 1975; 13: 2369.
25. Misra A, Garg SN. J. Polym. Sci. Polym. Phys. 1986; 24: 983.
26. Sakaguchi Y. Curr. Trend in Polym. Sci. 1996; 1: 157.
27. Van Bennekom ACM, Gaymans RJ, Polymer 1997; 38: 657.
28. Bouma GDW, Lohmeijer JHGM, Gaymans RJ. Polymer 2000; 41: 3965.
29. Bouma K, Gaymans RJ. Polym. Engg. Sci. 2001; 41: 466.
30. Agarwal S, de Wit G, Lemstra PJ. Polymer 2002; 43: 5709.
31. Bier P, Binsack R, Vernaleken H, Rempel D, Die Angew. Makromol. Chem. 1977; 65: 1
32. a) Nield E, US Patent 4,322,335; 1982 b) Jackson JB, Longman GW. Polymer 1969; 10: 873
33. Eisenbach CD, Stadler E, Enkelmann V. Macromol. Chem. Phys. 1995; 196: 833.
34. Frank WP, Zachmann HG. Progr. Colloid Polym. Sci. 1977; 62: 88.
35. Farikov S, Seganov I, Schultz JM. J. Appl. Polym. sci. 1986; 32: 3371.
36. Golike RC, Cobbs WH. J. Polym. Sci. Polym. Phys. Eds. 1961; 54: 277.
37. Jackson JB, Longman GW. Polymer 1969; 10: 873.
38. Van Krevelen DW. Properties of Polymers, 3rd ed.; Elsevier: Amsterdam, 1990
39. Manuel HJ, Gaymans RJ. Polymer 1993; 34: 636.
40. Bouma K, Regelink M, Gaymans RJ. J. Appl.Polym. sci. 2001; 80: 2676.
41. Asano T, Dzeick-Pickuth A, Zachmann HG. J. Mater. Sci. 1989; 24: 1967.

42. Roland CM. Polym. Eng. Sci. 1991; 31: 849.
43. Xue G, Ji G, Yan H, Guo M. Macromolecules 1998; 31: 7706
44. Xue G, Ji G, Li Y. J. Polym. Sci. Part B. Polym. Phys. 1998; 36: 1219.
45. Moore WR, Sheldon RP. Polymer 1961; 2: 315.
46. Lawton EL, Cates DM. J. Appl.Polym. sci., 1969; 13: 899.
47. Desai AB, Wilkes GL. J. Polym. Sci. Polym. Symp. 1974; 46: 291.
48. Markarewicz PJ, Wilkes GL. J. Polym. Sci. Polym. Phys. Ed. 1978; 16: 1529.
49. Billovits GF, Durning CJ. Polymer 1988; 29: 1468.
50. Im SS, Lee HS. J. Appl. Polym. Sci. 1989; 37: 1801.
51. Wei KY, Cuculo JA. J. Polym. Sci., Polym, Phys. Ed. 1980; 18: 343.
52. Phillips PJ. Macromolecules 1989; 22: 1649.
53. Siegmann A, Harget PJ. Bull. Am. Phys. Soc. 1973; 346: 1118.
54. Encyclopedia of polym. Sci. Engg. 1987; 10: 595.
55. Mahendrasingam A, Martin C, Fuller W, Blundell DJ, Oldman RJ, MacKerron DH, Harvie JL, Riekel C. Polymer 1999; 41: 1217.
56. Blundell DJ, Mahendrasingam A, Martin C, Fuller W, MacKerron DH, Harvie JL, Oldman RJ, Riekel C. Polymer 2000; 41: 7793.
57. Keum JK, Kim J, Lee SM, Song HH, Son YK, Choi JI, Im SS. Macromolecules 2003; 36: 9873.
58. Huisman R, Heuvel HM. J. Appl. Polym. Sci. 1989; 37: 595.
59. Brody H. J Macromol. Sci. Phys. 1983; B22: 407.
60. Gupta VB, Radhakrishnan J, Sett SK. J. Appl. Polym. Sci. 1995; 55: 247.
61. Gupta VB, Kumar S, J. Appl. Polym. Sci. 1981; 26: 1865.
62. Gupta VB, Ramesh C, Gupta AK. J. Appl. Polym. Sci. 1981; 29: 3115.
63. Ramesh C, Gupta VB, Radhakrishnan J. J. Macromol Sci Phys. 1997; B36: 281.
64. Smith FS, Steward RD. Polymer 1974; 16: 283.
65. Gupte KM, Motz H, Schultz JM. J. Polym. Sci. Polym. Phys. Ed. 1983; 21: 1927.
66. Althen G, Zachman HG. Makromol. Chem. 1979; 180: 2723.
67. Alfonso GC, Verdona MP, Wasiak A. Polymer 1978; 19: 711.
68. Sun T, Pereira JRC, Porter RS. J. Polym. Sci. Polym. Phys. Ed. 1984; 22: 1163.
69. Bonart R. Kolloid-Z 1966; 213: 16.
70. Asano T, Seto T. Polym. J. 1973; 5: 72.
71. Yeh GSY, Geil PH. J. Macromol. Sci. Part B 1967; 1: 235.
72. Yeh GSY, Geil PH. J. Macromol. Sci. Part B 1967; 1: 251.

73. Murthy NS, Correale ST, Minor H. Macromolecules 1991; 24: 1185.
74. Ward IM. Mechanical Properties of Solid Polymers, Interscience, New York, 1971.
75. Samuels RJ. J. Polym. Sci. (A-2) 1972; 10: 781.
76. Prevorsek DC, Kwon YD, Sharma RK. J. Mater. Sci. 1977; 12: 2310.
77. Schulz JM, Fakirov S. 'Solid State Behavior of Linear Polyesters and Polyamides, Prentice-Hall, Englewood Cliffs, NJ, 1990.
78. Dosiere M. Crystallization of Polymers, Kluwer, Dordrecht, 1992
79. Daubery RD, Bunn CW, Brown C. J. Proc. R. Soc, London, Ser. A 1954; 226: 531.
80. Kitano Y, Kinoshita Y, Ashida T. Polymer 1995; 36: 1947.
81. Fu Y, Busing WR, Jin Y, Affholter KA, Wunderlich B. Macromolecules 1993; 26: 2187.
82. Mahendrasingam A, Blundell DJ, Martin C, Fuller W, MacKerron DH, Harvie JL, Oldman RJ, Riekel C. Polymer 2000; 41: 7803.
83. Handbook of Polyesters, ed. S. Fakirov, Wiley-VCH, Weinberg 2002; 141
84. Sauer TH, Wendorff JH, Zimmermann HJ. J. Polym.Sci. Polym. Phys. Ed. 1987; 25: 2471.
85. Sun T, Zhang A, Li FM, Porter RS. Polymer 1988; 29: 2115.
86. Bonart R. Kolloid-Z 1966; 213: 1.
87. Bramer R, Ruland W. Macromol. Chem. Phys. 1976; 177: 3601.
88. Asano T, Balta Calleja, FJ, Flores A, Tanigaki M, Mina MF, Sawatari C, Itagaki H, Takahashi H, Hatta I. Polymer 1999; 40: 6475.
89. Ran S, Wang Z, Burger C, Chu B, Hsiao BS. Macromolecules 2002; 35: 10102.
90. Groenincks G, Reynaers H, Berghmans H, Smets G. J. Polym. Sci., Polym. Phys.Ed. 1980; 18: 1311.
91. Groenincks G, Reynaers H. J. Polym. Sci., Polym. Phys. Ed., 1980; l8: 1325.
92. Fakirov S, Fischer EW, Hoffman R, Smidt GF. Polymer 1977; 18: 1121.
93. Lin SB, Keoning JL. J. Polym. Sci., Polym. Symp. 1984; 71: 121.
94. Roberts RC. J. Polym. Lett. 1980; 8: 1311.
95. Holsworth PJ, Turner-Jones A. Polymer 1971; 12: 195.
96. Hoffmann JF. SPE trans. 1964; 4: 1.
97. Al Raheil IAM. Polymer International 1994; 35: 189.
98. Quida AMA, Al Raheil IAM. Polymer International 1995; 38: 367.
99. Pilati F. Compr. Polym. Sci., 1989; 5: 201.
100. Hsu LC. J.Macromol.Sci. Phys. 1967; 1: 801.

101. Droscher M, Wegner G. Polymer 1978; 19: 43.
102. Frank WP, Zachmann HG. Progr. Coolid. Polym. Sci. 1977; 62: 88.
103. Fakirov S, Seganov I, Kurdova E. Makromol. Chem. 1981; 82: 185.
104. Fakirov S, Seganov I, Prangowa L. Makromol. Chem. 1984; 184: 807.
105. Devotta I, Mashelkar RA. Chem Engng Sci 1993; 48: 1859.
106. Gaymans RJ, Amrithraj J, Kamp H. J Appl Polym Sci 1982; 27: 2513.
107. Kaushik A, Gupta SK. J Appl Polym Sci 1992; 54: 507.
108. Warner SB, Lee J. J Polym Sci, Polym Phys Ed 1994; 32: 1759.
109. Srinivasan R, Almonacil C, Narayan S, Desai P, Abhiraman AS. Macrmolecules 1998; 31: 6813.
110. Kang C-K. J Appl Polym Sci 1998; 68: 837.
111. Mallon FK, Ray WH. J. Appl. Polym. sci. 1998; 69: 1233.
112. Chen S-A, Chen F-L. J. Polym. Sci, Part A: Polym Chem 1987; 25: 533.
113. Ravindranath K, Mashelkar RA. J. Appl. Polym. sci. 1990; 39: 1325.
114. Zhi-Lian T, Gao Q, Nan-Xun H, Sironi C. J. Appl. Polym. sci. 1995; 57: 473.
115. Huang B, Walsh JJ. Polymer 1998; 39: 699.
116. Gao Q, Nan-Xun H, Zhi-Lian T, Gerking L. Chem Engng Sci 1997; 52: 371.
117. Mallon FK, Ray WH. J. Appl. Polym. sci. 1998; 69: 1233
118. Aharoni SM. In: Fakirov S, editor. Industrial scale production of polyesters. Handbook of thermoplastic polyesters, 1. New York: Wiley; 2002. p. 56.
119. Wendling PR. US Patent 4532319; 1985.
120. Mallon FK, Ray WH. J. Appl. Polym. sci. 1998; 69: 1203.
121. Yoo Y, Choi KY, Lee JH. Macromol. Chem. Phys. 2004; 205: 1863.
122. Tate S, Hashimoto H, Chiba A. US Pat. 4,613,664; 1986.
123. Tate S, Narusawa H, Watanabe Y, Chiba A. US Pat. 4,742,151; 1988.
124. Tate S, Watanabe Y, Chiba A. Polymer 1993; 34: 4974.
125. Kokkalas DE, Bikiaris DN, Karayannidis GP. J. Appl. Polym. sci. 1995; 55: 787.
126. Duh B. Polymer 2002; 43: 3147.
127. Schaaf E, Zimmerman H, Dietzel W, Lohmann P. Acta Polymerica 1981; 32: 250.
128. Kurita K, Hayashi M, Ohta T, Ishihara H, Okada F, Yoshikawa W, Chiba A, Tate S. US Patent 4851508; 1989
129. Cohn G. Polym. Prepr. 1989; 30: 160.
130. Cohn G. US Patent 4792573; 1988.
131. Rinehart VR. US Patent 4755587; 1988.

132. Ito M, Takahashi K, Kanamoto T. J. Appl. Polym. sci. 1990; 40: 1257.
133. Ito M, Wakayama Y, Kanamoto T. Polymer 1992; 48: 569.
134. Ito M, Wakayama Y, Kanamoto T. Sen-I-Gakkaishi 1994; 35: 1210.
135. Sasaki I, Mori H, Fujimoto M. EP0182352; 1985.
136. Boiko YM, Marikhin VA. Polym Sci USSR, Ser. 2000; A 42: 1169.
137. Ma Y, Agarwal US, Sikkema DJ, Lemstra PJ. Polymer 2003; 44: 4085.
138. Chang TM. Polym Engng Sci 1970; 10: 364.
139. Chang S, Sheu MF, Chen SM. J. Appl. Polym. sci. 1983; 28: 3289.
140. Chen FC, Griskey RG, Beyer GH. AIChEJ 1969; 15: 680.
141. Wu D, Chen F, Li R, Shi Y. Macromolecules 1997; 30, 6737.
142. Duh B. J. Appl. Polym. Sci. 2001; 81: 1748.
143. Medellin-Rodriguez FJ, Lopez-Guillen R, Waldo-Mendoza MA. J. Appl. Polym. Sci. 2000; 75: 78.
144. Schaaf E, Zimmerman H, Dietzel W, Lohmann P. Acta Polymerica 1981: 32:250.
145. Papaspyrides CD, Kampouris FM. Polymer 1984; 25: 791.
146. Duh B. U.S. Pat. 4,205,157; 1980
147. Duh B. U.S. Pat. 4,238,593; 1980
148. Jabarin SA, Lofgren EA, J. Appl. Polym. Sci. 1986; 32: 5315.
149. Karayannidis GP, Sideridou I, Zamboulis D, Stalidis G, Bikiaris D, Lazaridis N, Wilmes A. Angew. Makromol. Chem. 1991; 192: 155.
150. Kwon KC. J. Appl. Polym. Sci. 1998; 68: 837.
151. Gross SM, Roberts GW, Kiserow DJ, DeSimone JM. Macromolecules 2000; 33: 40.
152. James NR, Ramesh C, Sivaram S. Macromol. Chem. Phys. 2001; 202: 1200.
153. Takehiko O, Hideo K, Takeo S, Masataka Y. Japan. Kokai 77,148,92,09; 1977.
154. Rinehart VR. Eur. Pat. Appl. EP 284, 544; 1988.
155. Rinehart VR. US Pat. 4, 755, 587 05; 1988.
156. Scannapieco SN. US Pat. 4, 489, 497, 18; 1989.
157. Takuo N, Takatoshi K. Jpn. Kokai Tokkyo Koho JP. 01,75,520,22; 1989.
158. Van Erden D, Vadnais GL, Enriquez MC, Adams KG, Nelson JP. Eur. Pat. Appl. EP 856,537,5; 1998.
159. Rudolf P, Kurt H, Heinz H. PCT Int. Appl. No: 9611,978; 1996
160. Stouffer JM, Blanchard EN, Leffew KW. US Pat. 5, 510, 454; 1996.
161. Stouffer JM, Blanchard EN, Leffew KW. US Pat. 5, 540, 868 (1996)

162. Pilati F, Toselli M, Messori M, Manzoni C, Turturro T, Gattiglia EG. Polymer 1997; 38: 4469.
163. Ddaubeny Rde, Bunn CW, Brown CJ. Proc. Roy. Soc. 1954; 226: 531.
164. Miyagi A, Wunderlich B. J. Polym. Sci., Polym. Phys. Ed. 1972; 10: 2085.
165. Gross SM, Flowers D, Roberts G, Kiserow DJ, DeSimone JM. Macromolecules 1999; 32: 3167.
166. Iyer VS, Sehra JC, Ravindranath K, Sivaram S. Macromolecules 1993; 26: 1186.
167. Radhakrishnan S, Iyer VS, Sivaram S. Polymer 1994; 35: 3789.
168. Richardson MJ. In Developments in Polymer Characterization; J. V. Dawkins, Ed.; Applied Science Publishers: London 1978; 205.
169. Karayannidis GP, Kokalas DE, Bikiaris DN. J. Appl. Polym. Sci. 1995; 56: 405.
170. Pilati F, Marianucci E, Berti C. J. Appl. Polym. Sci. 1985; 30: 1267.
171. Cruz CA, Barlow JW, Paul DR. J. Appl. Polym. Sci. 1980; 25: 1549.
172. Nasser TR, Paul DR, Barlow JW. J. Appl. Polym. Sci. 1979; 23: 85.
173. Murff SR, Barlow JW, Paul DR. J. Appl. Polym. Sci. 1984; 29: 3288.
174. Linder H, Henrichs PM, Hewitt JM, Massa DJ. J. Chem. Phys., 1985; 82: 1585.
175. Chen XY, Birley AW. Br. Polym. J. 1985; 17: 347.
176. Hanrahan BD, Angeli SR, Runt J. Polym. Bull. 1986; 15: 455.
177. Zhang GY, Ma JW, Cui BX, Luo XL, Ma DZ. Macromol. Chem. and Phy. 2001; 202: 604.
178. Kong Y, Hay JN. Polymer 2002; 43: 1805.
179. Devaux J, Godard P, Mercier JP. Polym. Eng. Sci. 1982; 22: 229.
180. Wilkinson AN, Tattum SB, Ryan AJ. Polym. Bull. 2002; 48: 199.
181. Eguiazabal JI, Ucar G, Cortazar M, Iruin JJ. Polymer 1986; 27: 2013.
182. Michel GA, Roger PS. J. Polym. Sci; Polym. Phys. 1989; 27: 2587.
183. Stewart ME, Cox AJ, Naylor DM. Polymer 1993; 34: 4060.
184. Kotliar AM. J. Polym. Sci., Macromol. Rev. 1981; 16: 367.
185. Golvoy A, Cheung MF, Carduner KR, Rokosz MJ. Polym. Eng. Sci. 1989; 29: 1226.
186. Po R, Occhiello E, Giannotta G, Pelosini L, Abis L, Polym. Adv. Technol. 1996; 7: 365.
187. Cox AJ, Stewart ME, Shepherd FA, Light RR. WO 92/02584; 1992.
188. Hoffman DC. US 5,688,874; 1997.
189. Hait SB, Sivaram S. Macromol Chem Phys 1998; 199: 2689.

190. Hait SB, Sivaram S. US 6150493; 2000.
191. Godard P, Dekoninck JM, Devlesaver V, Devaux J. J. Polym. Sci., Polym. Chem. Ed. 1986; 24: 3301.
192. Berti C, Bonora V, Pilati F, Fiorini M. Makromol. Chem. 1992; 193: 1665.
193. Mercier JP, Groeninckx G, Lesne M. J. Polym. Sci., Part C 1967; 16: 2059.
194. James NR, Ramesh C, Sivaram S. Macromol Chem Phys 2001; 202: 2267.
195. Neil O, Allen G, James D, Joseph BD, Anthony SJ, Joseph MP, Michael SP, Jr. PCT Int. Appl. WO 2003040208 2003; 41.
196. Fustin CA, Bailly C, Clarkson GJ, Groote PD, Galow TH, Leigh DA, Robertson D, Slawin AMZ, Wong JKY. J. Am. Chem. Soc. 2003; 125: 2200.
197. Fustin CA, Bailly C, Clarkson GJ, Galow TH, Leigh DA. Macromolecules 2004; 37: 66.
198. Flory J. Principles of Polymer Chemistry, Cornell University Press, Ithaca, NJ, USA, 1953; 127.
199. Fiorini M, Pilati F, Berti C, Toselli M, Ignatov V. Polymer 1997; 38: 413.
200. Hanna S, Windle AH. Polymer 1988; 29: 207.
201. Kimura M, Salee G, Porter RS. J. Appl. Polym. Sci. 1984; 29: 1629.
202. Bloembergen S, Holden DA, Hamer GK, Bluhm TL, Marchessault RH. Macromolecules 1986; 19: 2865.
203. Bluhm TL, Hamer GK, Marchessault RH, Fyfe CA, Veregin RP. Macromolecules 1986; 19: 2871.
204. Kunioka M, Tamaki A, Doi Y. Macromolecules 1989; 22: 694.
205. Bloembergen S, Holden DA, Bluhm TL, Hamer GK, Marchessault RH. Macromolecules 1989; 22: 1663.
206. Kamiya N, Sakurai M, Inoue Y, Chujo R. Macromolecules 1991; 24: 3888.
207. Orts WJ, Marchessult RJ, Bluhm TL. Macromolecules 1991; 24: 6435.
208. Scandola M, Ceccorulli G, Pizzoli M, Gazzano M. Macromolecules 1992; 25: 1405.
209. VanderHart D, Orts WJ, Marchessault RH. Macromolecules 1995; 28: 6394.
210. Barker PA, Barham PJ, Martinez-Salazar. J. Polymer 1997; 38: 913.
211. Allegra G, Bassi IW. Adv. Polym. Sci. 1969; 6: 549.
212. Baozhong L, Jiayan Y, Seungwoo L, Moonhor R. Eur. Polym. J. 1999; 35: 1607.
213. Baozhong L, Jiayan Y, Seungwoo L, Moonhor R. Polymer 1999; 40: 5371.

214. Kugler J, Gilmer JW, Wiswe D, Zaccmann HG, Hahn K, Fischer EW. Macromolecules 1987; 20: 1116.
215. Fakirov S, Evstatiev M, Schultz JM. Polymer 1993; 34: 4669.
216. Fakirov S, Evstatiev M, Petrovich S. Macromolecules 1993; 26: 5219.
217. Lenz RW, Jin J, Feichtinger KA. Polymer 1983; 24: 327.
218. Chen G, Lenz RW. Polymer 1985; 26: 1307.
219. Lenz RW, Martin E, Schuler AN. J. Polym. Sci., Part A: Polym. Chem. Ed. 1973; 11: 2265.
220. Lenz RW, Ohata K, Funt J. J. Polym. Sci., Part A: Polym. Chem. Ed. 1973; 11: 2273.
221. Lenz RW, Go S. J. Polym. Sci., Part A: Polym. Chem. Ed. 1973; 2927.
222. Lenz RW, Go S. J. Polym. Sci. Part A: Polym. Chem. Ed. 1974; 12: 1.

CHAPTER 2

SCOPE AND OBJECTIVES OF THE PRESENT WORK

2.1 Introduction

The nature of semi crystalline morphology of crystallizable polymers is very important because it directly controls the physical and mechanical properties. Semi crystalline morphology of PET had been studied extensively since the polymer was synthesized for the first time. The structure and morphology can be modified by many methods. Thermal treatment is the most favored technique as it is a very simple method to practice. Solvent treatment also changes the morphology. Recently it has been shown that the semi crystalline morphology is modified during chain extension reaction in the solid state. Polycondensation of prepolymers in solid state has been developed mainly for commercial purposes. Industrially it is used to obtain high molecular weight PET, PBT, nylon 6 and nylon 66 which are used as engineering plastic materials. In all these cases, initially the materials are melt polymerized to about 0.6 dL/g viscosity then polymerized by solid state polymerization process. One of the key drawbacks of SSP is the slow reaction rate and polymerization time of about 15 h are not uncommon. In the solid state polymerization, reaction occurs in the amorphous phase and by the diffusion of the byproduct.

Recently, crystallization and SSP of polyester oligomers (PET and PEN) were studied[1]. Copolymer preparation of polyesters was extensively studied in the solid state[2-5]. Nirmala[2] et.al., studied the simultaneous solid state and exchange reactions in PET/PEN oligomers. Hait and Sivaram[3,4] demonstrated that carbonate-ester interchange reactions could occur along with solid state polymerization (SSP) in the case of PET/PC.

The primary focus of the present thesis is to study the structure and morphology development in PET based copolymers during chain extension reaction (solid state polymerization). To that end comonomers having distinct properties are chosen: 1) comonomer which is semi-rigid 2) highly flexible comonomer which can plasticize the PET and 3) rigid monomer which can form liquid crystal with PET.

Another important aspect of polymer crystallization is the role of orientation on crystallization. Hence, amorphous PET with varying degree of chain orientation is studied for the crystallization behavior and correlated with the amorphous orientation.

2.2 Objectives of the present work

2.2.1 Morphological Consequences of Interchange Reactions during Solid State Copolymerization in Poly (ethylene terephthalate) and Polycarbonate oligomers

Poly(ethylene terephthalate) (PET) is the most used member of thermoplastic polyester family. Some PET applications require modification of the base polymer. For example, in blow molding an increase in the glass transition temperature is useful in reducing the crystallization ability and increasing the melt strength. Also it is less tough and soluble in solvents such as trifluoroacetic acid (TFA) and o-chlorophenol. Bisphenol A polycarbonate has high impact strength and is soluble in common solvents such as chloroform. A copolymer or a blend made from the two could give a new material with combined properties. PET/PC blends are usually prepared by reactive processing[6,7]. PET and PC undergo transesterification to give block copolymers that subsequently turn into random copolymers. Controlling the transesterification levels is difficult in the melt process. Hait[3,4] et al found that transesterification between PET and PC can also take place in solid state, where the extent of transesterification will be lower. *The objective of the present work is to study the morphological consequences of interchange reactions during solid state copolymerization in poly(ethylene terephthalate) and polycarbonate oligomers. Oligomer blends were crystallized under chloroform vapors for 4 h to crystallize PC, while the PET crystallized during cooling after extrusion. Degree of randomness and percentage of transesterification at various levels of reaction will be determined by means of ^{1}HNMR. The structure and morphological changes occurring during SSP will be investigated by DSC and XRD.*

2.2.2 Effect of Poly(ethylene glycol) as an Additive on the Crystallization and Solid State Polymerization of Poly(ethylene terephthalate)

Solid state polymerization (SSP) is a technically important process in the manufacture of high molecular weight PET. Conventionally PET is synthesized by a combination of melt and SSP. Recently, it has been found that high molecular weight PET can be synthesized by SSP of very low molecular weight oligomer[1]. Since solid state polymerization requires crystalline precursors, oligomer crystallization is an important process[8]. Addition of suitable additives changes the crystallization behavior of the oligomers. PEG has good miscibility with PET and modifies the crystallization behavior. However, PEG can copolymerize with PET if the PEG ends are not capped. *The objective of the present work is to enhance the mobility of the amorphous phase PET oligomer and study its effect on the morphology and solid-state condensation. Hence it is proposed to plasticize the amorphous phase of PET oligomer by the addition of small quantities of low molecular*

weight PEG. Addition of plasticizers will have profound influence on the crystallization of the polymer. In the case of PEG, copolymer formation was confirmed by means of ^{1}HNMR. Morphological changes occurring at various levels of SSP will be monitored by using DSC and XRD.

2.2.3 Studies on the solid state polymerization of PET/POB oligomer blends

Copolyesters of poly(ethy1ene terephthalate) (PET) and p-hydroxybenzoic acid are well known as liquid-crystalline polymers[9,10]. P(ET-*co*-OB) is prepared by reactive blending of PET and *p*-acetoxybenzoic acid (ABA) to facilitate transesterification with loss of acetic acid to incorporate oxybenzoate units into the polymer. PET-*co*-OB is a liquid crystalline polymer when the fraction of oxybenzoate repeat units is at least 40 mol %. Taking into account all possible transesterification reactions between PET and POB during the synthesis, formation of a random polymer chain has to be assumed. Controlling the transesterification levels is difficult in the melt process. *The objective of the present work is to study the structure and morphology development during the synthesis of poly(ethylene terephthalate-co-oxybenzoate) copolymer by solid state polymerization. The structure and morphological changes occurring during SSP will be investigated by differential scanning calorimetry (DSC) and WAXD measurements. The copolymer obtained by solid state polymerization is compared with the copolymer obtained by standard melt polymerization.*

2.2.4 Effect of molecular orientation on the crystallization and melting behavior of Poly (ethylene terephthalate) fiber

Polyethylene terephthalate (PET) is perhaps one of the extensively studied and model semicrystalline polymer for crystallization studies because it can be obtained easily in amorphous form or semicrystalline form at room temperature. The effect of chain orientation on the crystallization of PET also attracted wide attention because its relevance in the polymer processing. In the presence of chain orientation, it has been shown that the rate of crystallization is strongly dependent on the degree of orientation and the key parameters are the initial orientation of the chains and the temperature of crystallization[11-15]. In most of the experiments oriented amorphous PET in the form of fibers are usually obtained by drawing fibers just below glass transition temperature[16-18]. This process always results in a skin whose orientation is significantly higher than that of the core. As a

result, crystallization behavior data obtained from these fibres do not accurately portray the influence of orientation on crystallization kinetics. In contrast, in this work we study PET fibres with different levels of amorphous orientation obtained by spinning PET with polystyrene (PS) skin, as a bicomponent fiber. This way, the shear stresses near the wall are absorbed by the PS skin and do not produce any shear induced orientation in the PET core. Fibers obtained after selectively removing the PS sheath enable us to study the effect of amorphous orientation on the crystallization behavior without the interference from the extraneous structure near the skin. *The objective of the present chapter is to study the effect of molecular orientation on the crystallization and melting behavior of poly (ethylene terephthalate)**.** Amorphous orientation and the amount of amorphous material oriented in the fibres are characterized by wide-angle x-ray scattering technique (WAXS) and are correlated with cold crystallization temperature and the heat of crystallization. The crystallization behavior of the oriented amorphous PET fiber was studied under free to relax and taut conditions using DSC.*

2.3 References

1. James, N. R.; Ramesh C.; Sivaram S. *Macromol. Chem. Phys.*, ***202***, 1200, (2001)
2. James, N. R.; Ramesh C.; Sivaram S. *Macromol. Chem. Phys.*, ***202***, 2267, (2001)
3. Hait, S. B.; Sivaram, S. *Macromol. Chem. Phys.*, **199**, 2689, (1998)
4. Hait, S. B.; Sivaram, S. US 6150493 A 21 Nov 2000
5. Fustin, C.A.; Bailly, C.; Clarkson, G. J.; De Groote, P.; Galow, T. H.; Leigh, D. A.; Robertson, D.; Slawin, A. M. Z.; Wong, J. K. Y.; *J. Am. Chem. Soc.*; **125,** 2200, (2003)
6. Devaux, J.; Godard, P.; Mercier, J. P. *J Polym Sci: Polym Phys Ed* **20**, 1875, (1982)
7. McAlea, K. P.; Schultz, J. M.; Gardner, K. H.; Wignall, G. D. *Polymer* **27**, 1581, (1986)
8. Gross, S. M.; Roberts, G. W.; Kiserow, D. J.; DeSimone, J. M. *Macromolecules* **33**, 40, (2000)
9. Jackson, W. J., Jr.; Kuhfuss, H. F. *J. Polym. Sci., Polym.Chem. Ed.* **1976**, *14*, 2043.
10. Kuhfuss, H. F.; Jackson, W. J. U.S. Pat. 3 778 410, 1973. Kuhfuss, H. F.; Jackson, W. J. U.S. Pat. 3 804 805, 1974.
11. Smith, F. S.; Steward, R. D. *Polymer* **16**, 283, (1974)

12. Gupte, K. M.; Motz, H.; Schultz, J. M. *J. Polym. Sci. Polym. Phys. Ed.* **21**, 1927, (1983)
13. Althen, G.; zachman, H. G. *Makromol. Chem.* **180**, 2723, (1979)
14. Alfonso, G. C.; Verdona, M. P.; Wasiak, A. *Polymer* **19**, 711, (1978)
15. Sun, T.; Pereira, J. R. C.; Porter, R. S. *J. Polym. Sci. Polym. Phys. Ed.* **22**, 1163, (1984)
16. Mahendrasingam, A.; Martin, C.; Fuller, W.; Blundell, D. J.; Oldman, R. J.; MacKerron, D. H.; Harvie, J. L.; Riekel, C. *Polymer* **41**, 1217, (1999)
17. Blundell, D. J.; Mahendrasingam, A.; Martin, C.; Fuller, W.; MacKerron, D. H.; Harvie, J. L.; Oldman, R. J.; Riekel, C. *Polymer*, **41**, 7793, (2000)
18. Keum, J. K.; Kim, J.; Lee, S. M.; Song, H. H.; Son, Y. K.; Choi, J. I.; Im, S. S. *Macromolecules* **36**, 9873, (2003)

CHAPTER 3

MORPHOLOGICAL CONSEQUENCES DURING SOLID STATE COPOLYMERIZATION OF POLY (ETHYLENE TEREPHTHALATE) AND POLYCARBONATE

3.1 Introduction:

Poly (ethylene terephthalate) (PET) is the most commercially successful member of the thermoplastic polyester family. Some PET applications require modification of the base polymer[1-3]. For example, in blow molding an increase in the glass transition temperature (T_g) is useful in reducing the crystallization ability and increasing the melt strength. It is relatively less tough and soluble in few solvents such as trifluoroacetic acid (TFA) and o-chlorophenol. On the other hand Bisphenol A polycarbonate (PC) has high impact strength and is soluble in common solvents such as chloroform. A copolymer or a blend made from the two could give a material with combined properties [1-8].

PET/PC blends have been studied extensively and many reports were published in the literature on the miscibility of these blends[1-19]. Paul et al[9,10] reported that the blends were miscible at higher PET content (above 70%), while others[11,13] found that blends were completely immiscible over all composition range. Wang et al[1] found that the blend became entirely miscible only after the transesterification reaction between PET and PC. Much of the previous research has been focused on preparing the miscible PET/PC blends by reactive blending via transesterification[1,4,5,9,10,15-19]. Transesterification reactions strongly depend on their initial compatibility and on the blending conditions. It is generally accepted that, as a result of transesterification reactions, the blend of homopolymers transform into block copolymers that subsequently transform into a random copolymer as block lengths gradually decrease[20]. Possible reactions in PET/PC blends during melt processing were well documented in the literature[4, 21-24].

Most of the transesterification reactions are carried out in the melt state. However, there are few reports describing transesterification reactions in solid state. Nirmala et al[25] studied the simultaneous solid state and exchange reactions in PET/PEN oligomers. Hait and Sivaram[26,27] demonstrated that carbonate-ester interchange reactions could occur along with the solid-state polymerization (SSP) in the case of PET/PC.

The focus of this chapter is to examine the structure and morphology development during ester-carbonate interchange reaction and solid state polymerization of PET/PC oligomer blend. The PET/PC oligomers were initially melt blended and crystallized. The crystallized blend was subjected to simultaneous solid state polymerization and ester-carbonate interchange reaction by holding the blend just below the melting temperature under reduced pressure. The change in the structure and morphology was monitored by ^{1}H NMR spectroscopy, DSC and X-ray diffraction.

3.2 Experimental:

3.2.1 *Preparation of oligomers:*

PET oligomer was prepared by hydrolysis of high molecular weight PET pellets (η_{inh}: 0.69 dL/g) obtained from Eastman Chemicals, USA. Hydrolysis was carried out using deionized water in a Parr reactor at 180^{o}C for 1.5 h. The oligomer obtained was filtered and dried at 60°C under reduced pressure. An oligomer of polycarbonate was prepared by melt polymerization of bisphenol A with diphenyl carbonate in the presence of a basic catalyst[28]. The inherent viscosities of the PET and PC oligomers were 0.16 dL/g and 0.14 dL/g (in phenol/1,1,2,2-tetrachloroethane) respectively.

3.2.2 *Preparation of oligomer blends:*

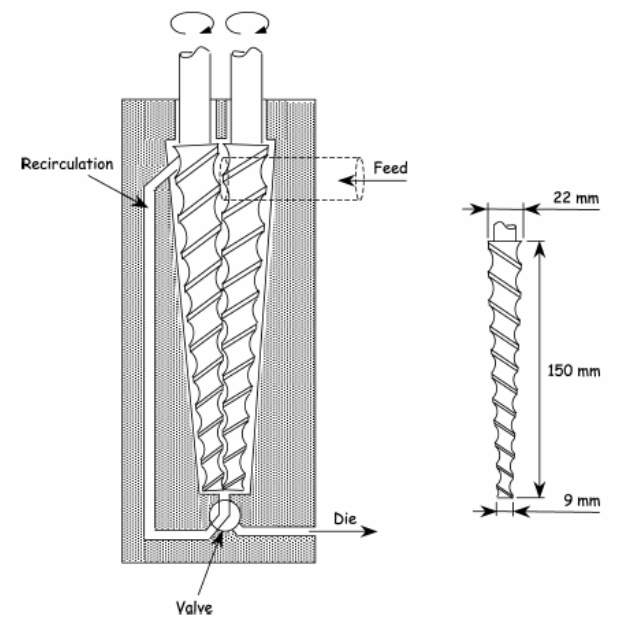

Figure 3.1: Assembly and profile of the screws in the twin-screw extruder.

The blends of PET and PC oligomers were prepared in Midi 2000 co-rotating twin-screw extruder from DSM Research (The Netherlands). Assembly and profile of the screws in the twin-screw extruder is shown in figure 3.1. The batch size was about 5 g and the oligomers were blended at 250^{o}C for 1 min., with a screw speed of 100 rpm to minimize the transesterification during blending.

3.2.3 *Crystallization and Solid state polymerization:*

The PET oligomer crystallized during cooling after extrusion, however, the PC oligomer in the blend was crystallized under chloroform vapors for 4 h at room temperature. The catalyst antimony trioxide (Sb_2O_3) (1000 ppm) was incorporated by refluxing the sample

in acetone for 1 h. Acetone was stripped off in a rotatory evaporator and the oligomer blend was dried under vacuum at 60^{o}C. The SSP was performed in a glass reactor according to a well defined time temperature protocol under reduced vacuum. Samples were periodically removed for structure and morphology characterization.

3.2.4 *Characterization:*

Inherent viscosities were measured at 30^{o}C in an automated Schott Gerate AVS 24 viscometer, using an Ubbelohde suspended level viscometer in phenol/1,1,2,2-tetrachloroethane (TCE) (60: 40, w/w) at a polymer concentration of 0.5%. The X-ray diffraction experiments were performed using a Rigaku Dmax 2500 diffractometer. The system consists of a rotating anode generator with a copper target and a wide-angle powder goniometer, having diffracted beam graphite monochromator. The generator was operated at 40 kV and 150 mA. All the experiments were performed in the reflection mode. The samples were scanned between 2θ = 5 to 35° at a speed of 1°/min. Calorimetric measurements were performed using a Perkin-Elmer thermal analyzer (DSC -7) at a heating/cooling rate of 10^{o}C/min in a nitrogen environment. ^{1}H NMR was performed in a Bruker DRX 500 spectrometer at 25^{o}C operating at 500 MHz. The samples were dissolved in $CDCl_3$/TFA (70:30, v/v) mixture and the spectra were internally referenced to tetramethyl silane.

3.3 Results and Discussions:

3.3.1 Solid state polymerization and interchange reaction:

Crystallized oligomer blends were subjected to SSP at 220°C for 20 h under dynamic reduced pressure. Table 3.1 and Figure 3.2 give the change in inherent viscosity (η_{inh}) with time during SSP. The starting SSP temperature is 190^{o}C and is dictated by the onset of melting of the crystallized sample. In general, PET oligomer displayed a higher onset of melting, but the PC component always showed lower melting temperature necessitating lower SSP temperature. The SSP temperature is progressively increased during the course of the reaction because the onset of melting shifted to higher temperature with increase in the SSP time. All the compositions underwent solid state polymerization to significant extent as indicated by the increase in inherent viscosity with time.

Table 3.1: Change in viscosity (η_{inh}) during SSP for PET/PC blend samples of different compositions.

SSP time	Inherent Viscosity (η_{inh}) dL/g (PET: PC)						
	0:100	**30:70**	**50:50**	**70:30**	**80:20**	**90:10**	**100:0**
0	0.17	0.17	0.16	0.19	0.2	0.19	0.16
2	0.26	0.2	0.17	0.22	0.23	0.22	0.23
5	0.38	0.27	0.24	0.28	0.3	0.29	0.27
8	0.44	0.43	0.34	0.46	0.44	0.4	0.4
10	0.46	0.51	0.54	0.56	0.61	0.51	0.43
15	0.49	0.56	0.75	0.72	0.72	0.65	0.56
20	0.5	0.61	0.79	0.81	0.82	0.69	0.67

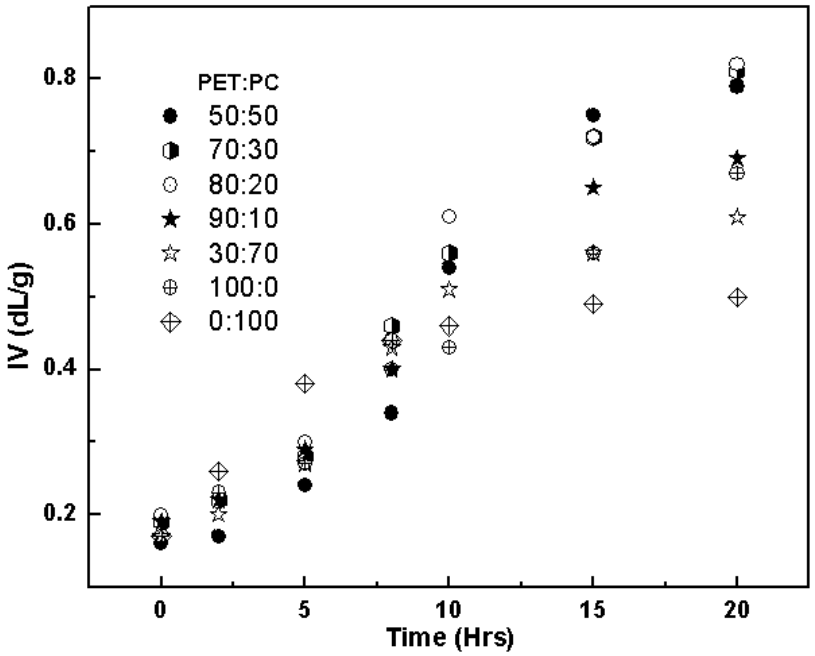

Figure 3.2: Change in inherent viscosity (η_{inh}) for PET/PC blend samples of different compositions during SSP.

The final viscosity attained by these blend samples differs with composition, even though the SSP time temperature protocol is the same for all samples. Nevertheless it must be kept in mind that the PET and PC have different set of Mark-Houwink constants for the given polymer-solvent combination. Hence, direct extrapolation of viscosity to molecular weight and comparison may not be appropriate.

It has been shown that PET and PC undergo interchange reaction in the melt state and hence it is reasonable to expect that PET and PC will undergo interchange reaction also in the solid state, albeit at lower rates. Figure 3.3 shows the NMR spectra for 70:30 and 30:70 PET/PC blend samples at various stages of SSP. In PET ^{1}H NMR spectra, 8.02 ppm corresponds to the four protons of terephthalic acid residue. The signals in the 7.00-7.20 ppm region correspond to the aromatic protons of bisphenol A in PC. Crystallized oligomer blend does not show signals in the range of 8.1 – 8.4 ppm indicating that no transesterification takes place during melt mixing the oligomers and subsequent crystallization. With progress in SSP, new NMR peaks start to appear at 8.14, 8.20 and 8.30 ppm indicating interchange reaction also occurring simultaneously with chain extension. The molecular structure of the copolymer may be analyzed from the NMR data. The ester-carbonate interchange reaction between PET and PC oligomers leads to the formation of a four-component polycondensate, which can be represented by the general formula

$$-[(A_1{-}B_1)_x-(A_2{-}B_1)_y]_m-[(A_1{-}B_2)_z-(A_2{-}B_2)_w]_n-$$

Where A_1 is the ethylene group, A_2 is the bisphenol A group, B_1 is the terephthalate unit and B_2 is the carbonate unit. The percentage transesterification and degree of randomness can be calculated from the triad mole fractions obtained from ^{1}H NMR. In term of triads, by considering the terephthalic unit B_1 as the central unit, in the final copolymers three different sequences can be identified as shown in Scheme 3.1.

Depending on the environment, the terephthalic protons in B_1 show signals at 8.14, 8.20 and 8.30 ppm corresponding to $A_1B_1A_2$ and $A_2B_1A_2$ triads respectively. The mole fractions of triads of type $A_iB_1A_k$ relative to the concentration of B_1 [$f(A_iB_1A_k)$] can be obtained directly from the integrated intensities of the appropriate NMR peaks. The degree of randomness (B_{B1}), which is indicative of how the A units are distributed around B_1, can be written as:

$$B_{B1} = f_{A1B1A2} \cdot (1/F_{A1} + 1/F_{A2})$$

Where f_{A1B1A2} is the mole fraction of $A_1B_1A_2$ triad, F_{A1} and F_{A2} are the mole fractions of ethylene glycol and bisphenol A respectively. The f_{A1B1A2} value is calculated from ^1H NMR spectra, by measuring the relative intensity of the signals due to the $A_1B_1A_2$ sequence. B_{B1} can assume values between 0 and 2. For random copolyesters B_{B1} is unity and if B_{B1} is less than unity, the units tend to cluster together in blocks of each unit. If B_{B1} is zero it indicates a mixture of homopolymers, whilst a value of 2 indicates an alternating distribution[29].

The degree of transesterification (DT) is

$(f_{A1B1A2} + f_{A2B1A2}) / (f_{A1B1A1} + f_{A1B1A2} + f_{A2B1A2}) = f_{A1B1A2} + f_{A2B1A2}$

where $f_{A1B1A1} + f_{A1B1A2} + f_{A2B1A2} = 1$

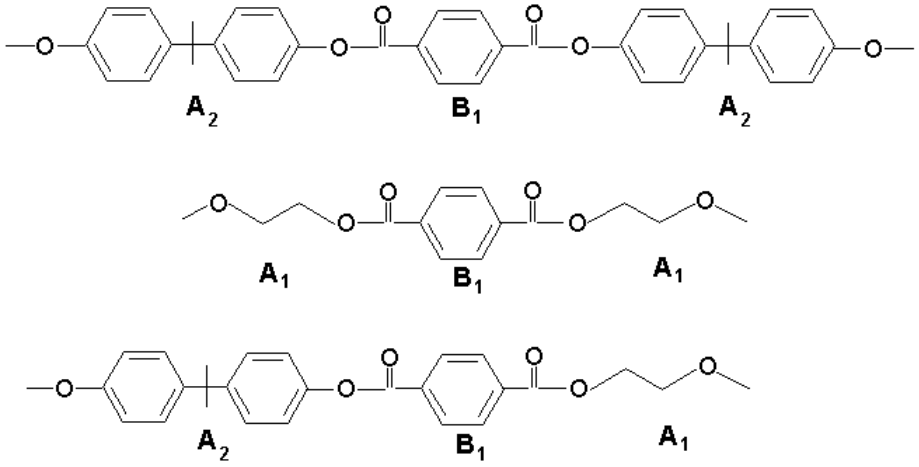

Scheme 3.1: Possible traids present in the PET/PC copolymer as terephthalic unit (B_1) as the central unit. A_1 is the ethylene group, A_2 the bisphenol A group

The degree of randomness and % of transesterification calculated from the NMR data is shown in Figure 3.4. It is apparent from the figure that the transesterification is minimum during the initial hour of reaction and the increase in the viscosity is due to self-condensation of homopolymers. However, transesterification becomes appreciable after 8 h of reaction. The degree of randomness is close to zero initially indicating long sequences of homopolymer blocks. The degree of randomness increases with increase in transesterification indicating the sequence of the blocks becoming shorter. However, degree of randomness is always below unity, indicating the presence of blocks of homopolymer chains. Small peak at about 4.3 and 6.8 ppm are also observed in the NMR spectra and are assigned to aromatic-aliphatic ether linkage and cyclic ethylene carbonate. These products arise from the side reactions as discussed in detail by Hait and Sivaram[26].

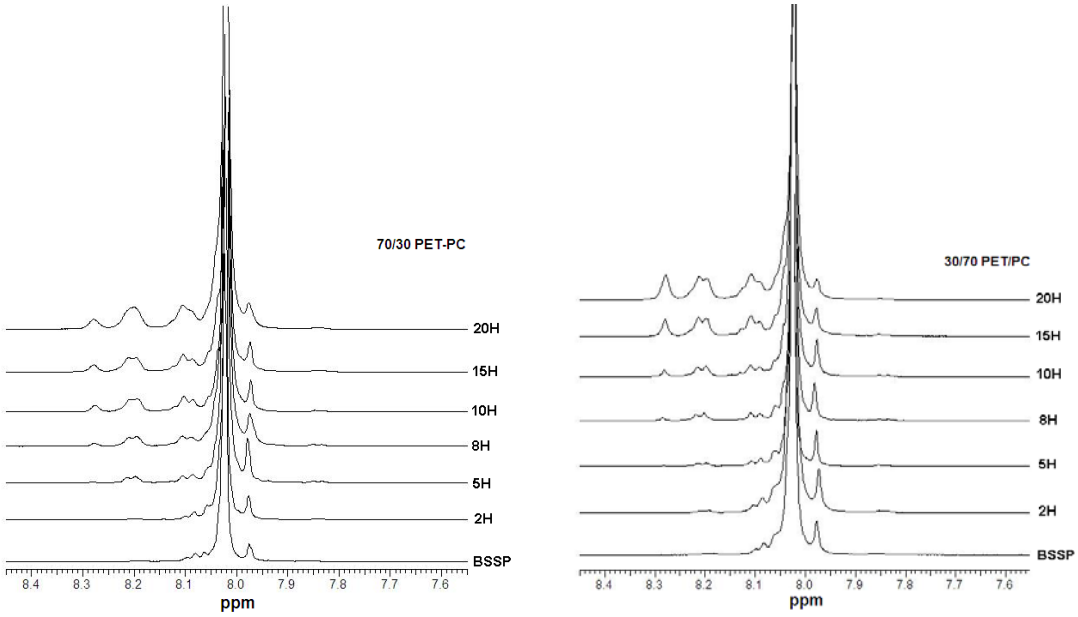

Figure3.3: [1]H NMR spectra at various stages of SSP for the compositions PET/PC 70/30 and 30/70.

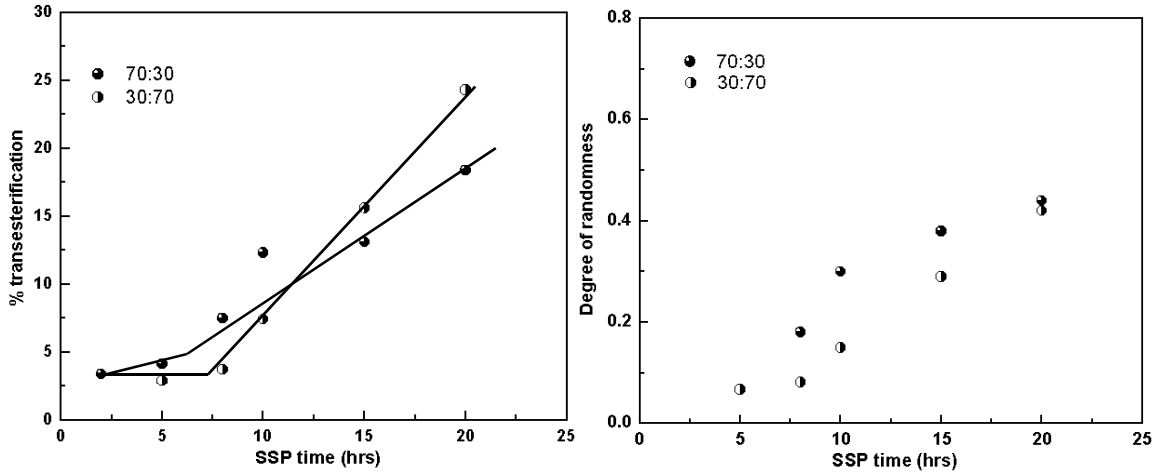

Figure 3.4: Degree of randomness and % of transesterification calculated for 70:30 and 30:70 PET/PC blend samples at various stages of SSP from [1]H NMR.

3.3.2 Structure and morphology

The change in the WAXS patterns of the 50/50, 70/30, 80/20, 90/10 and 30/70 PET/PC blend samples during the course of SSP are shown in Figure 3.5. All the compositions

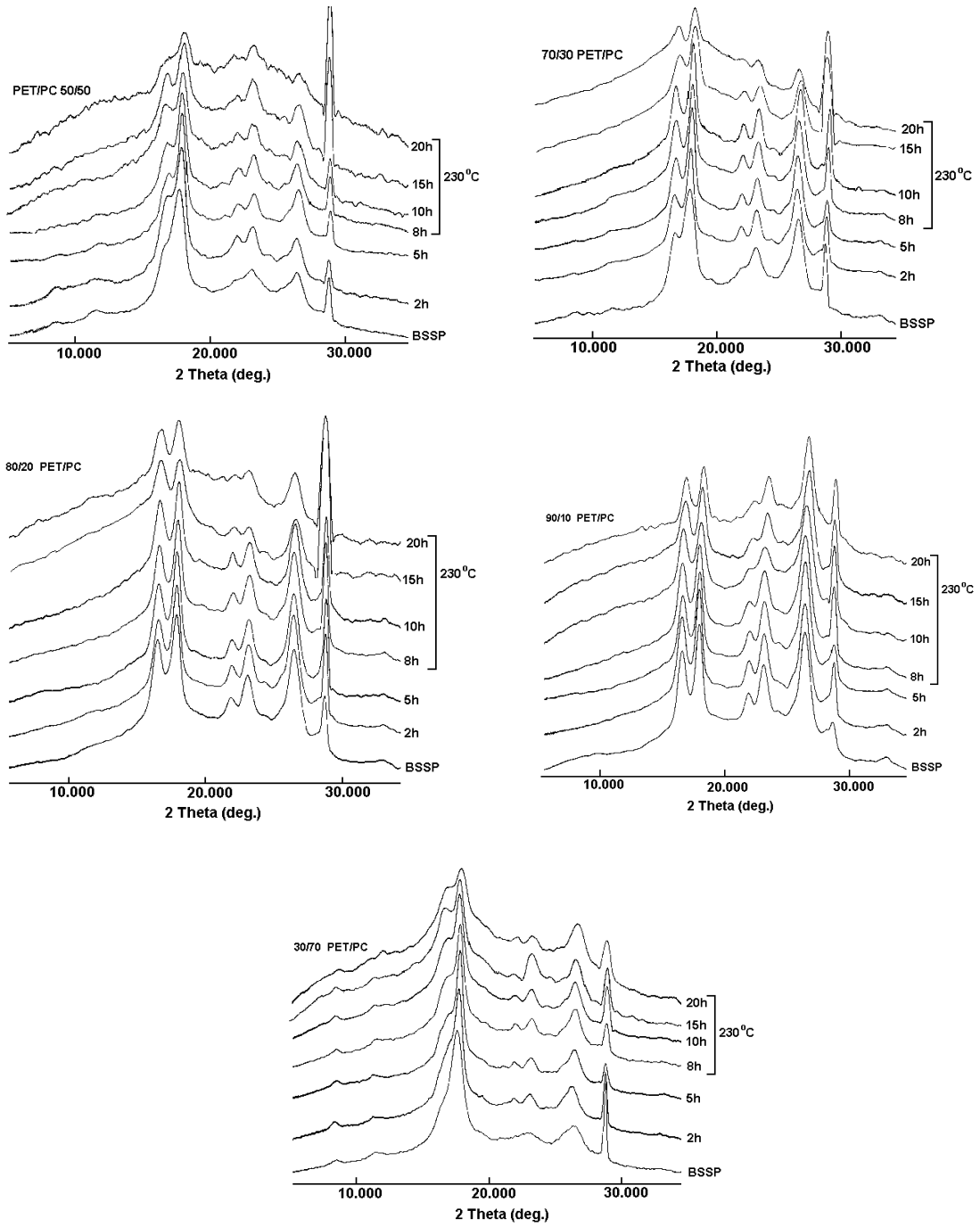

Figure 3.5: X ray diffraction patterns of 50/50, 70/30, 80/20, 90/10 and 30/70 PET/PC blend samples during the course of SSP.

exhibited similar behaviour. The before solid state polymerization (BSSP) sample shows a prominent peak at 2θ = 17.32° with a shoulder at 2θ = 16.25°. PET and PC have major reflections in the 2θ ranges from 14 to 20°. PC shows a major reflection at 2θ =17.02°

corresponding to 210 reflection and the other reflections are relatively weak[30]. In the case of PET, the strong reflections $0\bar{1}1$ and 010 occur at 15.92 and 17.46° respectively[31]. The other prominent reflections of PET are at 2θ = 21.16, 22.36 and 25.73° and are indexed as $\bar{1}11, \bar{1}10$ and 100[31]. In the blend samples, these reflections appear weak. This would imply that the crystallization of PET in the presence of PC is retarded, even though PET has a higher crystallization rate. To understand the crystallization behavior of PET/PC oligomeric blends, PET and PC oligomers were crystallized individually and physical mixtures were prepared in 30/70, 50/50 and 70/30 compositions at room temperature. The diffraction patterns of the mixtures are very similar to those of respective melt blended samples. This indicates that both PET and PC crystallize individually in the melt blended samples as in the case with homopolymers.

The X-ray diffraction patterns show increase in the amorphous content with progress in reaction. All the blend samples show decrease in crystallinity after 5 h of reaction, even though the reaction temperature is below the onset of melting. It is interesting to note that the amorphization starts after 5 h of SSP when the interchange reaction becomes prominent. It must be noted that though the amorphous fraction increased, the diffractograms still exhibited the basic shape of the before SSP diffractogram, indicating the existence of PET and PC crystals in the ASSP sample.

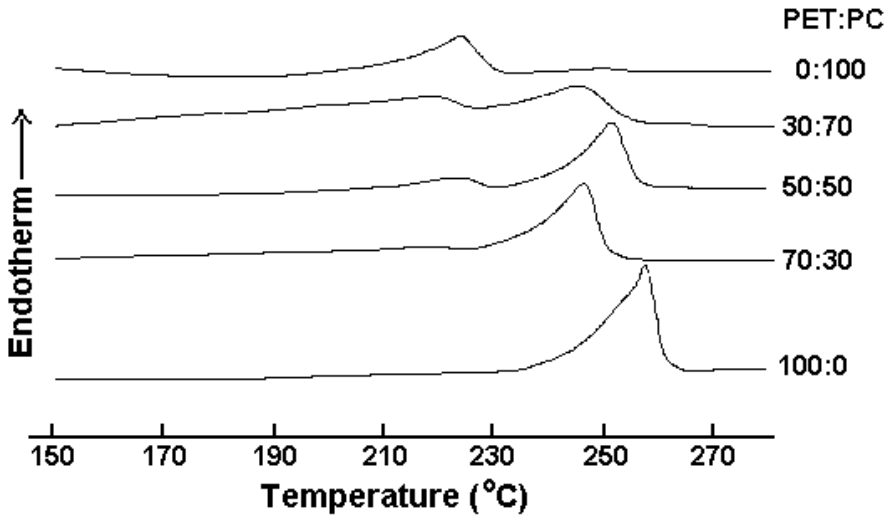

Figure 3.6: DSC thermograms of the crystallized oligomer samples PET, PC and blends of different compositions.

The thermal properties of the samples are studied in detail to understand the structure and morphology. DSC thermograms of the crystallized samples are shown in Figure 3.6. The thermograms of PET and PC oligomers are also sketched in the same figure for comparison. As seen from the Figure 3.6, the melting temperature of PET is depressed in the blend samples, however such depression is not obvious for the PC component. The behaviour of the melting endotherms with SSP and interchange reaction is shown in Figure 3.7 for the different compositions of PET/PC blends and homopolymers. The PC melting endotherm shifts to higher temperature with increasing reaction time, while the position of PET does not change. During the final stage of the reaction, the thermograms overlap. The heat of fusion is plotted with reaction time in Figure 3.8. Table 3.2 gives heat of fusion with reaction time for different compositions along with homopolymers. During initial stages the heat of fusion increases but after 5 h of reaction it starts decreasing indicating amorphization and is consistent with XRD data discussed above. However, under similar conditions the heat of fusion of the homopolymers shows an increase initially but becomes constant at later stages of reaction.

Table 3.2: Change in heat of fusion for different compositions of PET/PC blends along with homopolymers at different levels of SSP and transesterification

SSP time	**Heat of fusion (J/g) (PET: PC)**						
	0:100	**30:70**	**50:50**	**70:30**	**80:20**	**90:10**	**100:0**
0	24	45	43	45	47	51	51
2	36	46	57	57	54	58	59
5	40	42	47	52	51	61	65
8	40	40	45	50	53	60	66
10	40	35	40	48	46	54	65
15	41	25	37	40	44	50	66
20	40	21	27	27	32	50	66

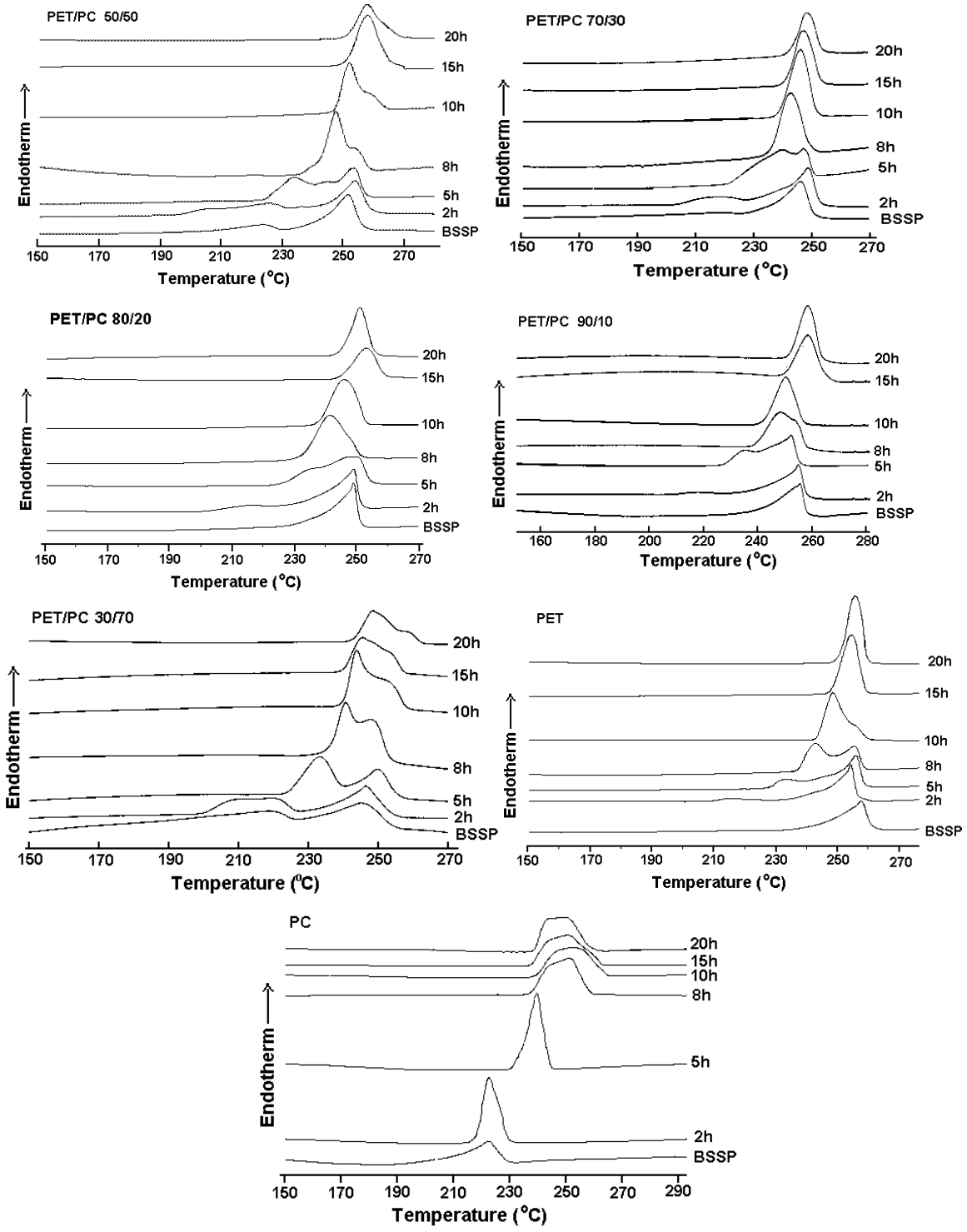

Figure 3.7: The melting behaviour of different composition PET/PC blend samples and homopolymers at various stages of SSP.

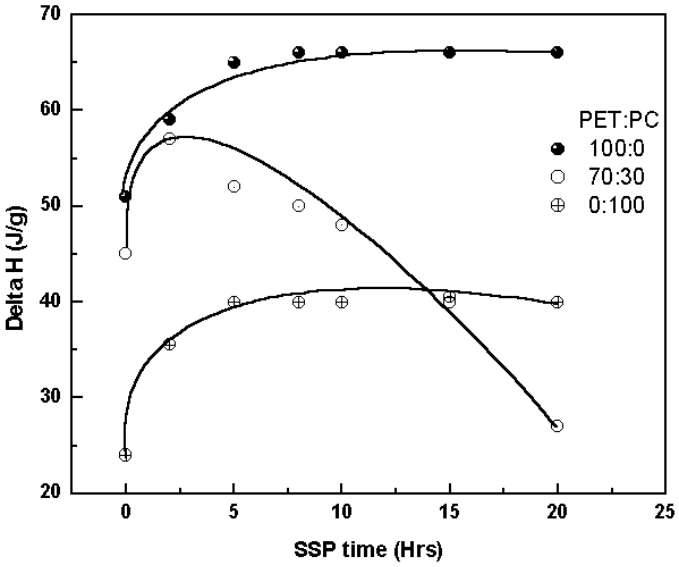

Figure 3.8: Change in heat of fusion of homopolymers PET, PC and 70/30 PET/PC blend at different level of SSP and transesterification.

It is worth comparing the behavior of PET-PC system with PET-PEN system. In the case of simultaneous solid state polymerization and exchange reactions of PET/PEN oligomer blends, such amorphization was not observed with the progress of the reaction in the solid state and the PET and PEN crystals remained unchanged[25]. The amorphization in the case of PET/PC may be explained on the basis of cocrystallization. PET and PEN have very similar chemical structure and crystallize in the triclinic structure. It has been shown that PET and PEN can cocrystallize in the same lattice[32-33]. Hence, it appears that in the case of PET-PEN system, the PET and PEN react to form a copolymer. The copolymer stem can be accommodated in the outer layer of the crystals of PET and PEN and this protects the crystal from further reaction. The reaction is not expected to take place within the crystals as these crystals are big and defect free. However, the situation is different for PET-PC system. PET and PC have different chemical structure and they crystallize in different crystal lattices and cannot cocrystallize. When PET-PC copolymer is formed on the outer layer, the stem is rejected from the crystal, thus exposing the inner layer for further reaction. Thus there is continuous reduction in the crystals leading to amorphization below the melting temperature. The mechanism of amorphization is schematically shown in Figure 3.9.

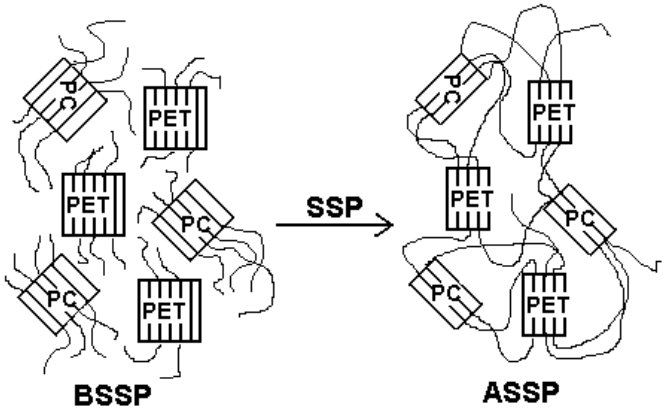

Figure 3.9: Schematic representation of mechanism of amorphisation in PET/PC oligomer blends during the SSP and transesterification.

Glass transition temperatures were not observed in the first heating runs for the BSSP sample because the starting sample was partially crystalline. However, glass transition is seen in the after SSP samples probably due to the increased amorphization and Figure 3.10 shows the variation of T_g with composition. As expected the T_g's of the samples solid state polymerized for 20 h show a linear relationship with composition and these values agree well with the computed values on the basis of linear relationship between T_g's of the components[34].

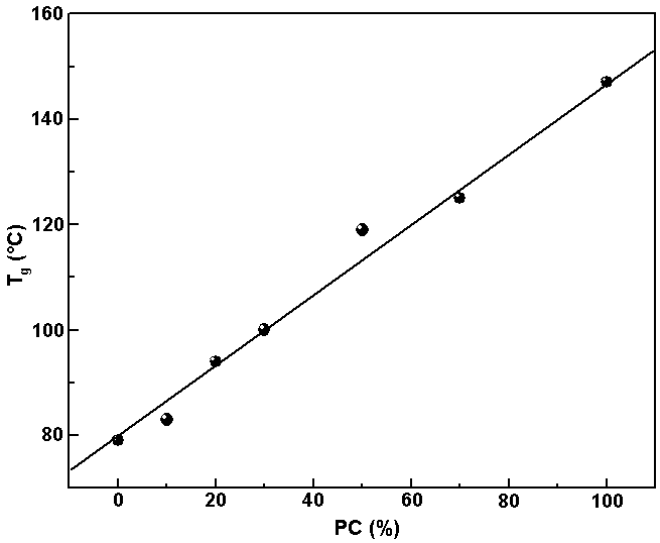

Figure 3.10: Dependence of glass transition temperature on the composition of PC in the copolymers

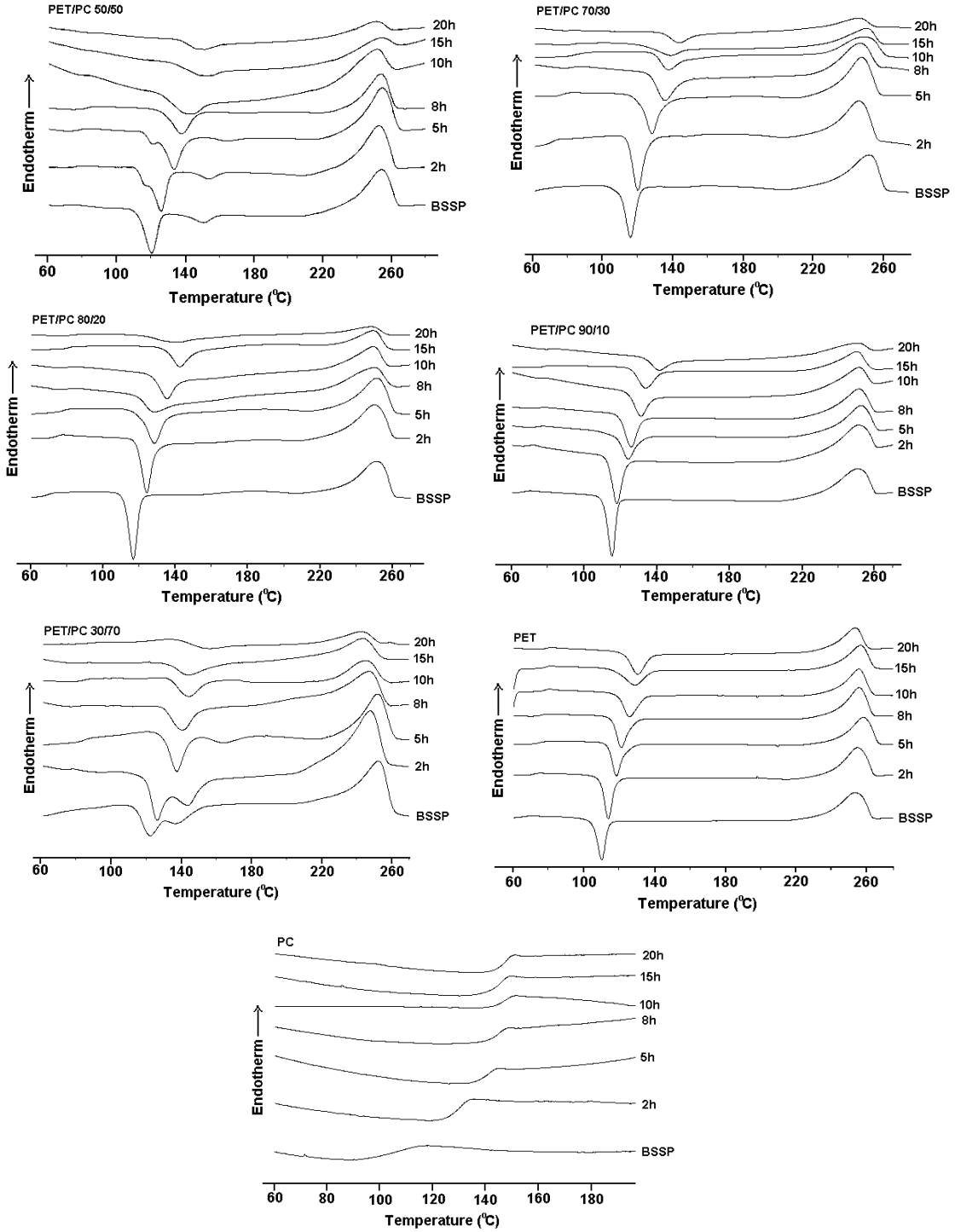

Figure 3.11: DSC thermograms of PET/PC blend samples and homopolymers at different levels of SSP and transesterification (Note: Samples were rapidly melted and quenched before scanning).

The melting endotherms in the first heating are not representative of the copolymer melting because the morphology has individual PET and PC crystals. Hence samples were melted and quenched and again heated in DSC to study its crystallization and melting

behavior. The thermograms are shown in Figure 3.11 for various compositions and homopolymers. All the samples showed the effect of transesterification on crystallization and melting. The cold crystallization peaks due to PET (T_{cc}) are evident for these samples. There is an additional crystallization exotherm for PET at higher temperature; however, the amount representing this peak is small. These peaks progressively shift towards higher temperature and become smaller and broader during SSP and transesterification. The heat of fusion and melting temperature also decreases. These suggest that crystallization is hindered due to the disruption of chain periodicity as a consequence of transesterification[35] as well as due to the increase in molecular weight.

3.4 Conclusions:

Poly(ethylene terephthalate-co-bisphenol A carbonate) was obtained by simultaneous solid state polymerization and transesterification of crystallized PET/PC oligomers. The ^{1}HNMR data indicates that interchange reactions are prevalent during later stages of SSP. The degree of randomness increases with increase in transesterification reaction. The ^{1}HNMR results are correlated with thermal and WAXS studies to understand the structure and morphology of the copolymer obtained. DSC and WAXS results reveal the amorphization of PET and PC crystals below the melting temperature with the progress of SSP and transesterification. DSC studies on the SSP samples showed that, with increase in transesterification and viscosity, the crystallization of the copolymers became more and more difficult.

3.5 References:

1. Porter RS, Wang LH. Polymer 1992; 33: 2019.
2. Porter RS, Jonza JM, Kimura M, Desper CR, George ER. Polym Eng Sci 1989; 29: 55.
3. Utaki LA, Polymer Alloys and Blends: Hanser: New York 1989.
4. Pilati F, Marianucci E, Berti C. J Appl Polym Sci 1985; 30: 1267.
5. Ignatov VN, Carraro C, Tartari V, Pippa R, Scapin M, Pilati F, Berti C, Toselli M, Fiorini M. Polymer 1997; 38: 195.
6. Ignatov VN, Carraro C, Tartari V, Pippa R, Scapin M, Pilati F, Berti C, Toselli M, Fiorini M. Polymer 1997; 38: 201.
7. Zheng WG, Wan ZH, Qi ZN, Wang FS. Polym Int 1994; 34: 301.
8. Zheng WG, Qi ZN, Wang FS. Polym Int 1994; 34: 307.

9. Nassar TR, Paul DR, Barlow JW. J Appl Polym Sci 1979; 23: 85.
10. Murff SR, Barlow JW, Paul DR. J Appl Polym Sci 1984; 29: 3231
11. Chen XY, Bireley AW. Br Polym J 1985; 17: 347.
12. Hanrahan BD, Angeli SR, Runt J. Polym Bull 1986; 15: 455.
13. Suzuki T, Tanaka H, Nishi T. Polymer 1989; 30: 1287.
14. Tan Q, Ma DZ, J Appl Polym Sci 1993; 48: 747.
15. Zhang GY, Ma JW, Cui BX, Luo XL, Ma DZ. Macromol Chem Phys 2001; 202: 604.
16. Marchese P, Celli A, Fioroni M. Macromol Chem Phys 2002; 203: 695.
17. Godard P, Dekoninck JM, Devlesaver V, Devaux J. J Polym Sci, Part A Polym. Chem 1986; 24: 3315.
18. Huang ZH, Wang LH. Makromol Chem Rapid Commun 1986; 7: 255.
19. Kong Y, Hay JN. Polymer 2002; 43: 1805.
20. Fiorini M, Pilati F, Berti C, Toselli M, Ignatov V. Polymer 1997; 38: 413.
21. Licciardello A, Auditore A, Samperi F, Puglisi C. Appl Surf Sci 2003; 203-204: 556.
22. Godard P, Dekoninck JM, Devlesaver V, Devaux J. J Polym Sci, Part A Polym Chem 1986; 24: 3301
23. Eguiazabal JI, Ucar G, Cortazar M, Iruin JJ. Polymer 1986; 27: 2013.
24. Berti C, Bonara V, Pilati F. Makromol Chem 1992; 193: 1665.
25. James NR, Ramesh C, Sivaram S. Macromol Chem Phys 2001; 202: 2267.
26. Hait SB, Sivaram S. Macromol Chem Phys 1998; 199: 2689.
27. Hait SB, Sivaram S. 2000;US 6150493.
28. Iyer VS. 1994; Ph. D. thesis: University of Poona.
29. Yamadera R, Murano M. J Polym Sci A 1967; 5: 2259.
30. Radhakrishnan S, Iyer VS, Sivaram S. Polymer 1994; 35: 3789.
31. Murthy NS, Correale ST, Minor H. Macromolecules 1991; 24: 1185.
32. Wendling J, Suter UW. Macromolecules 1998; 31: 2516.
33. Lu X, Windle AH. Polymer 1995; 36: 451.
34. Sperling LH, Introduction to Physical Polymer Science, John Wiley & Sons, New York 1992.
35. Lee SC, Yoon KH, Park IIH, Kim HC, Son TW. Polymer 1997; 38: 4831.

CHAPTER 4

EFFECT OF POLY(ETHYLENE GLYCOL) AS AN ADDITIVE ON THE CRYSTALLIZATION AND SOLID STATE POLYMERIZATION OF POLY (ETHYLENE TEREPHTHALATE)

4.1 Introduction

Solid state polymerization (SSP) has been widely used to produce high molecular weight poly(ethylene terephthalate) (PET) resins used for molding applications. Generally, PET prepolymer having an intrinsic viscosity [η] ≈ 0.5 dL/g is polymerized in the solid state at a temperature just below the polymer's melting temperature in a stream of inert gas or under reduced pressure to produce high molecular weight PET[1]. Major factors influencing the SSP rate include the catalyst (type and concentration)[2], temperature[3], particle size[3], gas flow[4,5] and concentration of carboxyl end groups or carboxyl content [6-8]. Recently, PET oligomer having an intrinsic viscosity [η] ≈ 0.2 dL/g has been polymerized in the solid state[9-11]. It is generally accepted that the polymerization proceeds by step reactions in the amorphous phase of the semicrystalline polymer[1,11]. However, an optimum amount of crystallinity is required to prevent sticking or coalescence of the particles[12-13]. Within the SSP temperature range, in the amorphous phase, the functional end groups of the polymer chains are sufficiently mobile and activated to collide and react with one another to further increase the molecular weight [11]. The mobility of the polymer chain in the solid state is much lower than in the melt state, which retards reactions between two chain ends[14]. Because of the restriction of mobility, the time needed to reach a particular molecular weight is generally much longer than that in melt or solution[14].

Plasticizers are often added to semicrystalline polymers to lower the glass transition temperature (T_g). Plasticizing the amorphous regions of the polymer sample should give the chains increased mobility for chain extension reactions and should increase the diffusion coefficient of the byproduct in solid state polymerization[17,18]. DeSimone et al used supercritical CO_2 as the sweep fluid in polycarbonate SSP. It enhances the chain mobility for chain extension reactions and increases the diffusion coefficient of the byproduct because of plasticization of the amorphous phase[17,18]. It is known that the glass transition temperature of PET is reduced by using a small amount of codiols or long diols (polyethers) as comonomers (internal plasticizers)[19-21]. Recently, Lin et al[22] synthesized PET copolymers with poly(ethylene glycol) methyl ether (one side end capped) end groups and demonstrated that low level of PEG end groups enhance the PET crystallization. Xue et al[23] showed that crystallinity of PET was improved by precipitating from a PEG solution at a low temperature.

In the present study for the first time we have explored the use of small amount (2.5-10%) of poly (ethylene glycol) and end capped poly (ethylene glycol) [Poly(ethylene glycol)

dimethyl ether (PEGDME)] of number average molecular weight 1000 as plasticizers with a view to understand the effect of plasticizer on the SSP of PET. It is expected that PEGDME just depresses the T_g and modifies the crystallization behavior of PET, while PEG apart from influencing the T_g and crystallization behavior, reacts with PET and forms a copolymer.

4.2 Experimental

4.2.1 Materials

The starting sample was a commercial high molecular weight PET having intrinsic viscosity of 0.69 dL/g from Eastmann chemicals and was used as received. Methanol, Phenol, 1,1,2,2-Tetra Chloroethane (TCE) was supplied by Sd Fine Chemicals Bombay and used after distillation. Trifluoro acetic acid (TFA) and chloroform-d needed for NMR were obtained from Aldrich Chemical Company Inc. USA, and were used as such. Poly(ethylene glycol) dimethyl ether (PEGDME) oligomer of number average molecular weight 1000 was obtained from Aldrich and Poly(ethylene glycol) of number average molecular weight 1000 was obtained from BDH chemicals Ltd., England. PEG and PEGDME were dried azeotropically with toluene before use.

4.2.2 Preparation of oligomer

PET oligomer was prepared by hydrolysis of high molecular weight PET pellets. Hydrolysis was carried out in deionized water in a Parr reactor at 180^{o}C. The oligomer obtained was filtered and dried at 60°C under reduced pressure. The inherent viscosity of the PET oligomer was 0.16 dL/g.

4.2.3 Blending of PEGDME and PEG with PET oligomer:

The PEGDME and PEG of different weight percentages were blended with the PET oligomer by melt mixing in a Midi 2000 co-rotating twin screw extruder from DSM Research (The Netherlands). The batch size was ~ 5 g and the oligomers were blended at 250^{o}C for 5 min., at a screw speed of 100 rpm.

4.2.4 Solid state polymerization

The PET oligomer crystallized during cooling after extrusion. The catalyst antimony trioxide (1000 ppm) was incorporated into PET by refluxing the sample in acetone for 1 h. Acetone was stripped off in a rotatory evaporator and the oligomer was dried under vacuum at 60^{o}C. The SSP was performed in a glass reactor according to a well defined

temperature protocol under reduced vacuum. Samples were periodically removed for characterization.

4.2.5 Characterization

Inherent viscosities were measured at 30^{o}C in an automated Schott Gerate AVS 24 viscometer, using an Ubbelohde suspended level viscometer in phenol/1,1,2,2-tetrachloroethane (TCE) (60: 40, w/w) at a polymer concentration of 0.5%. The X-ray diffraction experiments were performed using a Rigaku Dmax 2500 diffractometer. The system consists of a rotating anode generator with a copper target and a wide-angle powder goniometer, having diffracted beam graphite monochromator. The generator was operated at 40 kV and 150 mA. All the experiments were performed in the reflection mode. The samples were scanned between $2\theta = 5$ to 35° at a speed of 1°/min. Calorimetric measurements were performed using a Perkin-Elmer thermal analyzer (DSC -7) at a heating/cooling rate of 10^{o}C/min in a nitrogen environment. ^{1}H NMR was performed in a Bruker DRX 200 spectrometer at 25^{o}C operating at 200 MHz. The samples were dissolved in $CDCl_3$/TFA (70:30, v/v) mixture and the spectra were internally referenced to tetramethyl silane.

4.3 Results and Discussions

4.3.1 Plasticization of PET oligomers and its crystallization

The PET oligomers exhibit a glass transition temperature at 70°C. The addition of PEG and PEGDME has profound effect on the T_g. The glass transition temperature decreases rapidly with increasing PEG and PEGDME content as shown in Figure 4.1; the PET-PEGDME samples show marginally lower T_g compared with PET-PEG samples. Possibly the end caps (OCH_3) in the PEGDME generate larger free volume compared with PEG. The cold crystallization peak temperature (T_{cc}) on heating the amorphous samples, obtained by quench cooling, is shown in Figure 4.2. It is apparent from the figure that the incorporation of plasticizers decreases the T_{cc} indicating faster crystallization and also it depends on the amount of additive added to the oligomer. It is observed that both PEG and PEGDME enhanced the crystallization rate when crystallized from glassy state. This may be attributed to the plasticization of PET chains by the addition of PEG and PEGDME. However, when the samples are crystallized from the melt, different results are observed. In the case of PEG blended samples melt crystallization temperature (T_c), shown in Table 4.1 decreases with increasing amount of PEG while PEGDME does not affect the melt

crystallization temperature on cooling. Possibly that very small fraction of PEG reacts with PET during melt blending and forms a copolymer and decreases the crystallization temperature. Further, these results indicate that the additives do not influence the mobility of the polymer chains in the melt.

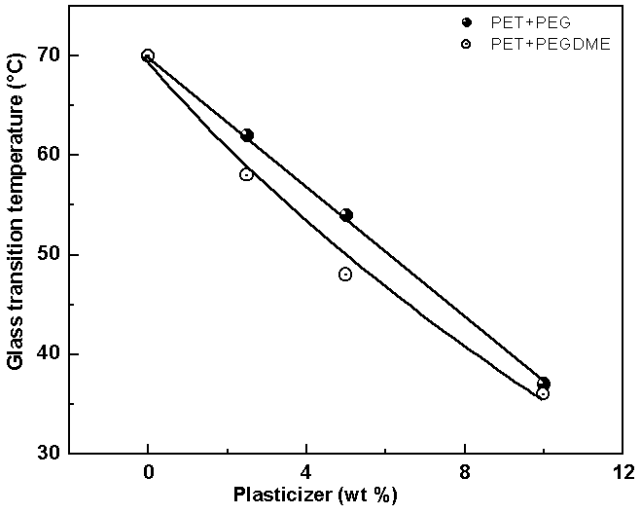

Figure 4.1: Change in glass transition temperature with the amount of plasticizer (wt/wt) incorporated in PET oligomer

4.3.2 Solid state polymerization of plasticized PET oligomer

Plasticized oligomer blends were subjected to SSP for 20 h at constant temperature under dynamic reduced pressure. The SSP temperature was determined by the onset of melting of the blend samples. The PET-PEG blend samples exhibited lower onset temperature compared to PET-PEGDME blends. Hence the former samples were solid state polymerized at 220^{o}C and the later samples at 230°C. Figure 4.3 a and b show the change in inherent viscosity (η_{inh}) with time for various samples. All the samples underwent SSP to a significant extent, as indicated by the increase in inherent viscosity (η_{inh}) with time. Starting η_{inh} for all the samples were 0.18 dL/g. Interestingly PET-PEG blend samples show higher viscosity compared to PET oligomer. On the other hand in the case of PET – PEGDME blends the PET oligomer shows higher viscosity. The effect of temperature is seen in the viscosity; PET polymerized at 230°C shows higher viscosity than the PET polymerized at 220°C. The present data clearly show that PEG enhances the SSP rate while PEGDME retards the SSP rate. It should be kept in mind that the PET-PEG samples are polymerized at a lower temperature even then these samples show higher viscosity than the PET-PEGDME samples polymerized at 230°C.

Table 4.1: Effect of plasticizer content on melt crystallization temperature.

Plasticizer content (wt%)	Melt crystallization temperature (°C)	
	PEG	PEGDME
0	214	214
5	207	213
10	203	211

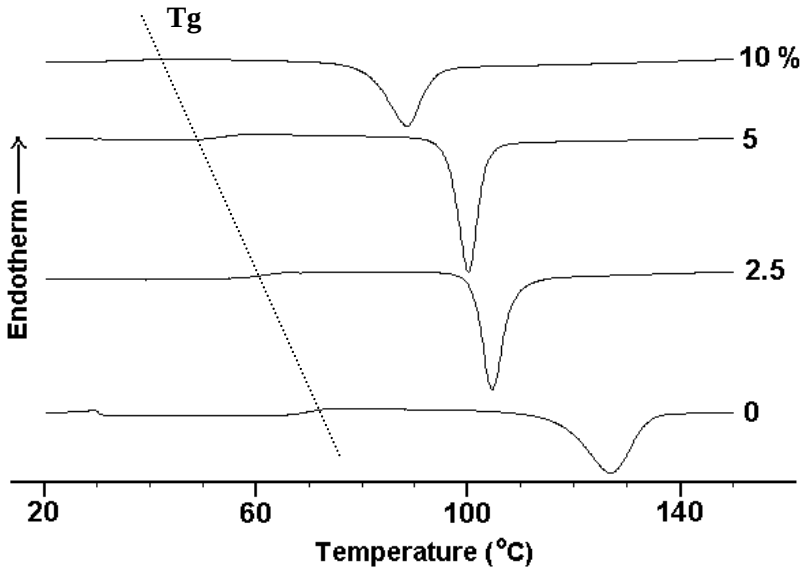

Figure 4.2: Effect of plasticizer content (PEG) on the cold crystallization temperature (T_c). (Note: Samples were rapidly melted and quenched before scanning).

Another important point is that the amount of PEG also influences the SSP. With increase in the amount of PEG, the viscosity also increases, while in the case of PEGDME the viscosity decreases with increase in the amount of PEGDME. The observed effects may be traced to the copolymer formation in the case of PET-PEG blends during the SSP while copolymer formation is prevented in the case of PET-PEGDME blends since PEGDME is end capped. James et al[11] reported that the crystallites do not undergo reorganization during SSP and the chain ends in the amorphous phase mainly control the SSP. Plasticizers reside in the amorphous phase and increase the mobility of the polymer chains. The increase in the amorphous mobility will increase the reaction rate. Indeed, the

PEG and PEGDME increase the amorphous mobility as evidenced from the T_g reduction. However, at the SSP temperature PEGDME may act as a barrier between the

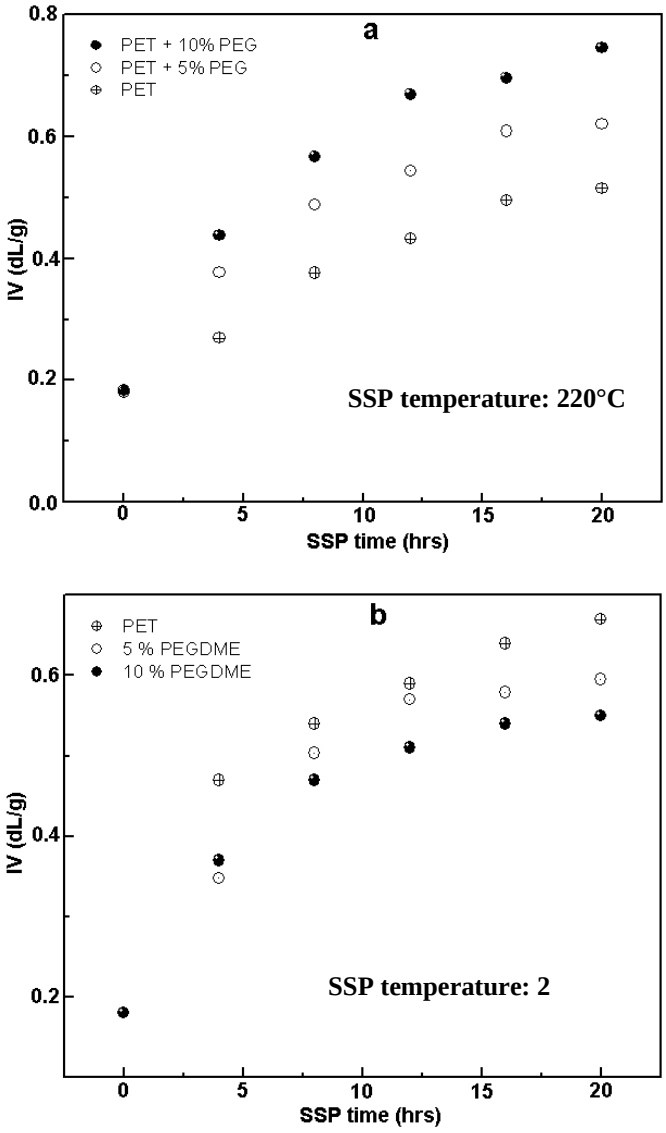

Figure 4.3: Changes in η_{inh} during SSP of a) PET blended with different amounts of PEG b) PET blended with different amounts of PEGDME

PET chain ends to collide in the amorphous region for the reaction to occur. The decrease in the viscosity with increase in the amount of PEGDME supports the above argument. However, in the case of reactive PEG, higher viscosities are observed. It may be because of the chain extension between PEG and PET oligomers in the amorphous region. Hydroxyl end groups of PEG oligomer react with the PET chain ends to form a copolymer and lead to build up in the viscosity. Indeed, the ^{1}H NMR studies on these samples show

that the PEG reacts with the PET during SSP forming a copolymer. Samples are dissolved in phenol/1,1,2,2-tetrachloroethane (TCE) (60: 40, w/w) and reprecipitated in methanol to remove the unreacted PEG and PEGDME in the samples. Figure 4.4 shows the ^{1}H NMR trace of the PEG and PEGDME blended samples before and after SSP and reprecipitated samples. In ^{1}H NMR spectra, 8.02 ppm corresponds to the four protons of terephthalic acid residue and 4.8 ppm corresponds to ethylene protons of PET. Peak at 3.8 ppm corresponds to the protons in PEG and PEGDME. As shown in the Figure 4.4, the peak at 3.8 ppm disappears in the case of PET-PEGDME sample (C) after dissolving and reprecipitating. It indicates that PEGDME does not form a copolymer with PET but remains in the amorphous phase and the dissolution and reprecipitation process removes it from the samples. On the other hand, PET-PEG retains (C) the peak at 3.8 ppm indicating the copolymer formation during SSP. The dissolution and reprecipitation process could not remove PEG as it reacted with PET and forms a copolymer. The amount of PEG incorporated into the PET is given in the Table 4.2.

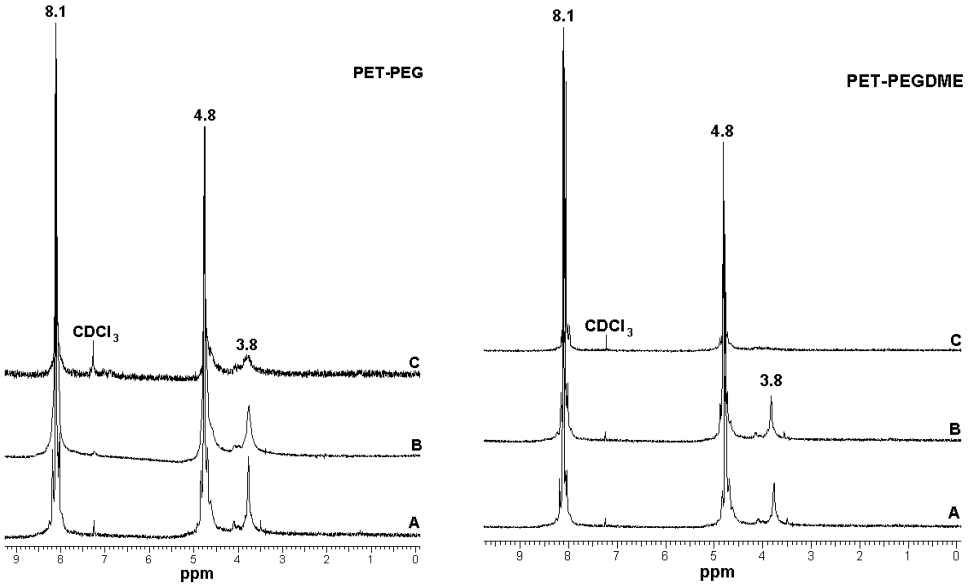

Figure 4.4: ^{1}H NMR spectra of after SSP samples of PET+10% PEG and PET+10% PEGDME A) BSSP B) ASSP C) Dissolved and reprecipitated

Table 4.2: ^{1}H NMR analysis of PET-PEG and PET-PEGDME samples at various conditions.

Sample Wt (%)	Loaded	BSSP	ASSP	Dissolved and reprecipitated
PEG	10	9.5	8.8	7.6
PEGDME	10	9.4	7.6	0.5

4.3.3 Structure and Morphology

4.3.3.1 X-ray diffraction studies

The change in the structure and morphology of plasticized and unplasticized PET samples during the course of SSP was monitored by WAXS and DSC. Figure 4.5 a-d shows the changes in the WAXS patterns of various samples during SSP. These WAXS patterns do not show any obvious change during SSP indicating that the crystals do not undergo major reorganization. Further, the peak positions are at 2θ = 15.92, 17.46, 21.16, 22.36 and 25.73° and indexed to $0\bar{1}1$, 010, $\bar{1}11$, $\bar{1}10$ and 100 reflections respectively based on PET crystal structure[24]. The crystal size was calculated from 010 reflection of PET and shown in Table 4.3 for various samples. It is obvious from the results that unplasticized PET oligomer shows thinner crystals of size close to 7 nm than plasticized PET with PEG and PEGDME, which is close to 9 nm. This may be due to the enhancement of crystallization rate of PET by the addition of plasticizers as discussed in the above part. As shown in the figure 4.5, after 4 h of SSP all the samples showed sharp reflections indicating the increase in crystal sizes because of the thermal annealing at SSP temperature. After 4 h of SSP there is no significant change observed in the diffractograms. Crystal sizes also do not vary much during the SSP. It indicates that the crystallites do not undergo changes or reorganization during SSP. The x-ray diffraction data indicates that PEG does not enter the lattice and remains in the amorphous phase. This result is not unexpected as the monomer lengths of PET and PEG are different and PET lattice cannot accommodate the PEG. Since the NMR spectra of PET-PEG blend and the PET-PEG copolymers are similar, the sequence lengths of PET and PEG segments could not be evaluated. Nevertheless, it is expected that long sequence of PET segments in these samples and PET can crystallize on its own[25].

Table 4.3: The crystal size data of various samples at different stages of SSP.

SSP time (h)	Crystal Size (nm)			
	PET	PET + PEGDME (5 %)	PET + PEG (5 %)	PET + PEG (10 %)
0	7	9	9	9
4	7	11	11	11
8	8	11	11	10
12	8	11	10	11
16	8	10	10	11
20	8	11	10	11

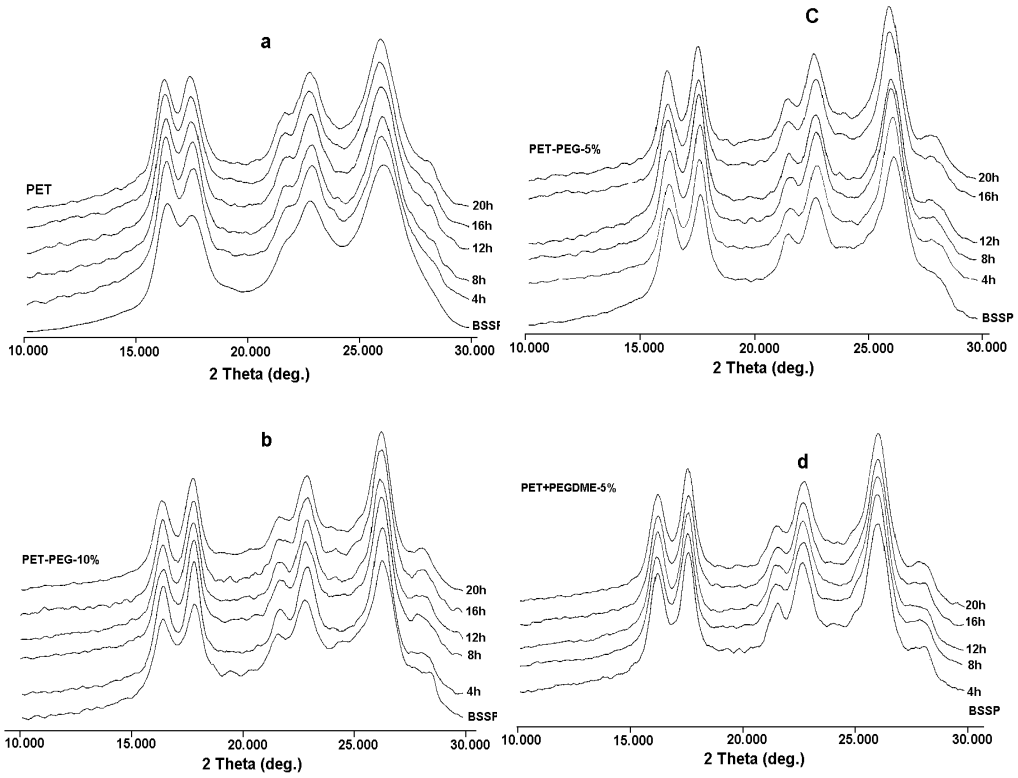

Figure 4.5: X ray diffraction patterns of a) PET b) PET+10% PEG blended sample c) PET+ 5% PEG blended sample d) PET+10% PEGDME blended sample at various stages of SSP

4.3.3.2 DSC studies

The thermal properties of the samples were studied in detail to understand the change in the structure and morphology during SSP. The melting temperature during the first heat as shown in Figure 4.6 does not change during SSP, while the heat of fusion increases indicating increase in crystallinity during SSP, however, considering the temperature and time the increase in the crystallinity is very marginal. T_m and ΔH are given in Table 4.4 for various samples during first heat. These results are in confirmation with WAXS data that during SSP the crystals do not undergo any changes, though the SSP is performed at temperatures close to the melting temperature. Hence WAXS and thermal data during first heat is not representative of the polymerized sample. However, the exotherm on the first cooling and the events occurring during the second heating are representative of the polymerized sample. Figure.4.7 and Figure 4.8 show the DSC thermograms for cooling and reheating. The thermal data obtained during cooling and second heating cycle are given in Table 4.5 and Table 4.6. The heat of fusion, when compared with the starting oligomer samples, decreases for all the samples indicating high molecular weight after SSP. Also, the PET-PEG sample shows the highest reduction in heat of fusion and is attributed to the copolymer formation, in which the PEG segments retard, the crystallization.

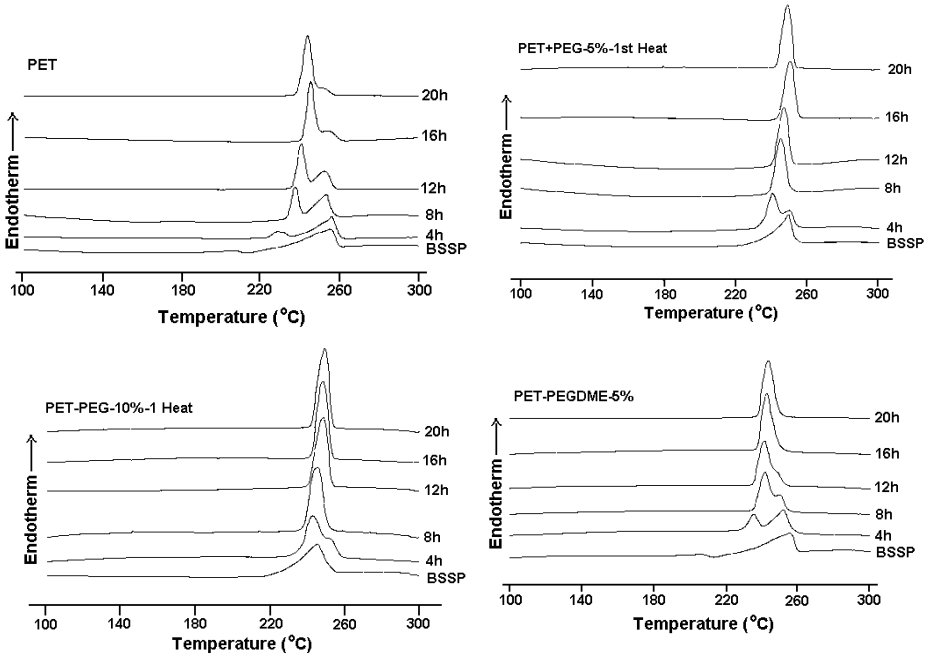

Figure 4.6: DSC thermograms of various samples during the course of SSP. (First heating)

Table 4.4: DSC data for various samples during first heat

SSP time (h)	PET		PET+PEGDME (5 %)		PET+PEG (5 %)		PET+PEG (10 %)	
	T_m (°C)	ΔH (J/g)	T_m (°C)	ΔH (J/g)	T_m (°C)	ΔH (J/g)	T_m (°C)	ΔH (J/g)
0	255	66	249	57	249	57	245	56
4	256	65	252	66	250	68	243	66
8	254	68	242	68	245	68	246	66
12	254	74	241	70	247	69	248	66
16	255	74	243	72	249	70	248	65
20	253	74	244	73	249	69	249	62

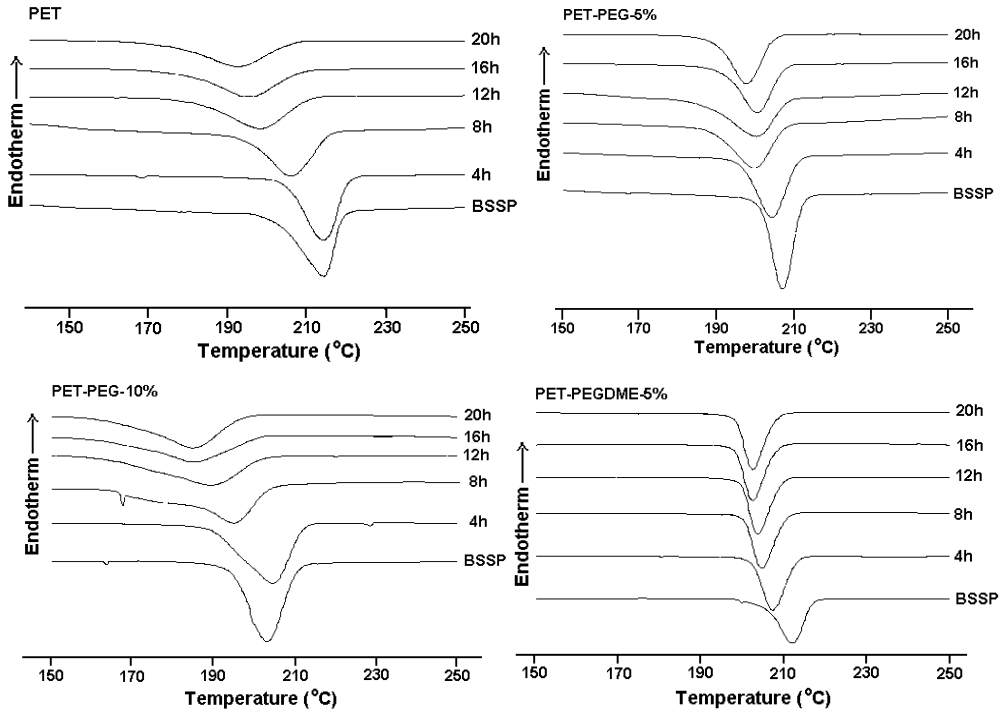

Figure 4.7: DSC thermograms of various samples during the course of SSP. (Cooling from the melt)

Table 4.5: DSC data for various samples during cooling

SSP conditions (h)	PET		PET+PEGDME (5 %)		PET+PEG (5 %)		PET+PEG (10 %)	
	T_{mc} (°C)	ΔH (J/g)	T_{mc} (°C)	ΔH (J/g)	T_{mc} (°C)	ΔH (J/g)	T_{mc} (°C)	ΔH (J/g)
0	214	58	213	49	207	54	203	45
4	214	53	207	48	204	46	204	44
8	206	47	205	48	200	43	195	40
12	198	49	204	47	200	43	189	36
16	195	42	203	46	200	42	185	32
20	193	42	203	46	198	41	185	32

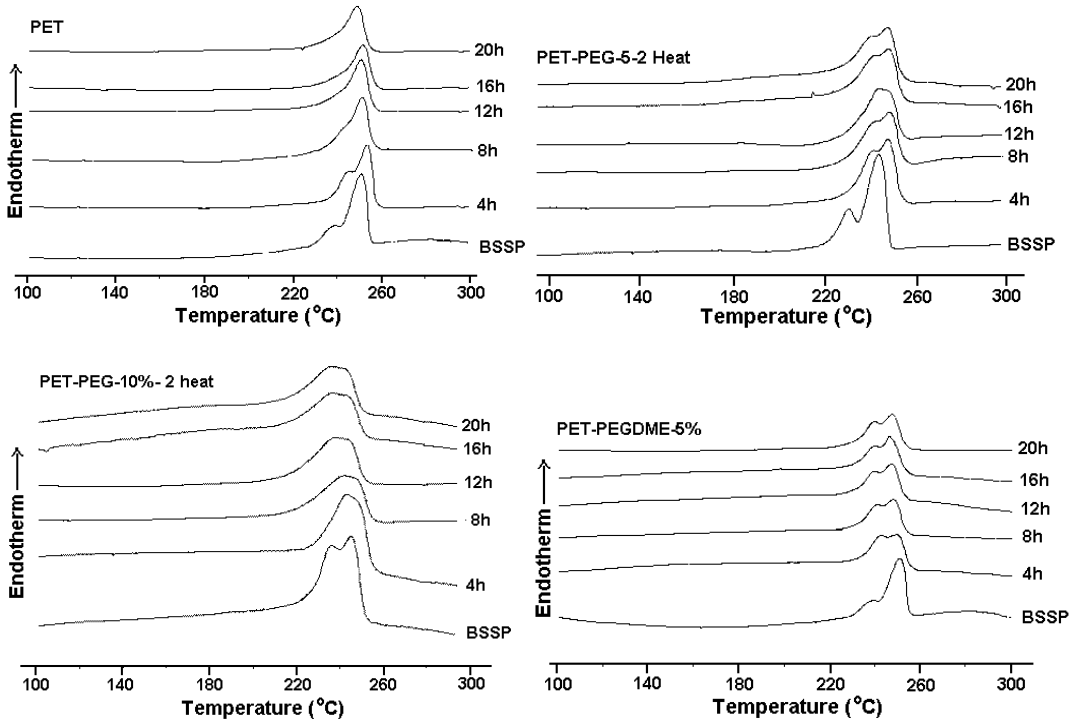

Figure 4.8: DSC thermograms of various samples during the course of SSP. (Second heating)

Table 4.6: DSC data for various samples during second heat

SSP conditions (h)	PET		PET+PEGDME (5 %)		PET+PEG (5 %)		PET+PEG (10 %)	
	T_m (°C)	ΔH (J/g)	T_m (°C)	ΔH (J/g)	T_m (°C)	ΔH (J/g)	T_m (°C)	ΔH (J/g)
0	251	54	251	50	243	53	245	48
4	254	59	250	46	248	42	244	41
8	252	43	248	46	248	37	242	34
12	251	44	247	45	244	38	238	34
16	252	40	247	44	247	38	237	31
20	249	40	248	43	247	38	237	31

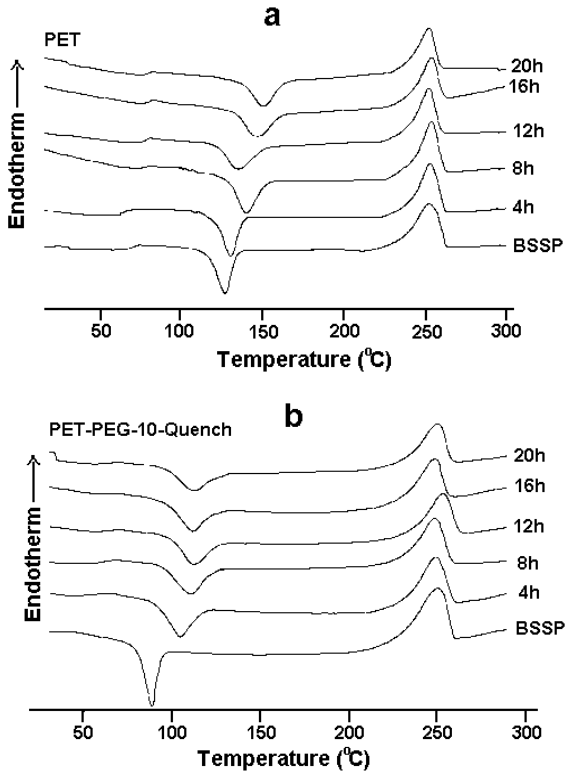

Figure 4.9: DSC thermograms of quenched PET and 10% PEG blended samples at various stages of SSP. (Note: Samples were rapidly melted and quenched before scanning.

The glass transition temperatures (T_g's) were not observed for the crystallized and SSP samples, as all these samples are crystalline in nature. Hence separate sets of DSC scans were performed for these samples by melting and rapidly quenching in ice water. On heating, these samples showed T_g, cold crystallization temperature (T_{cc}) and melting temperature. Figure 4.9 shows the thermograms of quenched PET and 10 % PEG incorporated samples at various stages of SSP as examples. Table 4.7 gives the T_g, T_{cc} and T_m before and after the solid state polymerization for all the samples. All the samples showed increase in T_g and T_{cc} with SSP time indicating the increase in molecular weight. T_{cc} peaks progressively shift towards higher temperature and become smaller and broader with the progress of SSP.

Table 4.7: DSC data for various samples BSSP and ASSP. (Note: Samples were rapidly melted and quenched before scanning)

Samples	**SSP conditions**	**T_g (^oC)**	**T_{cc} (^oC)**	**ΔH_c (J/g)**	**T_m (^oC)**	**ΔH_m (J/g)**
PET	BSSP	70	127	37	253	63
	ASSP	81	151	35	253	47
PET + PEGDME (5 %)	BSSP	48	94	31	252	70
	ASSP	62	108	26	251	47
PET + PEG (5 %)	BSSP	55	100	35	249	62
	ASSP	71	125	28	250	40
PET + PEG (10 %)	BSSP	37	89	27	250	60
	ASSP	65	112	23	250	39

4.4 Conclusions:

In this study we examined the effect of PEG and PEGDME of number average molecular weight 1000 on the crystallization and solid state polymerization of PET. Glass transition temperature and crystallization rate were strongly affected by both PEG and PEGDME.

Glass transition temperature of PET linearly depends on the amount of PEG and PEGDME incorporated. The plasticizers do not affect the crystalline morphology even though it influences the crystallization rate. PEG incorporated samples form copolymers and they show improved SSP rates compared to the SSP of PET oligomer under the similar conditions. On the other hand PEGDME sample cannot form a copolymer, and retarded the SSP. Structure and morphology studies indicate that the PEG segments remain in the amorphous phase of the copolymer. These results indicate that reduction in T_g alone cannot enhance the SSP rate of PET.

4.5 References:

1. Schulz JM, Fakirov S, Solid State Behaviour of Linear Polyesters and Polyamides, Prentice Hall, Engle wood cliffs, NJ 1990.
2. Kokkalas DE, Bikiaris DN, Karayannidis GP. J. Appl. Polym. Sci. 1995; 55: 787.
3. Papaspyrides CD, Kampouris FM. Polymer 1984; 25: 791.
4. Huang B, Walsh JJ, Polymer 1998; 39: 6991.
5. Mallon F, Beers K, Ives A, Ray WH. J. Appl. Polym. Sci. 1998; 69: 1789.
6. Duh B. J. Appl. Polym. Sci. 2002; 83: 1288.
7. Duh B. U.S. Pat. 4,205,157; 1980.
8. Duh B. U.S. Pat. 4,238,593; 1980.
9. Stouffer JM, Blanchard EN, Leffew KW. US Pat. 5, 510, 454; 1996.
10. Stouffer JM, Blanchard EN, Leffew KW. US Pat 5, 540, 868; 1996.
11. James NR, Ramesh C, Sivaram S. Macromol. Chem. Phys. 2001; 202: 1200.
12. Zimmerman J. J. Polym. Sci. 1964; 62: 995.
13. Chang TM. Polym. Eng. Sci. 1970; 10: 364.
14. Chen FC, Griskey RG, Beyer GH. AIChE J. 1969; 15: 680.
15. Jackson JWJ, Kuhfuss HF. J. Polym. Sci., Polym. Chem. Ed. 1976; 14: 2043.
16. Pohl HA. J. Am. Chem. Soc. 1951; 73: 5660.
17. Gross SM, Roberts GW, Kiserow DJ, DeSimone JM. Macromolecules 2000; 33: 40.
18. Shi C, DeSimone JM, Kiserow DJ, Roberts GW. Macromolecules 2001; 34: 7744.
19. Bier P, Binsack R, Vernaleken H, Rempel D. Angew Makromol Chem 1977; 65: 1.
20. Nield E. U.S. Pat. 4,322,335; 1982.
21. Jackson JB, Longman GW. Polymer 1969; 10: 873.

22. Lin Q, Unal S, Fornof AR, Wei Y, Li H, Armentrout RS, Long TE. Macromol Symp 2003; 199: 163
23. Xue G, Ji G, Yan H, Guo M. Macromolecules 1998; 31: 7706.
24. Daubery RD, Bunn CW, Brown C. J. Proc. R. Soc, London, Ser. A 1954; 226: 531.
25. Jun HW, Chae SH, Park SS, Myung HS, Im SS. Polymer 1999; 40: 1473.

CHAPTER 5

STUDIES ON THE SOLID STATE POLYMERIZATION OF PET/POB OLIGOMER BLENDS

5.1 Introduction:

Copolyesters of poly(ethy1ene terephthalate) (PET) and p-hydroxybenzoic acid are well known as liquid-crystalline polymers. Jackson and Kuhfuss first described the preparation and liquid crystallinity of poly(ethylene terephthalate-*co*-oxybenzoate) (P(ET-*co*-OB)), currently sold commercially as Rodrun LC-5000[1-3]. P(ET-*co*-OB) is prepared by reactive blending of PET and *p*-acetoxybenzoic acid (ABA) to facilitate transesterification with loss of acetic acid to incorporate oxybenzoate units into the polymer. PET-*co*-OB is a liquid crystalline polymer in which the fraction of oxybenzoate repeat units is at least 40 mol %. Recently Kang et al[4] synthesized and characterized PET copolymers modified with a broad range of *p*-acetoxybenzoic acid (PABA) compositions. It was found that PET copolyesters with a composition of more than 40 mol % PABA form thermotropic nematic liquid crystals. Extensive literature was published on the thermal properties[5-8], crystal structure[5,9,10], phase separation and morphology[5-7, 9,11], and sequence distribution[1,12-17] of the copolyesters. Ponrathnam et al[18] synthesized poly(ethylene terephthalate-co-oxybenzoate) via melt polyesterification route and studied for copolyesterification kinetics by evaluating the byproduct i.e. acetic acid. A series of co[poly (ethylene terephthalate-p–oxybenzoate)] copolyesters with POB content of 0-100 mol % were prepared by melt polycondensations of p-acetoxybenzoic acid with either PET or its oligomer and characterized for thermal stability, X-ray diffraction analysis, morphological observation by polarizing microscopy. Most of these studies did not consider the changes in molecular weight or viscosity with the progress of transesterification.

This chapter focuses on the preliminary examination of the structure and morphology development during the interchange reaction in the solid state polymerization of PET/POB oligomer blend. The PET/POB oligomers were initially melt blended. The crystallized blend was subjected to interchange reaction in the solid state by holding the blend just below the melting temperature under reduced pressure. The change in the structure and morphology was monitored by DSC and X-ray diffraction. PET/POB copolymer was also obtained by melt polymerization and the structure and morphology was compared to the copolymer formed by SSP.

5.2 Experimental:

5.2.1 *Preparation of PET oligomers:*

PET oligomer was prepared by glycolysis of high molecular weight PET pellets (η: 0.69 dL/g) obtained from Eastman Chemicals, USA. 50 g of PET pellets and 250 ml ethylene

glycol were taken in a 1000 ml round bottom flask. Temperature was raised to 190°C while the pellets were stirred thoroughly. Reaction was continued for 10h at 190°C. The residue was filtered and washed with hot water and methanol to remove the ethylene glycol and was dried at 80°C for 12h. The oligomer obtained was filtered and dried at 60°C under reduced pressure. The inherent viscosity of the PET oligomer was 0.16 dL/g in phenol/1,1,2,2-tetrachloroethane.

5.2.2 *Preparation of POB oligomers:*

POB oligomer was prepared by melt polymerization of 0.05 mol (9.008 g) of 4-acetoxybenzoic acid at 250°C under atmosphere pressure. Dry nitrogen was purged throughout the reaction to prevent oxidation and degradation. The progress of the reaction was monitored by distillation of the side product, acetic acid[19]. After the removal of 0.8 ml acetic acid the reaction was stopped and the oligomer was collected. Heating the oligomer to 190°C under vacuum sublimed the unreacted monomer.

5.2.3 *Preparation of poly(ethylene terephthalate-co-oxybenzoate) copolymer by melt condensation:*

A mixture of PET oligomer (70 mol %) and POB oligomer (30 mol%) was placed in a 80 ml glass lined electrically heated three necked reactor equipped with a glass stirrer. The reaction temperature was maintained at 275°C for 4 h. Dry nitrogen was purged throughout the reaction to prevent oxidation and degradation. The progress of the reaction was monitored by distillation of the side product, acetic acid[19]. After the removal of acetic acid the reaction was stopped and the copolymer was collected. Heating the copolymer to 190°C under vacuum sublimed unreacted monomer.

5.2.4 *Preparation of oligomer blends:*

The blends of PET and POB oligomers were prepared in a Midi 2000 co-rotating twin-screw extruder from DSM Research (The Netherlands). The batch size was about 5 g and the oligomers were blended at 330^{o}C for 1 min., with a screw speed of 100 rpm to minimize the transesterification during blending.

5.2.5 *Crystallization and solid state polymerization:*

The oligomer blend crystallized during cooling after extrusion and hence no separate crystallization step was needed. The catalyst zinc acetate (1 wt%) was incorporated by refluxing the sample in pet ether for 1 h. Pet ether was stripped off in a rotatory evaporator

and the oligomer blend was dried under vacuum at 60^{o}C. The SSP was performed in a glass reactor according to a well-defined time temperature protocol under reduced vacuum. Samples were periodically removed for structure and morphology characterization.

5.2.6 *Characterization:*

Polarized optical microscopic observation was performed on an Olympus PM-C35B polarizing microscope equipped with a video camera and also image plus software for data analysis. Magnification of 20X was used for the analysis. Samples were placed between a microscope glass slide and a cover slip. Images were captured using Image plus software. Thermal and WAXS analysis was performed according to the procedures described in the Chapter 3.

5.3 Results and Discussions:

5.3.1 Solid state polymerization:

Inherent viscosity of the PET oligomer is 0.15 dL/g. However, when it is melt blended with the POB oligomer the blend IV came down to 0.07 dL/g. The apparent reduction in the viscosity may be due to a decrease in the characteristics of the solvent in the presence of 4-acetoxybenzoic acid. The solvent tends towards a theta solvent there by decreasing the viscosity. The blend crystallized on cooling from the melt and is used as a precursor for SSP. The crystallized oligomer blend (PET/POB 70/30 mol/mol) is subjected to SSP at different time temperature protocol as shown in the table 5.1 under dynamic reduced pressure. Table 5.1 gives the change in inherent viscosity (η_{inh}) during SSP. The starting SSP temperature is 210^{o}C and is dictated by the onset of melting of the crystallized sample. The SSP temperature is progressively increased during the course of the reaction because the onset of melting shifted to higher temperature with increase in the SSP time. The sample underwent solid state polymerization to significant extent as indicated by the increase in inherent viscosity with time. Nevertheless it must be kept in mind that the PET and POB have different set of Mark-Houwink constants for the given polymer-solvent combination. Hence, direct extrapolation of viscosity to molecular weight and comparison may not be appropriate.

The copolyester synthesized according to the procedure reported elsewhere[19] shows the inherent viscosity 0.3 dL/g. It is known that the transesterification reaction is stopped once the evolution of acetic acid ceased to occur under atmosphere pressure. It has been shown

that PET and POB undergo interchange reaction in the melt state[1-15,18] and hence it is expected that PET and POB should undergo interchange reaction in the solid state, albeit at lower rates. It may be noted that the copolyesters obtained by melt polymerization and solid state polymerization are indeed oligomers as seen from the low viscosities.

Table 5.1: Change in inherent viscosity with SSP time temperature protocol

SSP conditions Temperature / Time	IV* (dL/g)
BSSP	0.07
200°C – 1 hr	0.11
210°C – 2 hr	0.11
220°C – 4 hr	0.12
230°C – 4 hr	0.25
230°C – 8 hr	0.29

* IV's are calculated with respect to the PET weight.

The infrared spectra are recorded for the sample at various stages of SSP. It is observed that the band due to C=O stretching reduced to a great extent with the progress of SSP. This is indicative of the elimination of acetic acid (acetyl C=O group) during the SSP and interchange reaction between PET and POB oligomers. Another important observation is the infrared spectra of the copolymer obtained by melt polymerization and SSP looks similar.

5.3.2 X- ray diffraction studies:

The room temperature structure of the samples was analyzed by WAXD. Figure 5.1 gives X-ray diffraction patterns of PET and POB oligomers. PET and POB have major reflections in the 2θ ranges from 14 to 30°. PET shows two strong reflections $0\bar{1}1$ and 010 at 15.92 and 17.46° respectively[20]. The other prominent reflections of PET are at 2θ = 21.16, 22.36 and 25.73° and are indexed as $\bar{1}11, \bar{1}10$ and 100[20]. POB diffraction pattern is comparable to the diffraction pattern reported in the literature[21,22]. The major reflection of POB occurs at 2θ =19.9° and the two weak reflections at 23 and 29°.

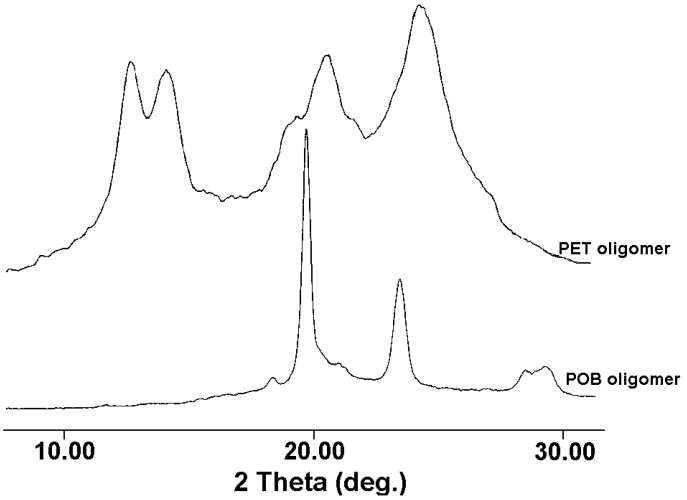

Figure 5.1: X ray diffraction pattern of POB and PET oligomer at room temperature

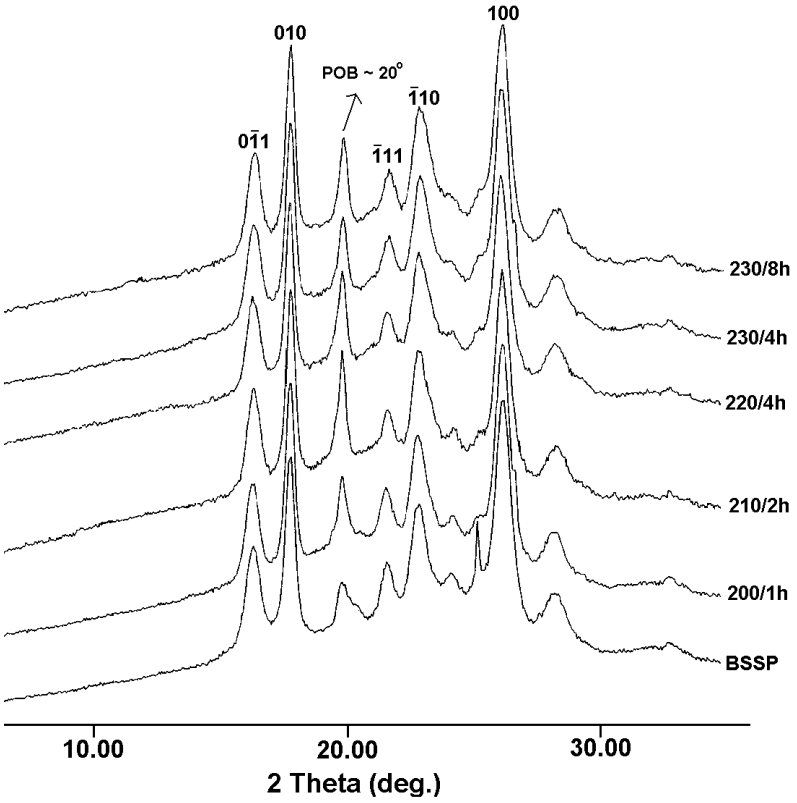

Figure 5.2: The change in the WAXS patterns of the 70/30 (PET/POB) blend during the course of SSP

The WAXD patterns of the 70/30 (PET/POB) blend before and during the course of SSP is shown in Figure 5.2. In the blend samples, PET reflections appear along with the POB reflections.

The XRD patterns are very sharp for the crystallized samples. The crystal size was calculated from 110 and 010 reflections of PET and from the reflection at 2θ ~ 19.9° for POB and are given in Table 5.2. The PET reflections are distinctly sharper in the blend sample compared to the homo oligomer pattern in the Figure 5.1. It appears that the POB helps to crystallize PET into big crystals.

Table 5.2: The crystal sizes calculated from 110 and 010 reflections of PET and from the reflection at 2θ ~ 19.9° for POB at various stages of SSP.

SSP conditions Temperature/ Time	**Crystal Size (nm) PET (From 010 reflection)**	**Crystal Size (nm) POB (from 2θ ~ 19.9° peak)**
BSSP	18	20
200/1 hr	21	21
210/2 hr	21	32
220/4 hr	21	20
230/4 hr	20	21
230/8 hr	19	23

A careful examination of the diffraction patterns after SSP shows that they do not vary significantly from the crystallized sample. Table 5.2 gives the crystal sizes during SSP for various samples and the crystal sizes do not vary significantly. This indicates that the crystallites do not undergo changes or reorganization during SSP. It has been shown elsewhere[23,24] that in the case of crystallized PET oligomers, the crystallites also do not undergo reorganization during SSP and the chain ends in the amorphous phase mainly control the SSP and it appears that a similar mechanism is operative for these blend samples as well. However in the case of blend samples, in addition to the chain extension reaction, exchange reaction between PET and POB also takes place simultaneously in the amorphous phase leading to the formation of copolymer. It is worth comparing the copolymer prepared by SSP route and by the melt polymerization method.

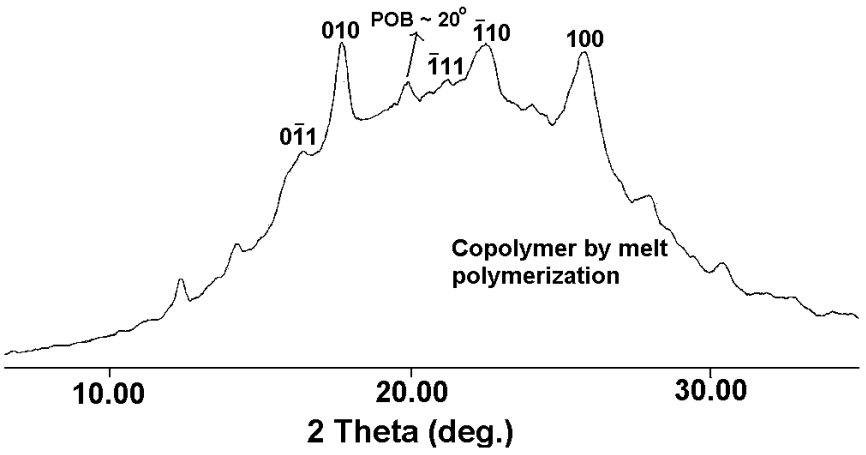

Figure 5.3: X-ray diffraction pattern of the copolymer prepared by melt polymerization

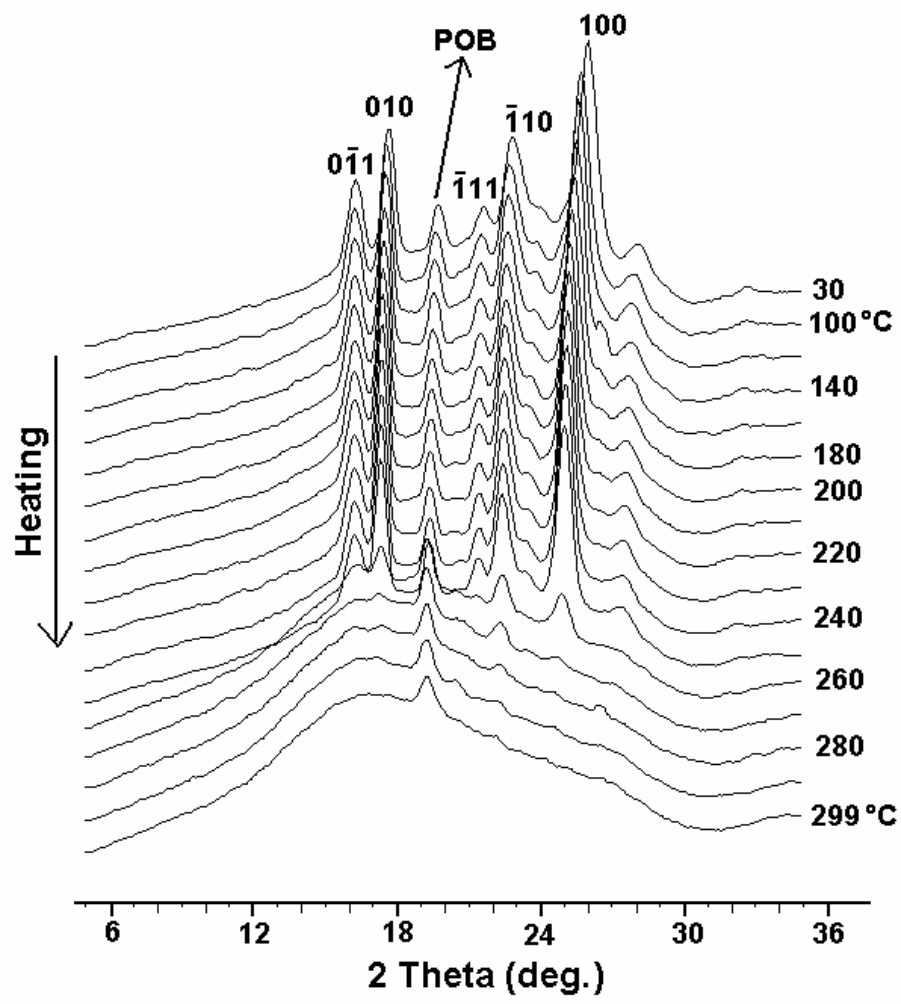

Figure 5.4: X-ray diffraction patterns obtained at various temperatures for the SSP performed sample.

The X-ray diffraction pattern of the copolymer prepared by melt polymerization shown in the figure 5.3 is different from the SSP diffractograms. By the addition of PABA into PET, the degree of crystallinity is decreased because of the disrupting order of the PET-PABA copolymer by the presence of PABA. It indicates that the copolymer formed by melt polymerization is a random copolymer, while the copolymer prepared by SSP is blocky in nature. The sample prepared by the SSP route is further heated in the X-ray hot stage up to 300°C to analyze the structure of the block copolymer obtained by SSP. The Figure 5.4 shows the overlay of the diffractograms obtained during various temperatures. With increasing temperature, the peaks due to PET vanishe at about 250°C, however, the peak due to POB at 2θ = 19.9° remains even at 300°C. This confirms the optical microscopy studies that the POB crystals do not melt even at 375°C.

5.3.3 Crystallization and melting behavior of copolyesters:

PET and POB oligomers show melting and crystallization behavior when subjected to a thermal cycle. The heating and cooling thermograms for POB oligomer is shown in Figure 5.5. POB shows melting temperature (T_m) ~ 320°C and melt crystallization temperature (T_c) ~ 287°C. On the other hand when POB is heated in a hot stage under polarizing microscope it shows distinct anisotropy even at 375°C as shown in the Figure 5.6, the maximum temperature reachable by the hot stage. The optical anisotropy at 375°C indicates the presence of crystals well above the melting temperature of POB. These may be arising from the long sequence POB.

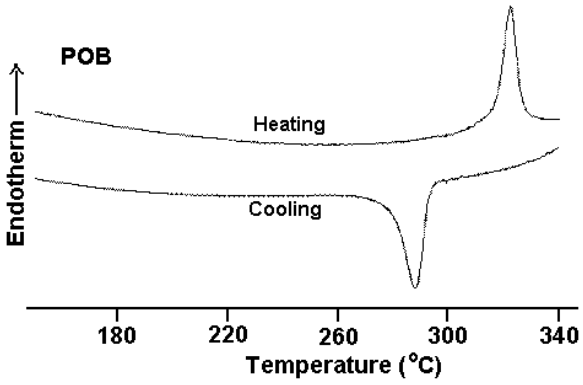

Figure 5.5: DSC thermograms of POB oligomer during heating and cooling.

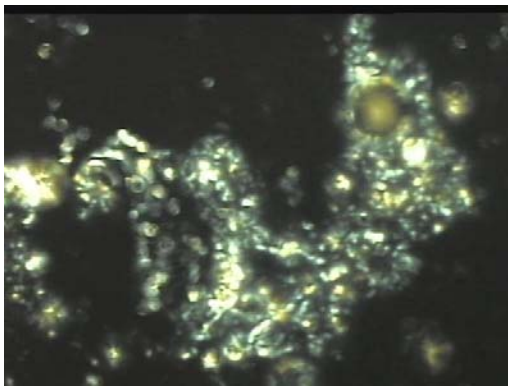

Figure 5.6: POB is heated in a hot stage under polarizing microscope at 375°C

PET/POB (70/30) oligomer blend shows melting temperature ~ 243°C. In the blend sample PET melting point is depressed by 15°C and POB melting is not observed. The behavior of the melting endotherms with SSP is shown in Figure 5.7.

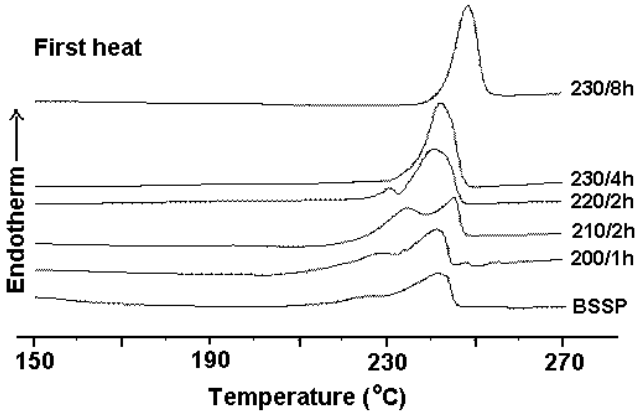

Figure 5.7: DSC thermograms of PET/POB (70/30) oligomer blend during SSP

The melting temperature does not change significantly but peaks become sharper during SSP, while the heat of fusion increases indicating increase in crystallinity during SSP. However, considering the temperature and time the increase in the crystallinity is marginal. These results are in confirmation with the WAXS data that during SSP the crystals do not undergo any changes, though the SSP is performed at temperatures close to the melting temperature. Hence WAXD and thermal data during first heat is not representative of the copolymer sample. However, melting the sample and the exotherm on the first cooling and the events occurring during the second heating are representative of the copolymer sample. Figure 5.8 shows the DSC thermograms for cooling and the

subsequent reheating. The heat of fusion and the melting temperature obtained during the

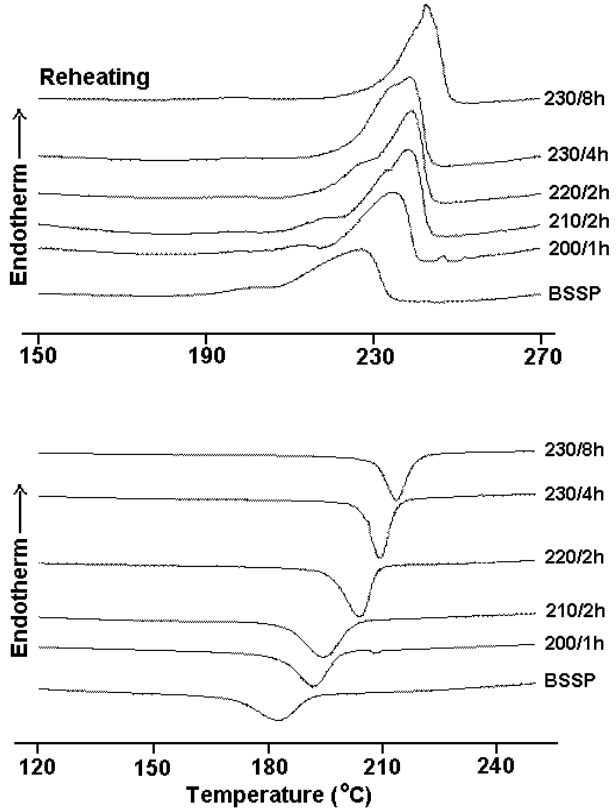

Figure 5.8: DSC thermograms of PET/POB (70/30) oligomer blend for cooling and reheating during SSP

different cycles is given in Table 5.3. The melting temperature during the second heat increases slightly during SSP and heat of fusion remains same at all the stages of SSP. Decrease in the melting temperature observed in the second heat when compared with the first heat represents the copolymer formation. However, the crystallization peak temperature on cooling from the melt showed that the crystallization rate of the PET increases with the progress of SSP. Table 5.3 shows the change in melt crystallization temperature with the progress of SSP. This may be due to complex structure of the copolymer formed during SSP. The copolymer contains different mesogen length (POB) and also the thermotropic behavior of the copolymer formed may enhance the crystallization rate.

Table 5.3: Thermal data for the SSP samples during heating, cooling and reheating at various stages of SSP

SSP conditions **Temperature/ Time**	First Heat		Cooling from the melt		Second heat	
	T_m (°C)	Δ Hm (J/g)	T_c (°C)	Δ Hc (J/g)	T_m (°C)	Δ Hm (J/g)
BSSP	242	42	183	34	227	35
200/1 hr	242	48	192	35	235	34
210/2 hr	245	50	195	39	238	40
220/4 hr	241	51	204	40	239	40
230/4 hr	242	53	209	38	239	39
230/8 hr	248	55	214	36	239	38
PET oligomer	255	66	214	58	251	54

Glass transition temperature (T_g) and cold crystallization temperatures (T_{cc}) are not seen during heating for SSP samples, as all these samples are highly crystalline. Hence separate sets of DSC scans are performed on these samples after melting and rapidly quenching in ice water. Figure 5.9 gives the DSC thermograms and Table 5.4 gives the data for the quenched samples.

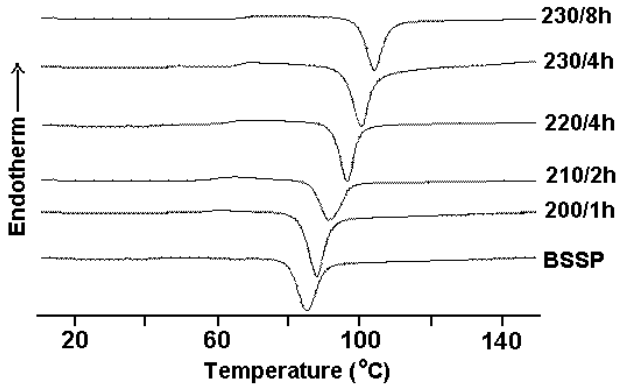

Figure 5.9: DSC thermograms of PET/POB (70/30) oligomer blend for the quenched samples

Table 5.4: Thermal data for quenched samples at various stages of SSP

SSP conditions Temperature/ Time	**T_g (^oC)**	**T_{cc} (^oC)**	**ΔH_c (J/g)**
BSSP	54	85	27
200/1 hr	57	88	26
210/2 hr	60	92	22
220/4 hr	63	97	24
230/4 hr	66	101	24
230/8 hr	68	104	24
PET oligomer	69	127	37

Results indicate that the T_g and T_{cc} decrease for the oligomer blend compared to PET. This may be due to molecular weight reduction of the blend after melt blending the oligomers. By performing SSP on these samples T_g and T_{cc} progressively increases with the SSP time/temperature protocol. The increase in the T_g may be attributed to the increase in the molecular weight. The increase in the cold crystallization temperature is indicative of decrease in the ability of the PET in the copolymer to crystallize with increase in the molecular weight. Evidently the POB blocks inhibit the crystallization of PET from the glassy state.

It is worth comparing the melting thermograms of the copolymer prepared by SSP and melt polymerization routes. Figure 5.10 shows the thermograms obtained during the second heating cycle. The thermograms look very different; the sample obtained by SSP route appears to be more crystalline than the sample prepared by melt polymerization. The sample obtained by the melt polymerization shows cold crystallization exotherm and melting endotherm at lower temperatures indicating that the sample is not crystallized during cooling from the melt. The lower melting point also indicates that the sample is more of a random copolymer. On the other hand the sample prepared by SSP does not show cold crystallization exotherm indicating the sample crystallized on cooling. Further, the sample shows higher melting temperature and heat of fusion (Table 5.5). These results indicate that the copolymer is more blocky in nature.

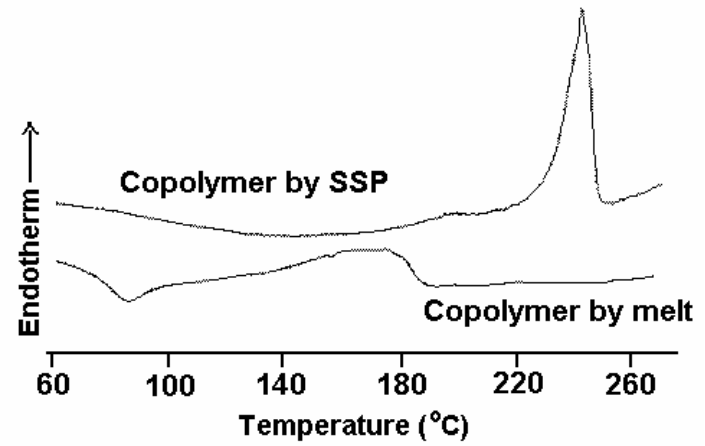

Figure 5.10: DSC thermograms obtained during the second heating cycle for copolymer prepared by SSP and melt polymerization.

Table 5.5: Thermal data for the copolymer prepared by SSP and melt polymerization route (second heating cycle)

Sample	T_m (°C)	Δ H (J/g)
SSP	243	36
Melt polymerization	175	22

5.4 Conclusions:

Oligomer blends are crystallized thermally to obtain suitable precursors for SSP. X-ray diffraction studies show that SSP and interchange reaction occurs only in the amorphous phase of the semicrystalline precursors. DSC results show that Tm of oligomers decreases in the blend sample. Melt crystallization temperature of PET increases with the progress of reaction indicating the enhancement of crystallization rate with the progress of reaction. It may be due to the nucleation of PET by unmelted long POB chains. On the other hand melt quenched samples showed that crystallization rate reduces with the progress of the SSP and interchange reaction indicating that the POB crystals inhibit crystallization of PET in the glassy state.

The preliminary work on the PET-POB blends indicate that the solid-state polymerization can be performed on PET and POB oligomer blends to obtain PET/POB copolymer. The morphology of the polymer obtained by SSP appears to be different from the sample obtained by melt polymerization. The SSP route gives block copolymer while the melt method gives a more random type of copolymer.

5.5 References:

1. Jackson WJ, Kuhfuss HF. J. Polym. Sci., Polym.Chem. Ed. 1976, 14, 2043.
2. Kuhfuss HF, Jackson WJ. U.S. Pat. 3 778 410; 1973.
3. Kuhfuss HF, Jackson WJ. U.S. Pat. 3 804 805; 1974.
4. Kang TK, Ha CS. J. Appl. Polym. Sci., 1999; 73: 1707.
5. Zachariades AE, Economy J, Logan JA. J. Appl. Polym. Sci. 1982; 27: 2009.
6. Zachariades AE, Logan JA. Polym. Eng. Sci. 1983; 23: 797.
7. Joseph E, Wilkes GL, Baird DG. Polymer 1985; 26: 689.
8. Meesiri W, Menczel J, Gaur U, Wunderlich B. J. Polym. Sci., Polym. Phys. Ed. 1982; 20: 719.
9. Sawyer LC. J. Polym. Sci., Polym. Lett. Ed. 1984; 22: 347.
10. Blackwell J, Lieser G, Gutierrez GA. Macromolecules 1983; 16: 1418.
11. Quach L, Hornbogen E, Volksen W, Economy J. J. Polym. Sci. Polym. Chem. Ed. 1989; 27: 775.
12. Mitchell GR, Ishii F. Polym. Commun. 1985; 26: 34.
13. Lenz RW, Jin J, Feichtinger KA. Polymer 1983; 24: 327.
14. Clements J, Humphreys J, Ward IM. J. Polym. Sci., Polym. Phys. Ed. 1986; 24: 2293.
15. Nicely VA, Dougherty JT, Renfro LW. Macromolecules 1987; 20: 573.
16. Amundson KR, Reimer JA, Denn MM. Macromolecules 1991; 24: 3250.
17. Bohme F, Komber H, Leistner D, Ratzsch M. Macromol. Chem. Phys. 1994; 195: 3233.
18. Mathew J, Ghadage RS, Ponrathnam S, Prasad SD. Macromolecules 1994; 27: 4021
19. Mathew J, Bahulekar RV, Ghadage RS, Rajan CR, Ponrathnam S, Prasad SD. Macromolecules 1992; 25: 7338
20. Murthy NS, Correale ST, Minor H. Macromolecules 1991; 24: 1185.
21. Shinn TH, Lin CC. J. Appl. Polym. Sci. 1993, 47, 1105.
22. Kang TK, Ha CS. J. Appl. Polym. Sci. 1999, 73, 1707.
23. James NR, Ramesh C, Sivaram S. Macromol. Chem. Phys. 2001; 202: 1200.
24. James NR, Ramesh C, Sivaram S. Macromol Chem Phys 2001; 202: 2267.

CHAPTER 6

EFFECT OF MOLECULAR ORIENTATION ON CRYSTALLIZATION AND MELTING BEHAVIOR OF POLY (ETHYLENE TEREPHTHALATE)

6.1 Introduction

Poly(ethylene terephthalate) (PET) is perhaps one of the extensively studied and a model semicrystalline polymer for crystallization studies because it can be obtained easily in amorphous or semicrystalline forms at room temperature[1-5]. The effect of chain orientation on the crystallization of PET has also attracted wide attention because of its relevance in polymer processing. The extent of the short or medium range order within the amorphous phase, the density, orientation, and the confirmation of the amorphous chain segments greatly influence the performance of a polymer. In particular case of fibers, mechanical properties such as modulus and tenacity, and diffusion behavior such as dye uptake and permeability, are influenced by the amorphous orientation.

In the presence of chain orientation, it has been shown that the rate of crystallization is strongly dependent on the degree of orientation and the key parameters being the initial orientation of the chains and the temperature of crystallization[6-11]. Orientation induced crystallization in PET is thought to be occurring through an intermediate phase called mesophase or transient phase[11,12]. Yeh and Gail observed paracrystalline order in quenched PET under electron microscopy[13,14]. Murthy et al. suggested that short-range order, as evidenced by the occurrence of two different interchain distances, act as incipient crystals for further crystallization[15]. *In situ* monitoring of the development of structure using synchrotron radiation source further reinforced the existence of mesophase order just before the crystallization[16-18].

Oriented amorphous fibers are usually obtained by drawing fibers just below glass transition temperature[16-18]. This process always results in a skin whose orientation is significantly higher than that of the core. As a result, crystallization behavior data obtained from these fibres do not accurately portray the influence of orientation on crystallization kinetics. In contrast, in this work we study PET fibres with different levels of amorphous orientation obtained by spinning PET with polystyrene (PS) skin, as a bicomponent fiber. This way, the shear stresses near the wall are absorbed by the PS skin and do not produce any shear induced orientation in the PET core. Fibers obtained after selectively removing the PS sheath enable us to study the effect of amorphous orientation on the crystallization behavior without the interference from the extraneous structure near the skin. PS was selected as sheath because the activation energy of elongational viscosity and glass transition temperature are higher than that of PET and it is expected to solidify at a point earlier than the solidification point of PET, which consequently brings about the suppression of PET structure development. It has been observed that the structure

development in the high-speed bicomponent spinning is significantly different from that of the corresponding single component fiber because of the mutual interaction of the two components. The relative differences in the inherent polymer characteristics, such as solidification temperature, activation energy of elongational viscosity and the initial viscosity are found to be some of the major factors influencing the mutual interaction between the component polymers. This may also lead to a significant difference in the fiber structure development. Thus, it may be possible to improve the structure of high-speed spun fibers via the choice of suitable component polymers. Degree of amorphous orientation (f_{am}) and the amount of amorphous material oriented in the fibres were characterized by wide-angle x-ray scattering technique (WAXS) and correlated with cold crystallization temperature (T_{cc}) and the heat of crystallization (ΔH_c) for the first time.

6.2 Experimental

6.2.1 Materilas

PET-PS bicomponent fibers were kindly provided by Prof. Kitutani, Tokyo Institute of Technology, Japan. PS sheath-PET core bicomponent fibers were prepared by coextruding the melt of PET (IV= 0.65dL/g) and PS at 295 °C at various spinning speeds from 1000 to 7000 m/min as discussed elsewhere[19]. The PS part was removed by dissolving in carbon tetrachloride. Another set of single filament standard fibers of PET was spun under similar conditions.

6.2.2 Measurements

The thermal behavior of the fibers was investigated by using DSC under constrained and unconstrained conditions. In the case of constrained condition, the fibers were wound on a small aluminum frame, which could fit in to the DSC sample pan. A tight knot was made on the ends of fiber to prevent the fiber from shrinking during DSC measurement. Wide-angle x-ray diffraction (WAXS) experiments were performed on theses fibers as described in chapter 3. The WAXS patterns were obtained from fibers that were cut into very small pieces by scissors.

The 2-D diffraction patterns were obtained using a Bruker AXS area detector. The data were collected on a Rigaku sealed tube generator with a sample to detector distance of 5.32 cm. Background-subtracted images were used for analysis. To determine the amorphous orientation, azimuthal scans were obtained over 360º of χ between 2θ values of 19.3º and 20.8º. This annular ring was between the 010 and $\bar{1}11$ reflections, an angular

range where the amorphous peak was reasonably intense and had least overlap from the crystalline reflections, when present. The profiles were fitted to two Gaussian peaks and a horizontal base-line. The width of the peak was used to calculate the degree of amorphous orientation f_{am} using expression for Herman's orientation function from the relation

$$f = (3\langle \cos^2 \phi \rangle - 1)/2 \qquad (1)$$

$$\langle \cos^2 \phi \rangle = \frac{\int_{-\pi/2}^{\pi/2} I(\phi) \cos^2 \phi \sin \phi d\phi}{\int_{-\pi/2}^{\pi/2} I(\phi) \sin \phi d\phi} \qquad (2)$$

$<\cos^2\phi>$ could be evaluated from the full-width at half-maximum ($\Delta\phi$) of the Gaussian azimuthal intensity distribution by evaluating the above integral for each value of $\Delta\phi$ from the relation

$$I(\phi) = \exp\left(\frac{-4\phi^2 \ln 2}{\Delta\phi^2}\right) \qquad (3)$$

We used the azimuthal intensity plots to calculate a second measure of amorphous orientation, the fraction of the oriented amorphous phase (F_{am}) as the ratio of the area of the amorphous peak above the base-line to the total amorphous area[20-23]. Where as the f_{am} is a measure of how well the chains are oriented, F_{am} is a measure of the fraction of the oriented amorphous phase. Both factors are known to influence the material properties.

Fibers spun at 6000 and 7000 m/min. showed crystalline reflections. The amorphous orientation in these fibers were analyzed from a sequence of radial scans obtained from 2θ = 5º to 40º at azimuthal angle 0º (equatorial) to meridional (90º) in steps of 10 degrees. Each of these scans was used to obtain the height of the amorphous halo. This height was then used to generate $I(\phi)$ plot, that was used to evaluate $\Delta\phi$ [21-23].

Crystalline orientations were calculated using the equations 1-3 by using the full-width at half maximum of the equatorial reflection $\bar{1}10$. This width was determined from the azimuthal scan through the crystalline reflections between 2θ values of 21.9º and 23.9º.

6.3 Results and Discussions

6.3.1 Wide-angle X-ray diffraction studies

WAXS patterns of the PET samples (PS removed) along with standard PET fibers spun at different speeds are shown in Figure 6.1. The scans for the bicomponent fibres do not show characteristic crystalline peaks until a spinning speed of 6000 m/min., is reached,

indicating that the spin line crystallization is suppressed in PET in these fibres. On the other hand in the standard PET fibres crystallinity develops at lower spinning speed: the standard PET fiber spun at 6000 m/min., (standard) is equivalent to PET-PS bicomponent (PS sheath) fibre spun at 7000 m/min. The key difference is that the shear induces skin to crystallize at lower spinning speed in standard PET fibers. Note also that the shape of the amorphous halo in the bicomponent fiber remains essentially unchanged until the onset of crystallization (5000 m/min.) whereas that in the straight PET fiber becomes asymmetric even at 2000 m/min., and this asymmetry increases until the onset of crystallization at 5000 m/min. The asymmetry in the shape of the amorphous suggests shear-induced enhancement of the short-range order in the amorphous domains near skin of the fiber[15]. Such enhancement is not seen in the bicomponent fibers.

A typical example of the azimuthal scans for completely amorphous and partially crystalline fibres spun at 3000 and 7000 m/min., respectively, are shown in Figure 6.2. The fibers spun at 3000 m/min. do not crystallize and the scattering is entirely due to the amorphous phase. On the other hand, the fibre spun at 7000 m/min. shows well-developed crystalline peaks and the azimuthal scan shows $\bar{1}10$, $\bar{1}11$, and 011 reflections. The degree of amorphous orientation (f_{am}) and, in the case of fibers spun at 6000 and 7000 m/min., which show crystalline peaks, the degree of crystallite orientation (f_c) could be calculated from the azimuthal scans. f_{am} and the amount of oriented amorphous fraction increase with increase in spinning speed and are shown in Figure 6.3. f_{am} increases linearly from 0.10 to 0.18 with spinning speed up to 5000 m/min, and jumps to 0.27 at higher speeds; this discontinuous increase is accompanied by the onset of spin-line crystallization.

The fraction of the oriented amorphous phase, which also increases with spinning speed, decreases when a part of this oriented amorphous phase crystallizes at a spinning speed of 5000 m/min., and then begins to increase at higher spinning speeds. These results indicate that there is a critical f_{am} for the onset of crystallization. Our data suggest this critical f_{am} for the onset of spin-line crystallization is ~0.18 (Figure 6.1a, 6.3a and Table 6.1). This is in surprising agreement with the results obtained on films using intrinsic fluorescence polarization measurements[24]. Note that these results are obtained for orientation-induced crystallization, and we can only speculate that a similar critical f_{am} could be present locally during crystallization in unoriented PET. We further speculate that these locally oriented amorphous domains constitute the nucleation sites for crystallization.

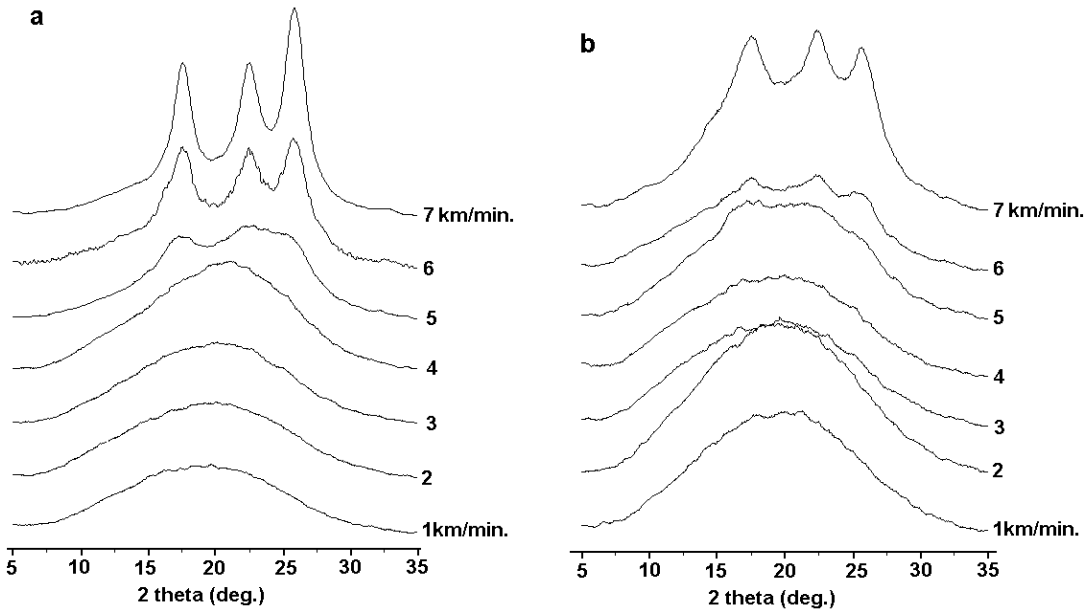

Figure 6.1: Powder diffraction patterns of the fibre samples (a) Standard PET fibers (b) Core PET fibers (PS removed)

The large increase in f_{am} after crystallization that we find in our fibres is in agreement with that reported for other fibers[23]. The large increase in f_{am} suggests that the transformation of the oriented amorphous phase with a $f_{am} \geq 0.18$ into crystals with a high degree of crystallite orientation (measured f_c, ~ 0.96), enhances the orientation of the surrounding amorphous matrix. This is suggestive of the strong interactions between the crystalline lamellae and the amorphous matrix. Given that crystallization occurs at the expense of oriented amorphous fraction one would expect that the amorphous chain segments that are left behind in the amorphous pool would be less oriented, and this is reflected in the sudden decrease in the fraction of the oriented amorphous phase.

These samples with varying degrees of amorphous orientation provide an opportunity to study the effect of amorphous orientation on crystallization. All the samples exhibit cold crystallization on heating above glass transition temperature. The cold crystallization temperature (T_{cc}) and the heat of crystallization (ΔH_c) decrease with increase in spinning speed and shown in Figure 6.4. Another point noted is the decrease in the heat of fusion as the amount of oriented phase increases with spinning speed. It is also interesting to note that the T_{cc} remains the same irrespective of whether the sample is constrained or not

during the DSC experiments. Table 1 shows the shrinkage in hot air at 100°C and are similar to the data obtained for the fibers obtained by single component spinning[25,26].

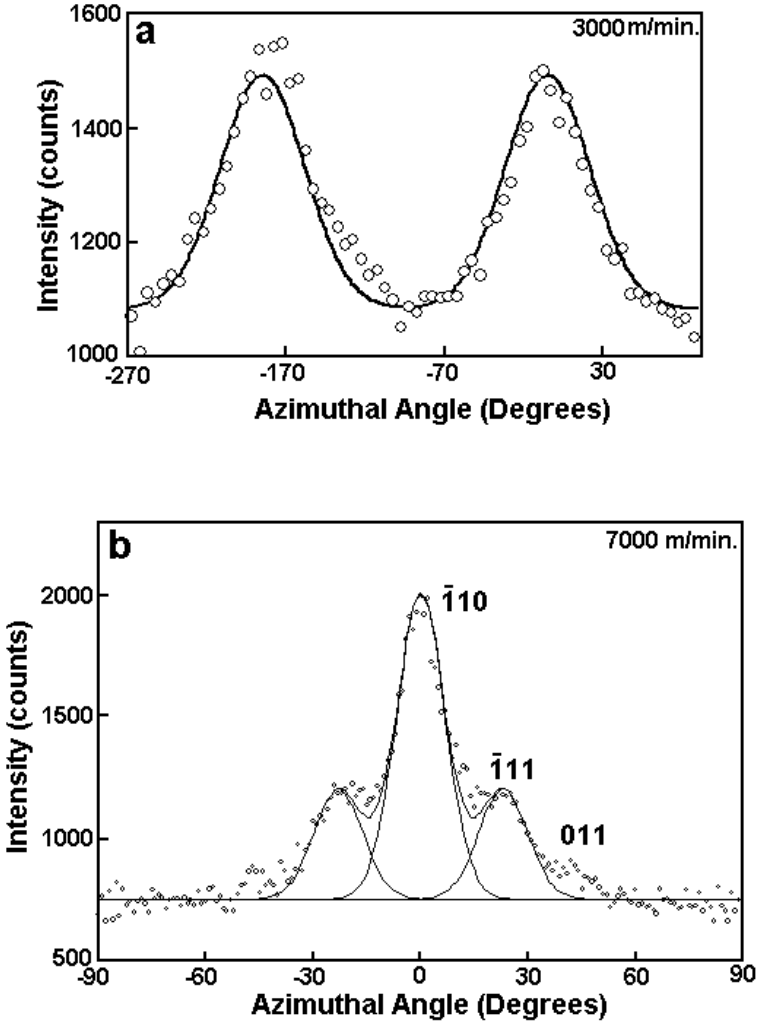

Figure 6.2: Azimuthal scans of two fibres: (a) Amorphous halo in a fiber spun at 3000 and (b) Crystalline peaks in a fiber spun at 7000 m/min.; the weak 011 reflection was not fitted.

These data indicate that the shrinkage force and T_{cc} are not correlated. Cold crystallization, because it depends on the internal structure present at the time of crystallization and not on external constraints, would be expected to be the same irrespective of whether the fiber is constrained or unconstrained during crystallization. Thus, T_{cc} is the same for both constrained and unconstrained specimens. But the effect of constrained and unconstrained conditions during DSC scanning is seen in the melting temperature. The constrained samples show consistently higher melting temperature than the corresponding

unconstrained fibers; the origin of such differences in the melting temperatures has been discussed in detail by Gupta et al[27].

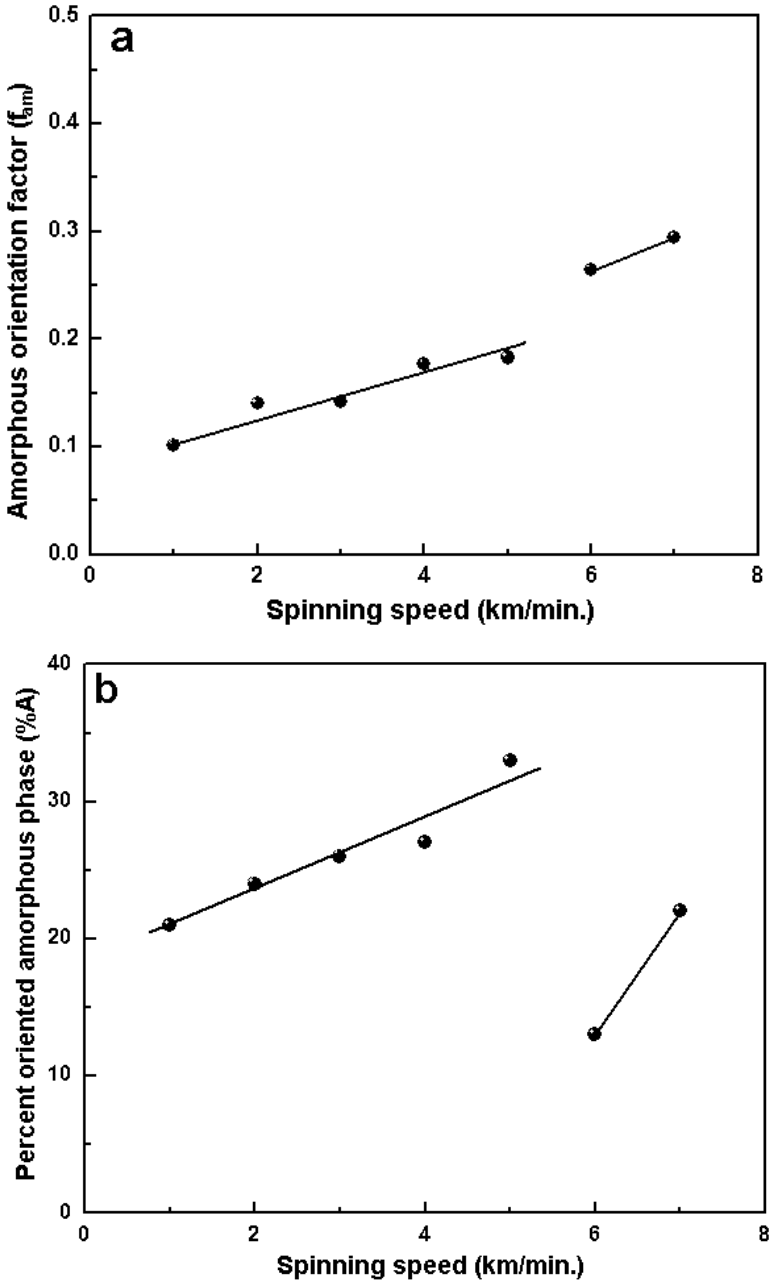

Figure 6.3: Variation of the (a) degree of amorphous orientation and (b) the fraction of the oriented amorphous phase with spinning speed.

Table 6.1: Structural parameters of the fibres

Spinning Speed (m/min.)	Hermans orientation function (f_{am})	% of oriented amorphous phase	Shrinkage at 100°C in hot air (%)	Cold crystallization temperature (°C)		Melting temperature (°C)	
				Unconstrained	Constrained	Unconstrained	Constrained
1000	0.102	21	27	134	133	257	260
2000	0.140	24	45	128	128	257	262
3000	0.142	26	53	117	122	256	261
4000	0.177	27	40	110	113	256	262
5000	0.183	33	28	107	107	256	262
6000	0.265	12	16	105	104	257	263
7000	0.295	19	6	102	101	257	265

Melting is governed by: $T_m = \Delta H/\Delta S$, where T_m is the melting point, ΔH is the enthalpy of melting, and ΔS is the change in the entropy during melting. When the fibers are held constrained during melting, there is a smaller change in entropy between the crystalline and the constrained oriented melt, and hence the constrained fibers show a higher T_m than the unconstrained fibers.

The decrease in the T_{cc} is indicative of the enhanced crystallization rate of the samples with increase in spinning speed (Figure 6.4a). The T_{cc} decreases with increase in the degree of amorphous orientation f_{am} as shown in Figure 6.5a and crystallization under constrained or unconstrained condition does not affect the T_{cc}. The extrapolation of the line shows that the sample with $f_{am} = 0.27$ will crystallize at T_g, (80 °C). Even though T_{cc} depends on heating rate, experiments with different heating rates led to the same extrapolated f_{am}=0.27. This implies that the T_{cc} of samples with $f_{am} \geq 0.27$ will be same as their T_g, because samples do not crystallize below T_g. It is interesting to note that as predicted in this work, Keum et al[18] using synchrotron data indeed show that the crystallization of mesophase occurs at about 80°C. If the crystallization is controlled by nucleation and growth, then orientation would not expect to have such a large influence on crystallization. It therefore appears that the crystallization occurs by spinodal decomposition[28,29]. The quantitative correlation between cold crystallization and amorphous orientation has been established for the first time and shows that the crystallization is very sensitive to amorphous orientation.

The correlation between T_{cc} and f_{am}, and the limiting T_{cc} of 80 ºC at $f_{am} > 0.27$ appears to be valid only for fully amorphous fibres. Because, in fibres spun at speeds greater than 6000 m/min. that show spin line crystallization $f_{am} > 0.27$ but $T_{cc} > 100$°C (Figure 6.5a). It could be that crystallites present in these fibres inhibit the crystallization of even the oriented amorphous phase. The crystallization, in these fibers probably proceeds by insertion of smaller crystallites between the larger lamellae formed during primary crystallization in the drawing step. The insertion requires higher activation energy and consequently slower crystallization rate compared to fibres that do not have preexisting lamellae. This appearance of these insertion-lamellae that follows primary crystallization has been reported by Lee et al[1], Wang et al[30] and Jonas et al[31].

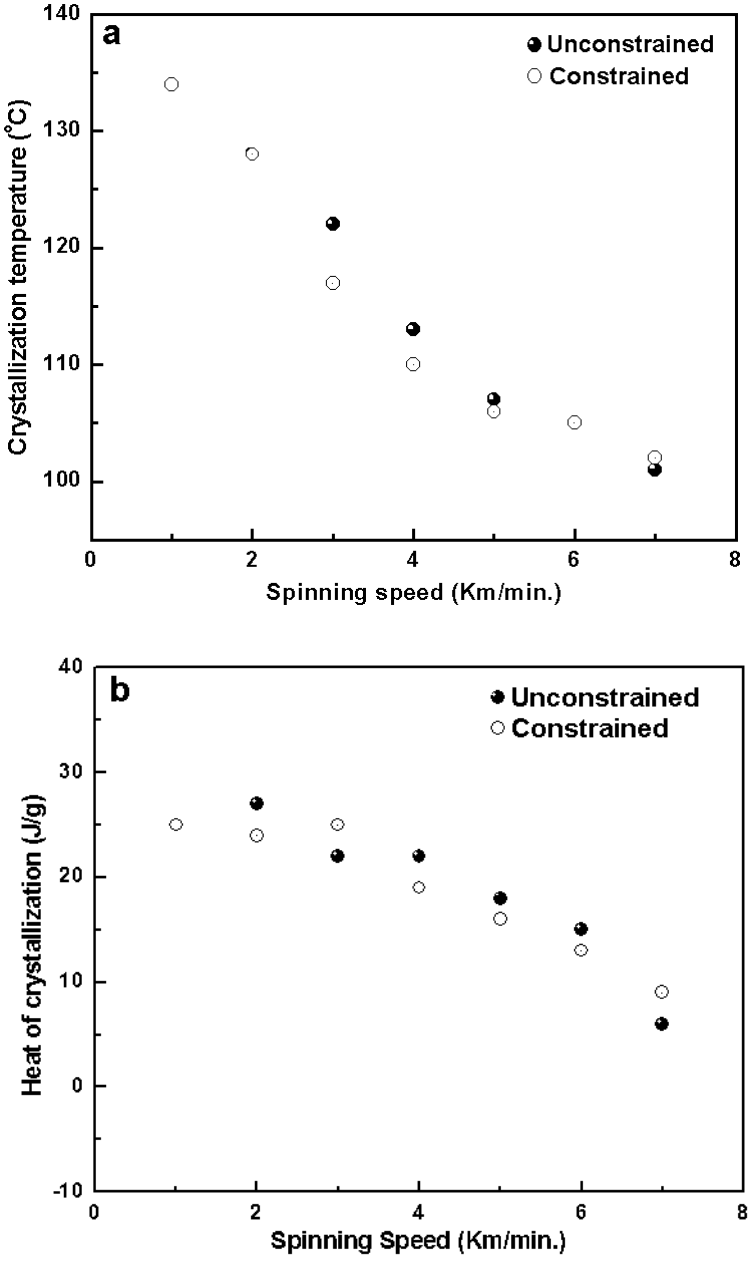

Figure 6.4: Variation of (a) cold crystallization temperature and (b) heat of crystallization with spinning speed

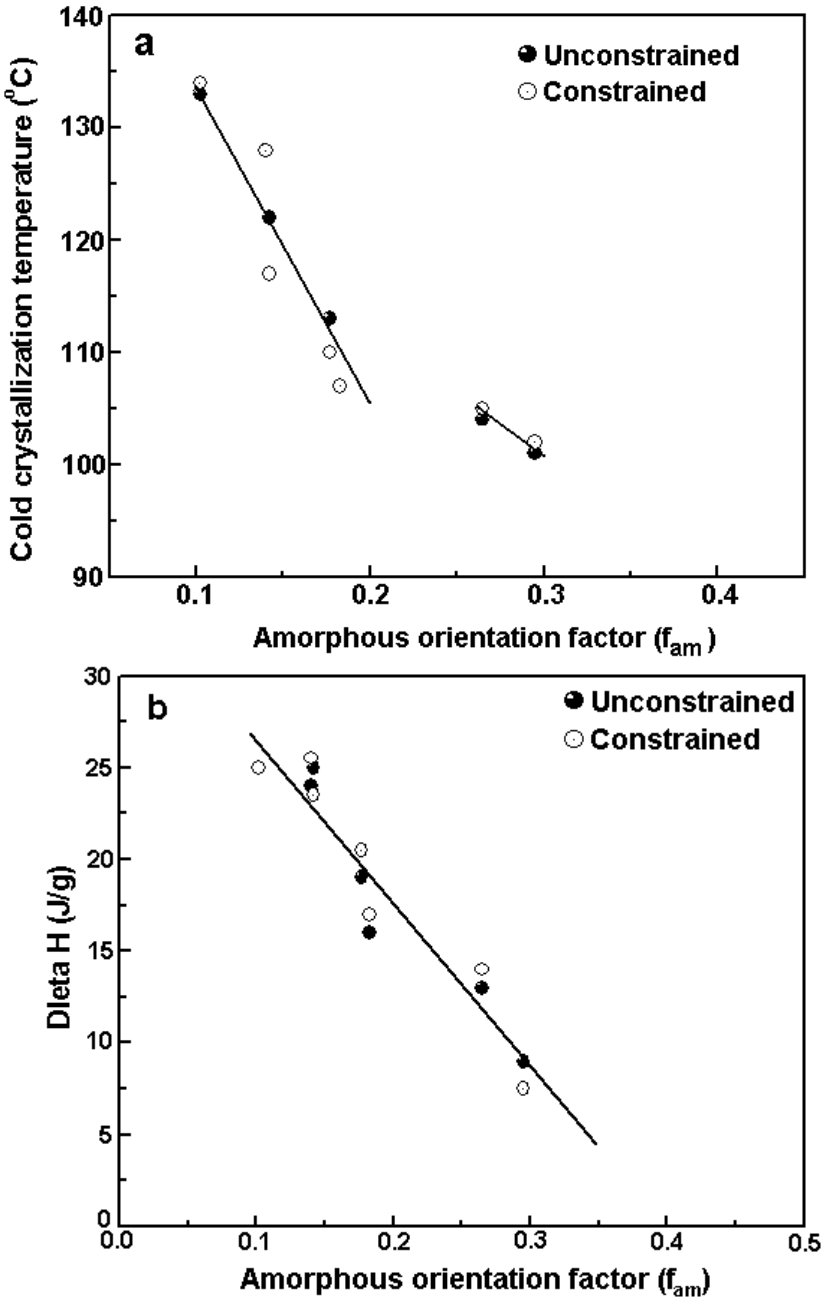

Figure 6.5: Dependence of (a) cold crystallization temperature and (b) heat of crystallization with the degree of amorphous orientation.

The heat of crystallization, ΔH_c, also decreases with increasing amorphous orientation, as shown in Figure 6.5b. It is seen from the figure that ΔH_c, unlike the T_{cc}, is not affected by the presence of pre-crystallized material. Extrapolation to x-axis shows that the $\Delta H_c=0$ for $f_{am}=0.40$. It is possible that above this critical orientation, a fraction of the chains will

spontaneously crystallize. The heat of crystallization that is released will provide for the increase in entropy of the fraction of the chains that become part of the unoriented amorphous phase and thus there is no net change in free energy. The highly oriented amorphous phase with very low ΔH_c may be considered as mesophase or transient phase. Keum et al.,[18] and Ran et al.[32] also observe mesophase in cold drawn amorphous PET film, which transforms into triclinic structure above Tg.

6.4 Conclusions

Analysis of fibers prepared such that the role of the skin is minimized allow us unambiguously ascertain the role of amorphous phase orientation on the crystallization. The cold crystallization temperature decreases linearly with increase in the degree of amorphous orientation. The results indicate that the crystallization is very sensitive to chain orientation and cold crystallization temperature approaches the Tg even at relatively low amorphous orientation of 0.27. The heat of crystallization also decreases with increase in amorphous orientation and extrapolates to zero when the f_{am} exceeds 0.40. This suggests that spinodal mechanism of crystallization at high degrees of amorphous orientation.

6.5 References

1. Lee B, Shin TJ, Lee SW, Yoon J, Kim J, Ree M. Macromolecules 2004; 37: 4174.
2. Lee B, Shin TJ, Lee SW, Yoon J, Kim J, Youn HS, Ree M. Polymer 2003; 44: 2509.
3. Lee JW, Lee SW, Lee B, Ree M. Macromol. Chem. Phys. 2001; 202: 3072.
4. Lee SW, Lee B, Ree M. Macromol. Chem. Phys. 2000; 201: 453.
5. Yu J, Zhou D, Chai W, Lee B, Lee SW, Yoon J, Ree M. Macromol. Res. 2003; 11: 25.
6. Smith FS, Steward RD. Polymer 1974; 16: 283.
7. Gupte KM, Motz H, Schultz JM. J. Polym. Sci. Polym. Phys. Ed. 1983; 21: 1927.
8. Althen G, Zachman HG. Makromol. Chem. 1979; 180: 2723.
9. Alfonso GC, Verdona, MP, Wasiak A. Polymer 1978; 19: 711.
10. Sun T, Pereira JRC, Porter RS. J. Polym. Sci. Polym. Phys. Ed. 1984; 22: 1163.
11. Bonart R. Kolloid-Z 1966; 213: 16.
12. Asano T, Seto T. Polym. J. 1973; 5: 72.
13. Yeh GSY, Geil PH. J. Macromol. Sci. Part B 1967; 1: 235.
14. Yeh GSY, Geil PH. J. Macromol. Sci. Part B 1967; 1: 251.
15. Murthy, NS, Correale ST, Minor H. Macromolecules 1991; 24: 1185.

16. Mahendrasingam A, Martin C, Fuller W, Blundell DJ, Oldman R J, MacKerron DH, Harvie JL, Riekel C. Polymer 1999; 41: 1217.
17. Blundell DJ, Mahendrasingam A, Martin C, Fuller W, MacKerron DH, Harvie JL, Oldman RJ, Riekel C. Polymer 2000; 41: 7793.
18. Keum JK, Kim J, Lee SM, Song HH, Son YK, Choi JI, Im SS. Macromolecules 2003; 36: 9873.
19. Kikutani T, Arikawa S, Takaku A, Okui N. Sen'i Gakkaishi 1995; 51: 408.
20. Murthy NS, Correale ST, Minor H, Macromolecules 1991; 24: 1185.
21. Murthy NS, Minor H, Bednarczyk C, Krimm S. Macromolecules 1993; 26: 1712.
22. Murthy NS, Bray RG, Correale ST, Moore RAF. Polymer 1995; 36: 3863.
23. Murthy NS, Bednarczyk C, Rim PB, Nelson CJ. J. Appl. Polym. Sci. 1997; 64: 1363.
24. Clauss B, Salem DR. Polymer 1985; 26: 1779.
25. Heuvel HM, Huisman R. J. Appl. Polym. Sci. 1978; 22: 2229.
26. Hamidi A, Abhiraman AS, Asher P, J. Appl. Polym. Sci. 1983; 28: 567.
27. Gupta VB, Jain AK. J. Macromol. Sci., Phys. 1990; B29: 49.
28. Matsuba G, Kanaya T, Saito M, Kaji K, Nishida K. Phys. Rev. 2000; E62: R1496.
29. Imai M, Kaji K, Kanaya T. Phys. Rev. Lett. 1993; 71: 4162.
30. Wang ZG, Hsiao BS, Sauer BB, Kampert WG. Polymer 1999; 40: 4615.
31. Jonas AM, Russel TP, Yoon DY. Coll. Polym. J. 1994; 272: 1344.
32. Ran S, Wang Z, Burger C, Chu B, Hsiao BS. Macromolecules 2002; 35: 10102.

CHAPTER 7

SUMMARY AND CONCLUSIONS

7.1 Summary

The key findings and conclusions of the present thesis are summarized below.

Poly(ethylene terephthalate) (PET) (IV:0.15 dL/g) oligomer was obtained by depolymerisation of high molecular weight PET. Polycarbonate (PC) oligomer (IV: 0.15 dL/g) was synthesized by standard melt polymerization procedure using bisphenol A and diphenyl carbonate in the presence of a basic catalyst. Blends of varying compositions were prepared by melt blending the chemically distinct PET and PC oligomers. The copolymer, poly(ethylene terephthalate-*co*-bisphenol A carbonate) was synthesized by simultaneous solid state polymerization and ester-carbonate interchange reaction between the oligomers of PET and PC. The reaction was carried out under reduced pressure at temperatures below the melting temperature of the blend samples. DSC and WAXS techniques characterized the structure and morphology of the blends, while ^{1}NMR spectroscopy was used to monitor the progress of interchange reactions between the oligomers. The studies have indicated the amorphisation of the PET and PC crystalline phases in solid state with the progress of solid-state polymerization and interchange reaction.

Poly (ethylene glycol) and end capped poly (ethylene glycol) [Poly(ethylene glycol) dimethyl ether (PEGDME)] of number average molecular weight 1000 is incorporated in to PET oligomer by melt mixing as additives. PEG and PEGDME reduce the glass transition temperature (T_g) of PET and it depends on amount of additive incorporated. Solid-state polymerization was performed on these samples using Sb_2O_3 as catalyst under reduced pressure at temperatures below the melting temperature of the samples. PEG forms a copolymer with PET and also it shows increase in inherent viscosity compared to PET oligomer SSP under the similar conditions. PEGDME is non reactive with PET and it sits in the amorphous region of PET, hence it could not accelerate the PET SSP. NMR, DSC and WAXS techniques characterized the structure and morphology of the blends, while ^{1}NMR spectroscopy was used to monitor the progress of interchange reactions between the oligomers.

POB oligomer is prepared by melt polymerization of 4-acetoxybenzoic acid at 250 °C under atmosphere pressure. The PET/POB oligomers are melt blended in the ratio 70/10. The crystallized blend is subjected to interchange reaction in the solid state by holding the blend just below the melting temperature under reduced pressure. The change in the

structure and morphology is monitored by DSC and X-ray diffraction. PET/POB copolymer is also obtained by melt polymerization and the structure and morphology are compared to the copolymer formed by SSP.

Amorphous poly (ethylene terephthalate) fibers in which the skin was removed were studied to expressly study the effect of amorphous molecular orientation on crystallization behavior. Thermal analysis was carried out on fibers with a wide range of molecular orientation using differential scanning calorimetry (DSC) under constrained and unconstrained conditions. The thermal behavior was correlated with structural characteristics such as amorphous orientation determined using wide-angle x-ray diffraction. We show for the first time a quantitative inverse linear relationship between the degree of amorphous orientation and the cold crystallization temperatures and heat of crystallization. Crystallization begins at a critical amorphous orientation of 0.18, and extrapolation shows that even at modest amorphous orientation of 0.27, the cold crystallization can start spontaneously at Tg and with no change in free energy.

7.2 Conclusions

- The key conclusion of this work is that amorphisation of PET and PC crystals were observed below the melting temperature of the homopolymers with the progress of SSP and transesterification. DSC and WAXS results reveal the amorphisation of PET and PC crystals. The ^{1}H NMR data indicates that interchange reactions are active during later stages of SSP. The degree of randomness increases with increase in transesterification reaction. DSC studies on the SSP samples showed that, with increase in transesterification and viscosity, the crystallization of the copolymers became more and more difficult. In the case of simultaneous solid state polymerization and exchange reactions of PET/PEN oligomer blends, such amorphization was not observed with the progress of the reaction in the solid state and the PET and PEN crystals remained unchanged[1].

- Another conclusion is that the glass transition temperature of PET oligomer is reduced by the incorporation of plasticizers, PEG and PEGDME (M_n~1000) and also it depends linearly on amount of additive incorporated. PEG and PEGDME have good miscibility with PET and alter the crystallization behavior of PET oligomers. The plasticizers do not affect the crystalline morphology even though it

influences the crystallization rate. The WAXS patterns show very sharp reflections indicating a well-developed crystalline phase with big crystals in the case of PEG and PEGDME incorporated samples. SSP results on these samples showed that enhancing the chain mobility alone will not help in building up the molecular weight. However, PEG incorporated samples forms copolymers and it shows very high SSP rates compared to PET oligomer SSP under the similar conditions. It is worth noting that PEG chain ends react with PET to enhance the SSP rate. In the case of PEGDME incorporated samples, PEGDME occupies in the amorphous region PET and it may not allow PET chain ends for extension. It may be the reason for low SSP rates.

- The preliminary work on the PET-POB blends indicate that the Solid-state polymerization can be performed on PET and POB oligomer blends to obtain PET/POB copolymer. The morphology of the polymer obtained by SSP appears to be different from the sample obtained by melt polymerization. The SSP route gives block copolymer while the melt method gives more random type of copolymer. The POB has profound influence on the crystallization behaviour of PET.

- Another important conclusion is that amorphous phase orientation plays a crucial role on the crystallization of PET fiber. The crystallization is very sensitive to chain orientation and cold crystallization temperature approaches the Tg even at relatively low amorphous orientation of 0.27. The heat of crystallization also decreases with increase in amorphous orientation and extrapolates to zero when the f_{am} exceeds 0.40. This suggests that spinodal mechanism of crystallization at high degrees of amorphous orientation.

7.3 Future Perspectives

These results obtained in the present study provide an excellent scope for further studies such as:

- In the present work the amorphisation of PET and PC crystals was observed below the melting temperature with the progress of SSP and transesterification. Similar kind of studies can be done to understand more about the amorphisation of crystals below the melting temperature by choosing different oligomers (one crystalline and another amorphous) during simultaneous SSP and transesterification.

- Poly(oxy benzoate) oligomers with controlled chain length can be prepared and copolymerized with polyester oligomers like PET, PBT and PEN by simultaneous SSP and transesterification. It is of interest to study the morphology changes when one of the components forms liquid crystalline nature during simultaneous SSP and transesterification.
- Crystallization of PET is very interesting in the presence of POB oligomers. A detailed study can be carried out on crystallization kinetics.

7.4 References

1. James NR, Ramesh C, Sivaram S. Macromol Chem Phys 2001; 202: 2267.

Synopsis

Introduction

The importance of polymer crystallization has increased in modern polymer industry, despite the recent decline in research activities. More than 80% of the commodity polymers made today are crystalline, and the subject of crystallization is still the number one issue concerning the performance of semicrystalline polymers. Although many believe the field of polymer crystallization has "matured", new problems and new knowledge continue to emerge, making research and education of this topic ever more challenging.

Poly(ethylene terephthalate) (PET) is one of the most commercially important polyesters with excellent thermal and chemical resistance and mechanical performance. With the high level of production and its low price, PET can be positioned between the technical polymers and commodities. The most important applications of PET are its use in textile filaments, packaging materials, and bottle production.

Most of the applications of PET require polymer of high molecular weight. PET having IV ~ 0.15 – 1.0 dL/g is very commonly available. Very high molecular weight PET (IV as high as 3 dL/g) can be achieved[1-3] by solid state polymerization. PET SSP was discussed thoroughly in the literature. Understanding the structure and morphology of the SSP precursors (prepolymer) and the morphology changes during the SSP is important for both for scientific and practical reasons. Even though the general characteristics of SSP of PET are well known, there have not been many reports on morphological analysis of the main variables involved in the process of polymerization. It is generally accepted that in SSP, reaction occurs in the amorphous phase and by the diffusion of the end groups and byproduct[4].

If the starting material is a semi-crystalline poly-condensate and not an amorphous one, there are two possible effects on the reaction rate. Firstly, the crystalline phase, as such, restricts chain mobility and diffusivity and so reduces the reaction rate. On the other hand, as the end groups are concentrated in the amorphous regions, a higher reaction rate may be expected; due to the higher local concentration of the reagent. A further advantage of the use of semi-crystalline polymer as the starting material is that polymer particles do not agglomerate in the reactor.

James et al[5] used crystallized oligomers of PET and PEN having [η] ~0.2 dL/g as prepolymers for SSP to understand the effect crystallization and morphology on the SSP rate. The results showed that the crystallites do not undergo reorganization during SSP and

the chain ends in the amorphous phase mainly control the SSP and lead to more tie molecules in the morphology.

Rodriguez et al[6] studied the effect of precursor crystallinity on the SSP of PET and showed that high crystallinities in precursors were required to obtain large increase in molecular weight. This is contrary to suggestions given by Chang et al[7] and Karayannidis et al[8] who concluded that because of the high crystallinity present, there would not be a high increase in molecular weight after SSP.

In the case of copolymers, transesterification reactions will takes place only in amorphous polymers or in the amorphous part of semicrystalline polymers. Even if reactions occur in crystallites they take place only in crystal defects. Nirmala et al[9] synthesized PET/PEN copolymers by simultaneous solid-state polymerization and transesterification. The invariance in WAXD pattern and DSC data indicate that the SSP and transesterification take place in the amorphous phase while crystalline phase remains unaltered. This suggests that the transesterification occurs only in the amorphous phase and at the crystal amorphous interface. This leads to the morphology in which PET and PEN crystallites are distributed in the amorphous PET/PEN copolymer matrix.

The effect of chain orientation on the crystallization of PET has also attracted wide attention because of its relevance in polymer processing. In the presence of chain orientation, it has been shown that the rate of crystallization is strongly dependent on the degree of orientation and the key parameters being the initial orientation of the chains and the temperature of crystallization[10-15]. Orientation induced crystallization in PET is thought to be occurring through an intermediate phase called mesophase or transient phase[15,16]. Murthy et al.[17] suggested that short range order, as evidenced by the occurrence of two different interchain distances, act as incipient crystals for further crystallization. PET fibres with different levels of amorphous orientation obtained by spinning PET with polystyrene (PS) skin, as a bicomponent fiber. This way, the shear stresses near the wall are absorbed by the PS skin and do not produce any shear induced orientation in the PET core. Fibers without the interference from the extraneous structure near the skin were obtained after selectively removing the PS sheath. These fibers were used to study the effect of amorphous orientation on the crystallization behavior in this thesis.

Objectives of the present work

The primary focus of the present thesis is to study the structure and morphology development in PET based copolymers during chain extension reaction (solid state polymerization). To that end comonomers having distinct properties are chosen: 1)

comonomer which is semi-rigid 2) highly flexible comonomer which can plasticize the PET and 3) rigid monomer which can form liquid crystal with PET.

Another important aspect of polymer crystallization is the role of orientation on crystallization. Hence, very specially spun PET fibers with varying degree of amorphous orientation are studied for the crystallization behavior and correlated with the amorphous orientation factor.

A. One of the objectives of the present work is to study the morphological changes of interchange reactions between poly(ethylene terephthalate) and polycarbonate oligomers during solid state copolymerization by using WAXD and DSC. Amount of transesterification and degree of randomness of the copolymer was analyzed by NMR analyses.
B. Another objective is to enhance the mobility of the amorphous phase of PET and study its effect on the SSP. Hence it is proposed to plasticize the amorphous phase by the addition of small quantities of low molecular weight plasticizers (PEG and PEGDME) and studying the solid state polymerization.

C. Another objective of the present work is to synthesize the copolymers of PET and POB from the blend of oligomers by simultaneous solid state polymerization and transesterification. Amount of transesterification of the copolymer was analyzed by NMR analyses. Structure and morphology of the copolymer formed is studied by differential scanning calorimetry (DSC) and WAXD measurements.

D. To study the effect of molecular orientation on the crystallization and melting behavior of poly (ethylene terephthalate) fiber**.** Amorphous orientation and the amount of amorphous material in the fibers are characterized by wide-angle x-ray scattering technique (WAXS) and correlated with cold crystallization temperature and the heat of crystallization.

The thesis has been divided into the following chapters.

Chapter 1: General introduction

A general literature background is presented on poly(ethylene terephthalate) crystallization, structure and morphology of PET, Solid state polymerization of PET,

structure and morphology changes in PET during SSP and copolymerization of PET with other comonomers via SSP and its structure and morphology.

Chapter 2: Scope and objectives of the present work

This chapter discusses the scope and objectives of the present work.

Chapter 3: Morphological consequences of interchange reactions during solid state copolymerization in poly (ethylene terephthalate) and polycarbonate oligomers.

This chapter describes the following

1. Preparation of PET and PC oligomers and oligomer blends in various compositions by melt blending.
2. Solid state polymerization of the crystallized oligomer mixtures.
3. Quantification of transesterification and degree of randomness of the copolymer by NMR analyses.
4. Understanding the changes in structure and morphology of the copolymer by differential scanning calorimetry (DSC) and WAXD measurements.

Chapter 4: Effect of poly(ethylene glycol) as an additive on the crystallization and solid state polymerization of poly(ethylene terephthalate).

This chapter describes the following

1. Effect of additives like PEG and PEGDME (M_n ~ 1000) on glass transition temperature and crystallization rate of PET oligomer.
2. Effect of these additives on rate of solid state polymerization.
3. Confirmation of copolymer formation by NMR analyses.
4. Understanding the changes in structure and morphology by differential scanning calorimetry (DSC) and WAXD measurements.

Chapter 5: Studies on simultaneous solid state polymerization and transesterification in poly(ethylene terephthalate) and poly(oxybenzoate) oligomers.

This chapter describes the following

1. Preparation of PET and poly(oxybenzoate) (POB) oligomers and oligomer blends in 70/30 molar compositions by melt blending.
2. Solid state polymerization of the crystallized oligomer mixtures.
3. Confirmation of copolymers formation by ^{1}H NMR analyses.
4. Understanding the changes in structure and morphology of the copolymer by differential scanning calorimetry (DSC) and WAXD measurements.

Chapter 6: Effect of molecular orientation on the crystallization and melting behavior of poly(ethylene terephthalate) fiber.

This chapter describes the following

1. Preparation of PET fibers with varying degree of orientation from bicomponent fibers.
2. Crystallization and melting behavior of the fiber under constrained and unconstrained state.
3. Correlation between amorphous orientation with cold crystallization temperature and the heat of crystallization.

Chapter 7: Summary and Conclusions

This chapter summarizes the results and conclusions of the work.

References:

1. Kurita K, Hayashi M, Ohta T, Ishihara H, Okada F, Yoshikawa W, Chiba A, Tate S. US Patent 4851508; 1989.
2. Cohn G. Polym Prepr; 1989; 30: 160.
3. Cohn G. US Patent 4792573; 1988.
4. Gross SM, Roberts GW, Kiserow DJ, DeSimone JM. Macromolecules 2000; 33: 40.
5. James NR, Ramesh C, Sivaram S. Macromol. Chem. Phys. 2001; 202: 1200.
6. Rodriguez M, Guillen RL, Mendoza MAW. J Appl Polym Sci 2000; 75: 78.
7. Chang S, Sheu MF, Chen SM. J Appl Polym Sci 1983; 28: 3289.
8. Karayannidis GP, Kokalas DE, Bikiaris DN. J Appl Polym Sci 1995; 56: 405.
9. James NR, Ramesh C, Sivaram S. Macromol. Chem. Phys. 2001; 202: 2267.
10. Smith FS, Steward RD. Polymer 1974; 16: 283.

11. Gupte KM, Motz H, Schultz JM. J. Polym. Sci. Polym. Phys. Ed. 1983; 21: 1927.
12. Althen G, Zachman HG. Makromol. Chem. 1979; 180: 2723.
13. Alfonso GC, Verdona, MP, Wasiak A. Polymer 1978; 19: 711.
14. Sun T, Pereira JRC, Porter RS. J. Polym. Sci. Polym. Phys. Ed. 1984; 22: 1163.
15. Bonart R. Kolloid-Z 1966; 213: 16.
16. Asano T, Seto T. Polym. J. 1973; 5: 72.
17. Murthy NS, Correale ST, Minor H. Macromolecules 1991; 24: 1185.

List of Publications

(From Ph.D. thesis)

1. Effect of molecular orientation on the crystallization and melting behavior of Poly (ethylene terephthalate) fiber

   E. Bhoje Gowd, C. Ramesh, Mark S. Byrne, N. Sanjeeva Murthy, and J. Radhakrishnan

   Polymer **45**, 6707 (2004)

2. Morphological Consequences of Interchange Reactions during Solid State Copolymerization in Poly (ethylene terephthalate) and Polycarbonate oligomers

   E. Bhoje Gowd and C. Ramesh

   Submitted to *Polymer*

3. Effect of poly(ethylene glycol) as plasticizer on the crystallization and solid state polymerization of poly (ethylene terephthalate)

   E. Bhoje Gowd and C. Ramesh

   Submitted to *Journal of Polymer science Part B: Polymer Physics*

List of related Publications

1. High Temperature X-ray Diffraction studies on the crystalline transitions in the α and γ forms of Nylon 6

   C. Ramesh and **E. Bhoje Gowd**

   Macromolecules **34**, 3308 (2001)

2. Studies on the crystallization and melting behavior of poly (ethylene 2,6-naphthalate)

   Nirmala R. James; **E. Bhoje Gowd**; C. Ramesh; S. Sivaram

   Int. J. Polym. Mat., **50(3-4)**, 335 (2001)

3. Crystalline transitions of the clathrate (δ) form of syndiotactic polystyrene during heating: Studies using high temperature X-ray diffraction

   E. Bhoje Gowd, Smitha S. Nair and C. Ramesh

   Macromolecules **35**, 8509 (2002)

4. Crystalline transitions of the clathrate (δ) form of syndiotactic polystyrene during heating: Studies using high temperature FTIR

   E. Bhoje Gowd, Smitha S. Nair, C. Ramesh and Kohji Tashiro

   Macromolecules **36**, 7388 (2003)

5. Main Chain Thermotropic Liquid Crystalline Polyurethanes Containing Biphenyl Mesogen Based on AB Type Self-Polycondensation Route: XRD and FT-IR Spectroscopic Studies

   T. Ranganathan, **E. Bhoje Gowd**, C. Ramesh and Anil Kumar

   Journal of Polymer science Part A: Polymer Chemistry (2005)
   (Accepted for publication)